

DOT/FAA/AR-08/37,P4

Air Traffic Organization
Operations Planning
Office of Aviation Research
and Development
Washington, DC 20591

Explicit Finite Element Modeling of Multilayer Composite Fabric for Gas Turbine Engine Containment Systems, Phase II

Part 4: Model Simulation for Ballistic Tests, Engine Fan Blade-Out, and Generic Engine

February 2009

Final Report

This document is available to the U.S. public through
the National Technical Information Service (NTIS),
Springfield, Virginia 22161.



U.S. Department of Transportation
Federal Aviation Administration

NOTICE

This document is disseminated under the sponsorship of the U.S. Department of Transportation in the interest of information exchange. The United States Government assumes no liability for the contents or use thereof. The United States Government does not endorse products or manufacturers. Trade or manufacturer's names appear herein solely because they are considered essential to the objective of this report. This document does not constitute FAA certification policy. Consult your local FAA aircraft certification office as to its use.

This report is available at the Federal Aviation Administration William J. Hughes Technical Center's Full-Text Technical Reports page: actlibrary.tc.faa.gov in Adobe Acrobat portable document format (PDF).

Technical Report Documentation Page

1. Report No. DOT/FAA/AR-08/37,P4		2. Government Accession No.		3. Recipient's Catalog No.	
4. Title and Subtitle EXPLICIT FINITE ELEMENT MODELING OF MULTILAYER COMPOSITE FABRIC FOR GAS TURBINE ENGINE CONTAINMENT SYSTEMS PHASE II, PART 4: MODEL SIMULATION FOR BALLISTIC TESTS, ENGINE FAN BLADE-OUT, AND GENERIC ENGINE				5. Report Date February 2009	
				6. Performing Organization Code	
7. Author(s) Ion V. Vintilescu				8. Performing Organization Report No.	
9. Performing Organization Name and Address Honeywell Engines, Systems & Services 111 S. 34th Street P.O. Box 52181 Phoenix, AZ 85072-2181				10. Work Unit No. (TRAIS)	
				11. Contract or Grant No.	
12. Sponsoring Agency Name and Address U.S. Department of Transportation Federal Aviation Administration Air Traffic Organization Operations Planning Office of Aviation Research and Development Washington, DC 20591				13. Type of Report and Period Covered Final Report	
				14. Sponsoring Agency Code ANM-100/AME-100	
15. Supplementary Notes The Federal Aviation Administration Aircraft Safety R&D Division COTR was Don Altobelli.					
16. Abstract Under the Federal Aviation Administration Airworthiness Assurance Center of Excellence, and with additional support from the Aircraft Catastrophic Failure Prevention program, Honeywell Engines, Systems & Services collaborated with Arizona State University, SRI International, and the National Aeronautics and Space Administration Glenn Research Center to develop a robust, explicit finite element analysis modeling methodology for gas turbine engines containment systems using multilayer composite fabrics. Honeywell's role was to simulate impact tests using LS-DYNA to validate the fabric material models (Tasks 1 and 2) and to apply the methodologies developed during this program to two engine fan blade containment analyses (Task 4). This report describes the work performed and the results obtained.					
17. Key Words Aircraft engine, Composite fabric, Material modeling, LS-DYNA, Fan containment, Kevlar, Zylon			18. Distribution Statement This document is available to the U.S. public through the National Technical Information Service (NTIS), Springfield, Virginia 22161.		
19. Security Classif. (of this report) Unclassified		20. Security Classif. (of this page) Unclassified		21. No. of Pages 85	22. Price

ACKNOWLEDGEMENTS

The investigator wishes to thank Mr. William Emmerling, Mr. Donald Altobelli, Mr. Chip Queitzsch, and Mr. Jim White of the Federal Aviation Administration for their technical and financial support. To meet the objectives of this project, there was a strong reliance on the technical collaborations with several other organizations that included Arizona State University (ASU), SRI International (SRI), and the National Aeronautics Space Administration Glenn Research Center (NASA-GRC). Some of the individuals who contributed immensely to this project included Dr. Subby Rajan and Dr. Barzin Mobasher of ASU, Dr. Don Shockey, Dr. Jeff Simons, and Mr. Dave Erlich of SRI, and Dr. J. M. Pereira and Mr. Duane Revilock of NASA-GRC; their support and cooperation in meeting the research objectives is greatly appreciated.

The technical support of Mr. Reha Gomuc of Honeywell Engines, Systems and Services was instrumental for the achievements of this project.

TABLE OF CONTENTS

	Page
EXECUTIVE SUMMARY	xv
1. INTRODUCTION	1
1.1 Purpose	1
1.2 Background	1
2. ROBUST FE MODEL DEVELOPMENT (TASK 1)	3
2.1 Objective	3
2.2 Analytical Procedure	3
2.3 The FE Model Description	5
2.4 Analysis Tools	6
2.5 Analysis Results	6
2.5.1 Pretest Ballistic Test Simulations (Task 1.7)	6
2.5.2 Ballistic Test-to-FE Analysis Results Comparison (Task 1.9)	7
2.5.3 Material Model and Methods Update (Task 1.10)	9
2.6 Conclusions for Task 1	20
3. MULTIPLE SHELL-ELEMENT LAYER MODELING (TASK 2)	21
3.1 Background and Objective	21
3.2 Perform Systematic Study—Bound the Problem (Task 2.1.2)	21
3.3 Problem Review With Livermore Software Technology Corporation (Task 2.2)	23
3.4 Demonstrate Results (Task 2.3)	25
3.5 Conclusions for Task 2	36
3.6 Phase II Model Improvements	39
3.7 Recommendations for Tasks 1 and 2	39
4. NUMERICAL SIMULATION OF ENGINE FAN BLADE-OUT TESTS (TASK 4)	39
4.1 Background and Objective	39
4.2 Analytical Procedure	40
4.2.1 Engine Fan Blade-Out Test Results	41

4.2.2	The FE Engine Fan Blade-Out Models	45
4.2.3	Qualitative Comparisons Between the Simulations and Tests	46
4.2.4	The LS-DYNA Simulation Procedure	47
4.3	ANALYSIS RESULTS	49
4.3.1	Results for the HTF7000 Engine Simulations	49
4.3.2	Results for the CFE738 Engine Simulations	57
4.4	Conclusions for Task 4	65
4.5	Generic Engine Fan Blade-Out Containment Model	66
4.5.1	Objective	66
4.5.2	Background	66
4.5.3	Generic Engine Model File Description	67
4.5.4	General Model Recommendations	69
5.	REFERENCES	70

LIST OF FIGURES

Figure		Page
1	Task 1 Process Flow Map	4
2	Honeywell LS-DYNA FE Model of a Ballistic Test With Two Different Projectiles	5
3	Stainless Steel Projectiles	5
4	Coordinate System Used for Definition of Projectile Rotation	6
5	The NASA-GRC Test LG572 Versus Analysis for One FE Shell Layer Simulation, SRI Model, Material Version 3.1	15
6	The NASA-GRC LG572-GIstat Data for One FE Shell Layer Simulation, SRI Model, Material Version 3.1	16
7	The NASA-GRC LG572-Fabric Matsum Data for One FE Shell Layer Simulation, SRI Model, Material Version 3.1	16
8	Simulation Results Showing Velocity Versus Time Compared to Test Final Projectile Velocity for NASA-GRC Test LG403	17
9	Simulation Results Showing Velocity Versus Time Compared to Test Final Projectile Velocity for NASA-GRC Test LG404	17
10	Simulation Results Showing Velocity Versus Time, Compared to Test Final Projectile Velocity for NASA-GRC Test LG411	18
11	Simulation Results Showing Velocity Versus Time Compared to Test Final Projectile Velocity for NASA-GRC Test LG432	18
12	Simulation Results Showing Velocity Versus Time Compared to Test Final Projectile Velocity for NASA-GRC Test LG655	19
13	Simulation Results Showing Velocity Versus Time Compared to Test Final Projectile Velocity for NASA-GRC Test LG657	19
14	Honeywell Generic Engine Model Versions	22
15	Results for Basic Honeywell Generic Engine Model, Three Layers, IHQ = 3, Material Model Version 2.1	24
16	Energy Balance From the GIstat File for Figure 14	25

17	Simulation of NASA-GRC Test LG411—Two FE Shell Layers, Honeywell Model, Material Version 3.1	26
18	The NASA-GRC Test LG411—G1stat Data for the Two FE Shell Layer Simulations, Honeywell Model, Material Version 3.1	27
19	Simulation of NASA-GRC Test LG411—Four FE Shell Layers, Honeywell Model, Material Version 3.1	27
20	The NASA-GRC Test LG411—G1stat Data for the Four FE Shell Layer Simulations, Honeywell Model, Material Version 3.1	28
21	Simulation of NASA-GRC Test LG411—Eight FE Shell Layers, Honeywell Model, Material Version 3.1	28
22	The NASA-GRC Test LG411—G1stat Data for the Eight FE Shell Layer Simulations, Honeywell Model, Material Version 3.1	29
23	Simulation of NASA-GRC Test LG411—12 FE Shell Layers, Honeywell Model, Material Version 3.1	29
24	The NASA-GRC Test LG411—G1stat Data for the 12 FE Shell Layer Simulations, Honeywell Model, Material Version 3.1	30
25	Simulation of NASA-GRC Test LG411—24 Shell Layers, Honeywell Model, Material Version 3.1	30
26	The NASA-GRC Test LG411—G1stat Data for the 24 FE Shell Layer Simulations, Honeywell Model, Material Version 3.1	31
27	The FE Model of the Honeywell Basic Generic Blade Containment Model	31
28	Ballistic Test Case Simulations Results Showing Velocity Versus Time Compared to Test Final Projectile Velocity for NASA-GRC Test LG411	34
29	Ballistic Test Case Simulations Results Showing Velocity Versus Time Compared to Test Final Projectile Velocity for NASA-GRC Test LG655	34
30	Ballistic Test Case Simulations Results Showing Velocity Versus Time Compared to Test Final Projectile Velocity for NASA-GRC Test LG657	35
31	Velocity Plots for Simulations Using the Basic Generic Blade Containment Model	35
32	Material Model Calibration Thought Process Map	38
33	The HTF7000 Honeywell Turbofan Engine Overall View	41

34	The HTF7000 Fan Containment Housing Following Blade-Out Test	42
35	The CFE738 Turbofan Engine Overall View	43
36	The CFE738 Fan Containment Housing Following Blade-Out Test, Internal View	43
37	The CFE738 Trailing Fan Blade Damage After the Fan Blade-Out Test	44
38	The CFE738 Fan Containment Housing Following Blade-Out Test, External View	44
39	The HTF7000 LS-DYNA Model for Fan Blade-Out Containment Analysis	45
40	The CFE738 LS-DYNA Model for Fan Blade-Out Containment Analysis	46
41	The HTF7000 Fan Blade-Out Simulation Results of Phase I	47
42	The HTF7000 Engine Blade Orientation and Deformed Blade Prediction for Simulation Using One Kevlar Shell Layer With Wetted Ends, Material Model Version 2.1, and Individual Contact Cards	50
43	The HTF7000 Engine Fabric Aspect Showing Penetration for Simulation Using One Kevlar Shell Layer With Wetted Ends, Material Model Version 2.1, and Individual Contact Cards	50
44	The HTF7000 Engine Global G1stat Data for Simulation Using One Kevlar Shell Layer With Wetted Ends, Material Model Version 2.1, and Individual Contact Cards	52
45	The HTF7000 Engine Fabric Matsum Data for Simulation Using One Kevlar Shell Layer With Wetted Ends, Material Model Version 2.1, and Individual Contact Cards	52
46	The HTF7000 Engine Blade Kinetic Energy Data for Simulations Using One Kevlar Shell Layer and Material Model Version 2.1	53
47	The HTF7000 Engine Fabric Aspect for Simulation Using One Kevlar Shell Layer, Material Model Version 3.1, Individual Contact Cards With Friction, and IHQ = 4	53
48	The HTF7000 Engine Global G1stat Data for Simulation Using One Kevlar Shell Layer, Material Model Version 3.1, Individual Contact Cards With Friction, and IHQ = 4	54
49	The HTF7000 Engine Fabric Matsum Data for Simulation Using One Kevlar Shell Layer, Material Model Version 3.1, Individual Contact Cards With Friction, and IHQ = 4	54

50	The HTF7000 Engine Fabric Aspect for Simulation Using Three Kevlar Shell Layers, Material Model Version 3.1, Individual Contact Cards With Friction, and IHQ = 3	55
51	The HTF7000 Engine Global Gstat Data for Simulation Using Three Kevlar Shell Layers, Material Model Version 3.1, Individual Contact Cards With Friction, and IHQ = 3	55
52	The HTF7000 Engine Fabric Matsum Data for Simulation Using Three Kevlar Shell Layers, Material Model Version 3.1, Individual Contact Cards With Friction, and IHQ = 3	56
53	The HTF7000 Engine Blade Kinetic Energy Data for Simulations Using Kevlar Material Model Versions 2.1 and 3.1, and Single and Multiple Shell Layers	57
54	The CFE738 Engine Blade Orientation and Deformed Trailing Blade for Simulation Using One Kevlar Shell Layer, Material Model Version 2.1, Individual Contact Cards, No Friction, and IHQ = 3	58
55	The CFE738 Engine Fabric Aspect for Simulation Using One Kevlar Shell Layer, Material Model Version 2.1, Individual Contact Cards, No Friction, and IHQ = 3	58
56	The CFE738 Engine Global Gstat Data for Simulation Using One Kevlar Shell Layer, Material Model Version 2.1, Individual Contact Cards, No Friction, and IHQ = 3	59
57	The CFE738 Engine Fabric Matsum Data for Simulation Using One Kevlar Shell Layer, Material Model Version 2.1, Individual Contact Cards, No Friction, and IHQ = 3	59
58	The CFE738 Engine Fabric and Blade Aspect for Simulation Using One Kevlar Shell Layer, Material Model Version 3.1, Individual Contact Cards With Friction, and IHQ = 4	61
59	The CFE738 Engine Global Gstat Data for Simulation Using One Kevlar Shell Layer, Material Model Version 3.1, Individual Contact Cards With Friction, and IHQ = 4	61
60	The CFE738 Engine Fabric Matsum Data for Simulation Using One Kevlar Shell Layer, Material Model Version 3.1, Individual Contact Cards With Friction, and IHQ = 4	62
61	The CFE738 Engine Fabric and Blade Aspect for Simulation Using Four Kevlar Shell Layers, Material Model Version 3.1, Individual Contact Cards With Friction, and IHQ = 4	62

62	The CFE738 Engine Close-Up of the Damaged Fabric in the Blade-Out Test Containment Housing	63
63	The CFE738 Engine Global G1stat Data for Simulation Using Four Kevlar Shell Layers, Material Model Version 3.1, Individual Contact Cards With Friction, and IHQ = 4	63
64	The CFE738 Engine Fabric Matsum Data for Simulation Using Four Kevlar Shell Layers, Material Model Version 3.1, Individual Contact Cards With Friction, and IHQ = 4	64
65	The CFE738 Engine Blade Kinetic Energy Data for Simulations Using Kevlar Material Model Versions 2.1 and 3.1, and Single and Multiple Shell Layers	64
66	Generic Engine Fan Blade Containment Model	67

LIST OF TABLES

Table		Page
1	Honeywell Pretest Ballistic Simulation Results Summary	7
2	Differences Between SRI and Honeywell Contact Formulation in the Ballistic Model	8
3	Measured Results of the NASA-GRC Ballistic Tests for all Cases Using Kevlar	10
4	The ASU, Honeywell, and SRI Simulation Results for Kevlar Material Model Version 3.1 Using SRI FE Model	10
5	The ASU, Honeywell, and SRI Simulation Results for Kevlar Material Model Versions 2.1 and 3.1 Using Both SRI and Honeywell Models	14
6	The ASU, Honeywell, and SRI Simulation Results, Kevlar Material Model Versions 3.1 and 2.1, Both SRI and Honeywell Ballistic Models	32

LIST OF ACRONYMS AND DEFINITIONS

ASU	Arizona State University
FAA	Federal Aviation Administration
FD	Dynamic coefficient of friction (card 2 of CONTACT card)
FE	Finite element
FS	Static coefficient of friction (card 2 of the CONTACT card)
Glstat	ASCII output file that stores total energies during an LS-DYNA simulation
IHQ	Hourglass viscosity type in the CONTROL_HOURLASS card
LS-DYNA	Finite element code used primarily for dynamic modeling
LSTC	Livermore Software Technology Corporation
Matsum	ASCII output file that stores material energies during simulation
NASA-GRC	National Aeronautics and Space Administration Glenn Research Center
SFS	Penalty stiffness scale factor
SRI	SRI International
TSSFAC	Time-step scale factor

EXECUTIVE SUMMARY

A team consisting of Arizona State University (ASU), Honeywell Engines, Systems & Services (Honeywell), the National Aeronautics and Space Administration Glenn Research Center (NASA-GRC), and SRI International (SRI) collaborated to develop computational models and verification testing for designing and evaluating turbine engine fan blade fabric containment structures. This research was conducted under the Federal Aviation Administration Airworthiness Assurance Center of Excellence and sponsored by the Aircraft Catastrophic Failure Prevention Program. The research was directed towards improving the modeling of a turbine engine fabric containment structure for an engine blade-out containment demonstration test required for certification of aircraft engines.

In Phase I, progress was made in testing and computational analysis. A material model was developed for Kevlar[®] and Zylon[®] fabrics. Static tests of containment wraps subjected to loads through a blunt-nose impactor were performed at ASU. Ballistic tests of containment wraps subjected to a high-velocity blunt projectile were performed at NASA-GRC. These tests provided test cases (benchmark results) to validate the developed finite element (FE) methodology. While the work performed in Phase I met the stated objectives, improvements in robustness and confidence of the FE simulations and predictions were desired.

The research conducted in Phase II brought a new level of capability to designing and developing fan blade containment systems for turbine engines. To achieve the program objectives, a program plan consisting of the following four technical tasks was developed and implemented:

- Task 1: Robust FE Model Development. The objective of this task was to increase confidence and robustness in the material models for the Kevlar and Zylon material models developed in Phase I.
- Task 2: Improve FE Modeling Capability for Multiple Layers of Fabric. In Phase I, most of the LS-DYNA[®] models used a single-element through the thickness to model the fabric, ranging from 1 to 24 layers.
- Task 3: 1500 denier (D) Zylon Material Model Development. In Phase I, limited ballistic and static tests of 1500 D Zylon indicated this configuration of Zylon might have the potential to offer a 60-percent weight advantage over a similar configuration of Kevlar 49 fabric for the same fragment energy. The objective of this task was to develop and validate a material model for 1500 D Zylon. It should be noted that during this research, it was discovered that Zylon was found to have excessive deterioration due to heat and humidity. As a result, it was decided that the remainder of this research would focus only on Kevlar fabrics.
- Task 4: Engine Simulations. As in Phase I, the objective of this task was to validate improvements to the material models and FE methods developed under Phase II as they relate to propulsion engine fan blade containment. Existing fabric material model and

modeling methods and their improvements will be validated using fan containment test data.

Each member of the team developed a comprehensive report describing the details of the research task and the findings. The comprehensive report consists of the following four report parts:

- Arizona State University Department of Civil Engineering, Part 1: Fabric Material Tests
- NASA-Glenn Research Center, Part 2: Ballistic Impact Testing
- SRI International, Part 3: Material Model Development and Simulation of Experiments
- Honeywell Engines, Systems & Services, Part 4: Model Simulation for Ballistic Tests, Engine Fan Blade-Out, and Generic Engine

Honeywell's role in this project was to incorporate the fabric material models (produced by SRI) into the LS-DYNA finite element (FE) program, to simulate ballistic tests with LS-DYNA to validate the fabric material models, and to apply the methodologies developed during this program to two, full-scale, engine fan blade containment analyses. This report (part 4) describes work performed under Contract No. 01-C-AW-ASU, Subagreement 04-441-13, (Tasks 1, 2, 3, and 4) during the period September 2004 through June 2007 and the results of the analytical simulations.

Overall, the analytical results correlated with the ballistic test results. Acceptable correlation was obtained between the simulation and ballistic test results for Kevlar using both single or multiple shell-element layer approaches for simulating all the fabric layers. The energy absorption of the fabric systems was successfully simulated. The overall deflection behavior was acceptable. Similar, successful analysis-to-test correlations were also obtained when up to four layers of shell elements were used to model all fabric layers. The sensitivity of the results to analysis parameters and solution algorithms, and to the program version and computer platform choices is discussed.

In addition, two, full-scale engine fan blade-out events were successfully simulated using the fabric material models and the developed analytical methodologies. Acceptable correlation was obtained between the simulation results and the engine containment test results using the new Kevlar model and both the single and multiple shell layer modeling techniques.

Based on the experience gained during the execution of the above simulations, a generic engine fan blade-out containment FE model, including fabric wraps, was created. The purpose of this model was to provide LS-DYNA users with generic guidelines for modeling fabric wraps in fan blade containment-related applications.

1. INTRODUCTION.

1.1 PURPOSE.

The primary focus of this research was to address the technology gaps in containment events simulation and to develop a robust modeling methodology for the analysis of a fan blade-out event in a multilayer fabric containment system. Specific program objectives were to:

- Combine the LS-DYNA[®] modeling expertise of Honeywell Engines, Systems & Services (Honeywell) with the material modeling capability of SRI International (SRI), the ballistic testing capabilities of National Aeronautics Space Administration Glenn Research Center (NASA-GRC), and the experimental facilities and finite element (FE) analysis and modeling capabilities of Arizona State University (ASU).
- Incorporate the material models (developed by SRI) into the LS-DYNA modeling methodology (developed by Honeywell), and correlate with the results from controlled laboratory hardware tests, and then develop new methodologies, if necessary.
- Develop methodologies for numerical simulation of engine fan blade-out events with fiber fabric wraps using SRI's material models and Honeywell's LS-DYNA modeling methodology. Validate the methodologies using existing engine fan blade-out containment test results from Honeywell.
- Compare the efficiency of Kevlar[®] and Zylon[®] wraps through laboratory hardware tests and LS-DYNA analysis of the test coupons.
- Explore the potential of 1500 denier (D) Zylon for future gas turbine engine containment systems.

During this study, the planned development of Zylon material models was suspended due to potential material strength degradation issues under environmental conditions. Funding was redirected toward completion of Tasks 1 and 2 with Kevlar material.

1.2 BACKGROUND.

Fiber fabric wraps are widely used in the containment systems of aerospace gas turbine engines. Such systems are especially cost-effective for containing engine debris during a possible engine fan blade-out event. Compared to traditional metallic containment systems, fabric wrap systems have very high strength per unit weight properties and are inexpensive to manufacture.

LS-DYNA is a commercial, FE program widely used in the analysis of gas turbine engine rotor containment applications. This program was used successfully at Honeywell as an analysis tool to design and optimize containment structures. Although there are challenges involved due to the complexity of these types of analyses, many successful modeling experiences exist, especially for containment systems using metallic materials. On the other hand, the modeling and analysis of a typical fan blade-out event in a multilayer, fiber fabric containment system has

always been a difficult task, mainly due to the lack of accurate, numerical, modeling techniques and material formulations. To properly take advantage of the fabric containment systems, it is necessary to have a robust, FE analysis modeling methodology that integrates the representative material behavior and the problem-specific analysis techniques. The resulting tool can then be used to analyze and optimize the performance of the fabric-based containment systems.

Progress was made in Phase I that addressed the above-mentioned issues [1-4]. The combined efforts of Honeywell, SRI, NASA-GRC, and ASU resulted in the following major accomplishments:

- A fabric material model was developed for Kevlar and Zylon fabrics. Independent laboratory tests conducted at ASU and SRI formed the basis of this model. These material models were general enough to be used as the constitutive model for both static and dynamic and explicit FE analyses.
- Static tests of containment wraps subjected to loads through a blunt-nose impactor were conducted at ASU. Ballistic tests (conducted at NASA-GRC) of containment wraps subjected to a high-velocity projectile provided test cases (benchmark results) to validate the developed FE methodology.
- The material models (developed in Phase I, Task 1) were used by the research team in the FE simulation of static and ballistic tests. The static test results were validated by ASU using the ABAQUS FE program. The ballistic test results were validated by Honeywell and SRI using the LS-DYNA FE program.
- The knowledge gained from Phase I, Tasks 1-3 was used by Honeywell for the numerical simulation of engine fan blade-out events involving existing production engine models and was compared to the test results (employing Kevlar containment).
- An understanding of the relative comparison between Kevlar and Zylon materials in turbine engine blade-out containment systems was achieved.

It was clear from Phase I that the developed FE analysis procedure provides a reliable simulation of the various tests, including actual engine fan blade-out events. While the work performed in Phase I met the stated objectives, the confidence of the FE simulations and predictions needed to increase.

For Phase II, the research was divided into four major tasks:

- Task 1: Robust FE Model Development. The objective of this task was to increase confidence in the material models for 1420 D Kevlar 49 17x17 (Kevlar) and 500 D Zylon AS 35x35 (Zylon), and to increase confidence that these models and methodologies, which were developed previously, could accurately predict off-design conditions.

- Task 2: Improve FE Modeling Capability for Multiple Layers of Fabric. In Phase I, most LS-DYNA models used a single shell FE through the thickness of the fabric to model the fabric, which ranged from 1 to 24 layers (wraps). Although this technique is simple, it does not provide the predictive capability of computing the number of penetrated fabric layers during a containment event. Therefore, the containment margin (in terms of the number of unpenetrated layers versus total number of layers) cannot be accurately predicted. The objective of Task 2 was to improve the modeling capability for multiple layers of fabric using multiple layers of shell elements.
- Task 3: 1500 D Zylon Material Model Development. In Phase I, limited ballistic and static tests of 1500 D Zylon (17x17 weave) indicated that 1500 D Zylon potentially offers a 60-percent weight advantage over Kevlar for the same fragment energy. 1500 D Zylon seemingly enables either a dramatic increase in fan containment safety margin, a decrease in engine weight, or a combination of both. The objective of Task 3 was to develop and validate a material model for 1500 D Zylon.
- Task 4: Engine Simulation. As in Phase I, the objective of Task 4 was to validate improvements to the material models and FE methods developed under this program as they relate to propulsion engine fan blade containment. Existing fabric material models and modeling methods, along with improvements to the material models and methods, were validated using fan containment test data.

2. ROBUST FE MODEL DEVELOPMENT (TASK 1).

2.1 OBJECTIVE.

The objective of Task 1 was to increase confidence in the material models for Kevlar and Zylon, and to increase the confidence that these models and single shell-element layer methodologies, which were previously developed for straight (zero degree pitch and yaw) projectile ballistic tests, can accurately predict ballistic tests using rotated projectiles (shot at an angle).

2.2 ANALYTICAL PROCEDURE.

The existing LS-DYNA, user-defined, material model for fabrics is based on two submodels: the material model and the failure model. The material model relates the stresses and strains and is based on the results of simple tension and compression tests. The failure model is strain-based and depends on the results of high strain rate tensile tests. SRI and ASU were tasked to develop new material models by performing various tests and LS-DYNA simulations. The objective of Task 1 was to compare the results of the FE ballistic test simulations to the ballistic test results using the latest material models.

To achieve that objective, Honeywell simulated the Kevlar and Zylon ballistic tests conducted at NASA-GRC using various prototype material models and compared the simulation results to the actual test results. The detailed steps for the correlation efforts are below. Figure 1 schematically illustrates the overall process followed during the execution of Task 1.

1. Honeywell conducted pretest simulations of the proposed ballistic tests using the fabric material model developed in Phase I (version 1.0). The purpose of this task was to assess the best way to test the fabric and determine the desired projectile velocity.
2. ASU and SRI developed new material models (versions 2.1, 3.0, and 3.1) using the methodology described in Phase II Parts 1 and 3 (ASU and SRI, respectively).
3. The ballistic tests were conducted at NASA-GRC and the details of the test procedures and results are reported in Phase II Part 2.
4. A fabric material model code (common for Kevlar and Zylon and provided by SRI) was compiled with the standard LS-DYNA binary files to obtain a user-defined executable. The typical LS-DYNA input deck included: the model file (FE nodes and elements), the user-controlled material input parameters (different sets for Kevlar and Zylon), the contact file defining the contact types to be used, and the control parameters required to run the LS-DYNA code.
5. Each test condition was properly simulated by changing input parameters, such as the fabric material constants, the projectile speed, and the number of fabric layers.
6. Similar to work performed in Phase I, the energy absorbed by the fabric system and the general behavior of the test specimen were compared. Recommendations for further material model and methodologies development were made based on the level of correlation between the analyses and the test results.

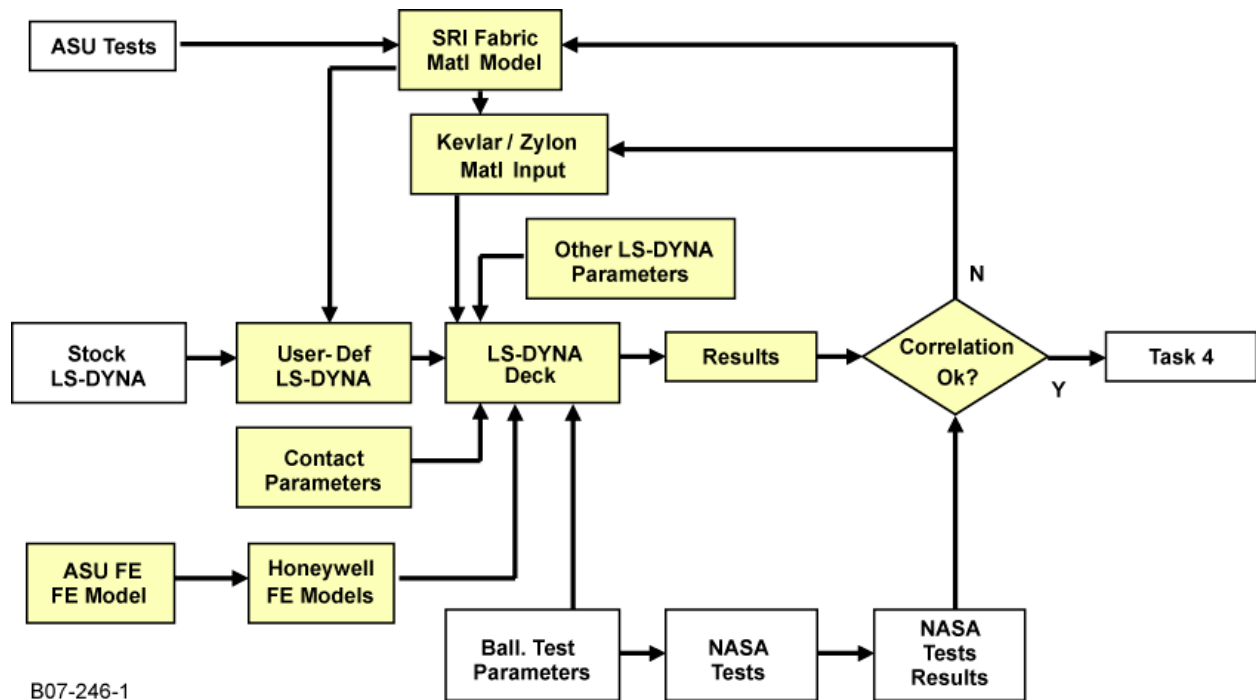


Figure 1. Task 1 Process Flow Map

2.3 THE FE MODEL DESCRIPTION.

In Phase I, ballistic tests and their respective simulations were conducted for one projectile orientation (straight) and one specific projectile design. For Phase II, ballistic tests in Task 1 were conducted by NASA-GRC with different projectile roll, pitch, and yaw orientations and two projectile configurations. The previous “old” (referred to as projectile A) and current “new” (referred to as projectile B) configurations of the projectile are shown in figures 2 and 3. The new blunt-nose configuration has the same mass and impact energy as the old (Phase I) projectile. The detailed description of the test setup can be found in Part 2 (NASA-GRC) of this four-part report.

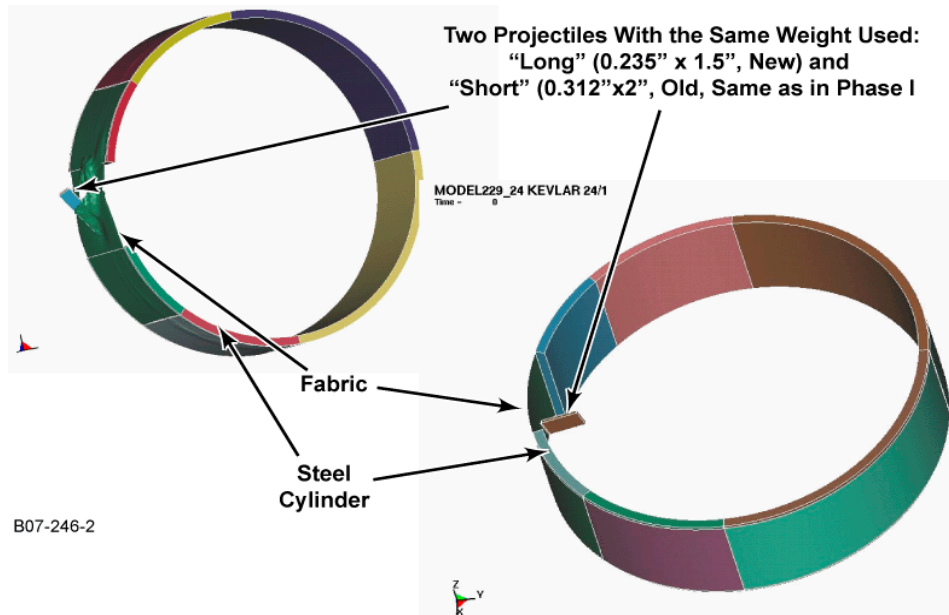


Figure 2. Honeywell LS-DYNA FE Model of a Ballistic Test Showing Two Different Projectiles



Figure 3. Stainless Steel Projectiles (Left View—Projectile A; Right View—Projectile B)

2.4 ANALYSIS TOOLS.

The same version of the LS-DYNA software was used throughout this project, unless otherwise specified. This type of analysis, which involves high nonlinearities, failure, and contact interactions, is sensitive to program version, the computer platform used, the number of microprocessor(s) and/or type(s), and the operating system. To ensure consistency of the results, the following parameters were intentionally kept constant during this project:

- Standard LS-DYNA file: ls970_d_5434_ibm : LS-DYNA SMP Version 970, Revision 5434a (double precision)
- IBM 275 UNIX machines with operating system version 10.2, single or dual processor

2.5 ANALYSIS RESULTS.

2.5.1 Pretest Ballistic Test Simulations (Task 1.7).

An initial set of pretest simulations of the proposed ballistic tests was performed by Honeywell using the fabric material model version 1.0 (developed in Phase I) along with the single shell methodology of Phase I. Similar to Phase I, the energy absorbed by the fabric system and the general behavior of the test specimen were predicted.

The coordinate system used for projectile rotation, in both test and simulations, was agreed upon between NASA-GRC and Honeywell (see figure 4). The pretest simulations were used to determine which rotations to perform first and which direction of rotation (roll, pitch, or yaw) produced a more significant effect on the fabric failure mechanism. For the 32-layer tests, Honeywell provided an estimated projectile velocity, prior to the tests at NASA-GRC, based on a set of simulations with various velocities. The results of the pretest simulations are shown in table 1.

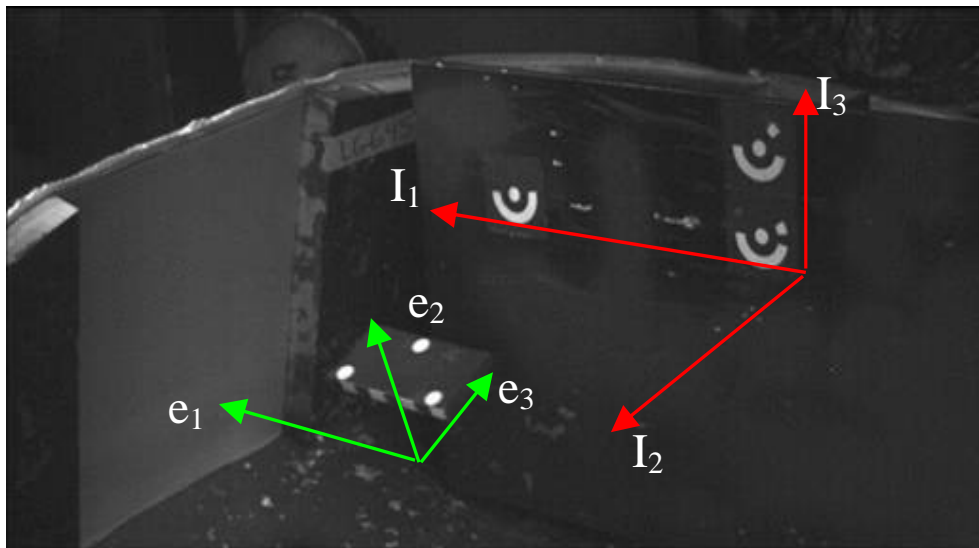


Figure 4. Coordinate System Used for Definition of Projectile Rotation

Table 1. Honeywell Pretest Ballistic Simulation Results Summary

Task No.	Model No.	Fabric Layers	Fabric	Penetrator	Roll (degrees)	Yaw (degrees)	Observations	Impact Velocity (ft/sec)	Impact Energy (in.*lb)	Exit Energy (in.*lb)	Absorbed Energy in.*lb
1.7.2.1	1	8	Kevlar	Old	0	0		875	103030	84188	18842
	2	2	Kevlar	Old	0	0		345	16040	8817	7223
	3	4	Kevlar	Old	0	0		904	110150	99196	10954
	4	8	Kevlar	Old	0	45		875	103030	81150	21880
	5	8	Kevlar	Old	0	90	Bending proj.	875	103040	55132	47908
	6	8	Kevlar	Old	45	0		875	103030	91828	11202
	7	8	Kevlar	Old	45	45	Roll first	875	103030	65525	37505
	8	8	Kevlar	Old	45	90	Roll first	875	103030	86407	16623
	9	8	Kevlar	Old	90	0		875	103030	92241	10789
	10	8	Kevlar	Old	90	45	Roll first	875	103030	80412	22618
	11	8	Kevlar	Old	90	90	Roll first	875	103030	82663	20367
	12	8	Kevlar	New	0	0		875	105410	90633	14777
	13	8	Kevlar	New	0	45	Bending proj.	875	105410	75289	30121
	14	8	Kevlar	New	0	90		875	105410	40104	65306
	15	8	Kevlar	New	45	0		875	105410	94467	10943
	16	8	Kevlar	New	45	45	Roll first	875	105410	81665	23745
	17	8	Kevlar	New	45	90	Roll first	875	105410	53967	51443
	18	8	Kevlar	New	90	0		875	105410	96700	8710
	19	8	Kevlar	New	90	45	Roll first	875	105410	84873	20537
	20	8	Kevlar	New	90	90	Part. Cont.	875	105410	40275	65135
1.7.2.2	21	8	Zylon	Old	0	0		904	110150	92258	17892
	22	4	Zylon	Old	0	0		891	110150	98095	12055
	23	8	Zylon	Old	0	45		904	110150	85050	25100
	24	8	Zylon	Old	0	90		904	110160	47872	62288
	25	8	Zylon	Old	45	0		904	110150	100000	10150
	26	8	Zylon	Old	45	45	Roll first	904	110150	77290	32860
	27	8	Zylon	Old	45	90	Roll first	904	103030	83536	19494
	28	8	Zylon	Old	90	0		904	110150	98404	11746
	29	8	Zylon	Old	90	45	Roll first	904	110150	85804	24346
	30	8	Zylon	Old	90	90	Roll first	904	110150	75469	34681
	31	8	Zylon	New	0	0		904	112480	95986	16494
	32	8	Zylon	New	0	45		904	112690	80894	31796
	33	8	Zylon	New	0	90	Part. Cont.	904	111840	46976	64864
	34	8	Zylon	New	45	0		904	112520	102860	9660
	35	8	Zylon	New	45	45	Roll first	904	112310	93043	19267
	36	8	Zylon	New	45	90	Roll first	904	112700	68599	44101
	37	8	Zylon	New	90	0		904	112700	102710	9990
	38	8	Zylon	New	90	45	Roll first	904	112700	85312	27388
	39	8	Zylon	New	90	90	Part. Cont.	904	112700	56001	56699
	40	32	Kevlar	Old	0	0		1000	131480	32241	99239
	41	32	Zylon	Old	0	0		1150	178210	39617	138593
	42	8	Kevlar	Old	45	45	Yaw first	875	103030	87612	15418
	43	8	Kevlar	Old	90	90	Yaw first	875	103030	84629	18401
	44	8	Kevlar	New	45	45	Yaw first	875	105410	82532	22878
	45	8	Kevlar	New	90	90	Yaw first	875	105410	56251	49159
	46	8	Zylon	Old	45	45	Yaw first	904	110150	95534	14616
	47	8	Zylon	Old	90	90	Yaw first	904	110150	76144	34006
	48	8	Zylon	New	45	45	Yaw first	904	112700	90339	22361
	49	8	Zylon	New	90	90	Yaw first	904	112700	60152	52548

Part. Cont. = Partially contained
 Bending proj. = Bending projectile observations

2.5.2 Ballistic Test-to-FE Analysis Results Comparison (Task 1.9).

Phase I used only Honeywell-developed LS-DYNA models and methodology for simulation. For Phase II, Task 1, SRI-developed models and methodology were also considered. The SRI FE model has three notable minor differences when compared to the Honeywell model: (1) the fabric is straight in the contact area, (2) the ring/projectile mesh is more refined, and (3) the projectile has a rounded tip. The differences in the LS-DYNA contact formulation are shown in table 2; the main difference is the use of a single contact card for the whole model in the SRI version, versus a contact card for each part in contact in the Honeywell version. A comparison showing minor differences between the two models in ballistic test simulations is detailed in Part

I (ASU) of this report. SRI developed single and multiple FE shell-element layer models. One FE shell-element layer was used to simulate four fabric wraps. This approach was used to model 4, 8, 16, 24, and 32 fabric wraps.

Table 2. Differences Between SRI and Honeywell Contact Formulation in the Ballistic Model

Definition	SRI	Honeywell
Fabric		
	HOURGLASS	HOURGLASS
IHQ	2 (viscous form hourglass control)	4 (stiffness form hourglass control)
QM	0.15 (membrane hourglass coefficient)	0.1 (hourglass coefficient - default)
QB, QW	0.0 (bending/warping hourglass coefficient)	0.1 (should equal QM)
Metal		
	HOURGLASS	HOURGLASS
IHQ	4 (stiffness form hourglass control)	4 (stiffness form hourglass control)
QM	0.0 (hourglass coefficient)	0.1 (hourglass coefficient - default)
IBQ	0 (bulk viscosity type for solids only)	1 (bulk viscosity type - for solids only - default)
QB, QW	0.0 (bending/warping hourglass coefficient)	0.1 (should equal QM)
	CONTACT_ERODING_SINGLE_SURFACE_ID	CONTACT_AUTOMATIC_SURFACE_TO_SURFACE
Card 1		
SSTYP	5 (include all)	3 (Part identification)
Card 2		
FS	0.2 (static friction coefficient)	0
FD	0.2 (dynamic friction coefficient)	0
DT	0.0 (death time)	1.00E+20
Card 3		
SFS	1.0 (scale factor on penalty stiffness - default))	0.1
SFM	1.0 (scale factor on penalty stiffness)	0.1
SFST	0.0 (scale true thickness)	1.0 (default)
SFMT	0.0 (scale true thickness)	1.0 (default)
Card A		
SOFSCCL	0.02	0.1 (default) (not used for SOFT=2)
IGAP	1	2
	DAMPING_PART_STIFFNESS	
COEF	0.25	not used
	CONTROL_SHELL	
THEORY	2	2
	CONTROL_ENERGY	
HGEN	0	2 (hourglass energy is computed)
	CONTROL_TIMESTEP	
TSSFAC	0.0 (scale factor for computed time step)	0.9

The material model for Kevlar version 1.0, developed in Phase I, was improved during Phase II to version 2.1. Due to a minor change in the material model algorithm, a limited set of simulations was initially run using Honeywell models for ballistic tests (from Phase I), to confirm that version 2.1 produced similar results.

A new material model, version 3.0, was developed by SRI using results of the tensile and high strain-rate tests (performed by ASU and SRI, respectively) during Phase II. All team members (ASU, SRI, and Honeywell) simulated the NASA-GRC ballistic tests presented in Part 2 of Phase II, using the material model version 3.0 for Kevlar and Zylon. The SRI-developed models that were used followed the approach of one FE shell-element layer to simulate four fabric wraps. The comparison was unsuccessful, as the absorbed energy of the simulation did not match the absorbed energy measured during the tests.

2.5.3 Material Model and Methods Update (Task 1.10).

The initially unsuccessful material model version 3.0 was improved to version 3.1. The details of the material model development are explained in Part 3 (SRI) of Phase II. Simulations of ballistic tests using Kevlar were performed using material model version 3.1 and the two similar LS-DYNA FE models developed by Honeywell and SRI.

Each member of the team simulated a set of ballistic tests, and several tests were simulated by all the members to verify platform and operating system consistency. Honeywell used the UNIX operating system and double precision, ASU used Windows[®] XP[®] and single precision, and SRI used a double-precision Linux operating system. All members used LS-DYNA, SMP version 970, release 5434a.

SRI models with single and multiple layers were used for simulations of Kevlar ballistic tests from Phase I (cases LG403, LG404, LG411, LG432 and LG572) and Phase II (cases LG594, LG609, LG610, LG611, LG612, LG618, LG620, LG655, LG657, LG688, LG689, LG692 and LG694). As previously mentioned, these models use one FE shell-element layer to simulate four fabric wraps, resulting in both single and multiple shell-element layer models, depending on the actual number of fabric wraps for each test case. NASA-GRC ballistic test results for these cases are shown in table 3. The absorbed kinetic energy of the simulations was compared to the absorbed kinetic energy measured during the tests (table 4) for all cases simulated using material version 3.1 and the SRI-developed models. A visual comparison of the fabric deformation results of the LS-DYNA simulations versus fabric deformation during the test was also performed.

Table 3. Measured Results of the NASA-GRC Ballistic Tests for all Cases Using Kevlar

NASA-GRC Test No.	Projectile Type ¹	Fabric Layers	Rotation Angle ²			Before Impact		After Impact		Absorbed Energy	
			Pitch (deg)	Roll (deg)	Yaw (deg)	Velocity (ft/sec)	Energy (ft*lb)	Velocity (ft/sec)	Energy (ft*lb)	Energy (ft*lb)	%
LG403	Old	4	0	0	0	899.0	105785	846.5	93791	11994	11.3
LG404	Old	8	0	0	0	895.7	104816	820.2	87899	16917	16.1
LG411	Old	24	0	0	0	885.8	101557	413.4	22117	79440	78.2
LG432	Old	16	0	0	0	895.7	105542	649.6	55517	50024	47.4
LG572	Old	2	21	0	13	346.6	16006	295.0	11591	4415	27.6
LG609	New	8	0.87	37.4	1.63	913.7	107185	825.4	87470	19715	18.4
LG610	New	8	0.7	25.3	11.9	888.1	101257	809.7	84168	17089	16.9
LG611	Old	8	-1.7	30.9	-11	905.7	109290	798.1	84858	24432	22.4
LG612	Old	8	-3.7	22.8	-0.5	898.3	107504	822.7	90187	17317	16.1
LG618	New	8	6.31	-47	51.6	866.4	96375	558.9	40105	56271	58.4
LG655	Old	32	1.29	-32	2.57	1131.7	170651	830.6	91921	78730	46.1
LG656	Old	32	-2.3	8.98	-10	967.3	124670	469.2	29337	95333	76.5
LG657	Old	32	9.73	-22	1.42	829.7	91724	0.0	0	91724	100.0
LG688	Old	8	-21	10.5	62.8	870.9	101064	549.3	40207	60858	60.2
LG692	Old	8	2.31	38.2	41.5	885.3	104432	602.6	48376	56055	53.7
LG594	New	8	6.6	27	47.8	843.9	89810	484.5	29606	60204	67.0
LG689	Old	8	-1.3	-13	49.7	896.3	106751	655.1	57029	49722	46.6
LG620	New	8	0.18	-38	55.1	893.8	103861	580.8	43849	60011	57.8

¹Refers to projectile shape, see figure 2.

²0/0/0 refers to straight projectile.

Table 4. The ASU, Honeywell, and SRI Simulation Results for Kevlar Material Model Version 3.1 Using SRI FE Model

NASA-GRC Test No.	Run By	FE Shell Layers	Before Impact		After Impact		Absorbed Energy		Difference vs Test (%)
			Velocity (ft/sec)	Energy (ft*lb)	Velocity (ft/sec)	Energy (ft*lb)	Energy (ft*lb)	(%)	
LG403	ASU	1	900.0	106032	856	95806	10226	9.6	1.7
	HON	1	900.0	106032	853	95162	10870	10.3	1.1
	SRI	1	900.0	106032	855	95712	10320	9.7	1.6
LG404	ASU	1	896.7	105048	809	85447	19601	18.7	-2.5
	ASU	2	896.7	105048	803	84339	20709	19.7	-3.6
	HON	1	896.7	105048	809	85496	19553	18.6	-2.5
	HON	2	896.7	105048	811	85968	19080	18.2	-2.0
	SRI	2	896.7	105048	809	85496	19553	18.6	-2.7

Table 4. The ASU, Honeywell, and SRI Simulation Results for Kevlar Material Model Version 3.1 Using SRI FE Model (Continued)

NASA-GRC Test No.	Run By	FE Shell Layers	Before Impact		After Impact		Absorbed Energy		Difference vs Test (%)
			Velocity (ft/sec)	Energy (ft*lb)	Velocity (ft/sec)	Energy (ft*lb)	Energy (ft*lb)	(%)	
LG411	ASU	1	885.8	101558	540	37718	63840	62.9	15.4
	ASU	6	885.8	101558	536	37175	64383	63.4	14.8
	HON	1	885.8	101558	539	37625	63932	63.0	15.3
	HON	6	885.8	101558	557	40148	61410	60.5	17.8
	SRI	6	885.8	101558	508	33422	68136	67.1	11.1
LG432	ASU	1	895.8	105578	680	60816	44763	42.4	5.0
	ASU	4	895.8	105578	671	59227	46352	43.9	3.5
	HON	1	895.8	105578	694	63449	42129	39.9	7.5
	HON	4	895.8	105578	677	60309	45269	42.9	4.5
	SRI	4	895.8	105578	676	60032	45547	43.1	4.3
LG572	ASU	1	346.7	16012	292	11343	4669	29.2	-1.6
	HON	1	346.7	16012	293	11415	4597	28.7	-1.1
	SRI	1	346.6	16006	292	11322	4685	29.3	-1.7
LG609	ASU	1	913.4	107103	841	90738	16365	15.3	3.1
	ASU	2	913.4	107103	840	90622	16481	15.4	3.0
	HON	1	913.3	107087	838	90228	16859	15.7	2.7
	HON	2	913.3	107087	840	90672	16415	15.3	3.1
	SRI	2	913.3	107087	842	91019	16068	15.0	3.4
LG610	ASU	1	888.4	101322	790	80118	21204	20.9	-4.1
	ASU	2	888.4	101322	792	80486	20836	20.6	-3.7
	HON	1	888.3	101311	790	80185	21126	20.9	-4.0
	HON	2	888.3	101311	791	80276	21035	20.8	-3.9
	SRI	2	888.3	101311	785	79113	22198	21.9	-5.1
LG611	ASU	1	905.8	109325	786	82305	27019	24.7	-2.4
	ASU	2	905.8	109325	791	83448	25877	23.7	-1.3
	HON	1	905.8	109319	790	83089	26230	24.0	-1.6
	HON	2	905.8	109319	792	83534	25785	23.6	-1.2
	SRI	2	905.8	109319	794	83946	25373	23.2	-0.9
LG612	ASU	1	898.3	107522	774	79731	27791	25.8	-9.7
	ASU	2	898.3	107522	784	81798	25724	23.9	-7.8
	SRI	2	898.3	107522	785	82158	25365	23.6	-7.5
LG618	ASU	1	866.7	96439	0	0	96439	100.0	-41.6
	ASU	2	866.7	96439	607	47229	49209	51.0	7.4
	SRI	2	866.7	96439	596	45553	50885	52.8	5.6

Table 4. The ASU, Honeywell, and SRI Simulation Results for Kevlar Material Model Version 3.1 Using SRI FE Model (Continued)

NASA-GRC Test No.	Run By	FE Shell Layers	Before Impact		After Impact		Absorbed Energy		Difference vs Test (%)
			Velocity (ft/sec)	Energy (ft*lb)	Velocity (ft/sec)	Energy (ft*lb)	Energy (ft*lb)	(%)	
LG655	ASU	1	1131.7	170632	719	68818	101814	59.7	-13.5
	ASU	8	1131.7	170632	894	106496	64136	37.6	8.5
	HON	1	1131.7	170636	716	68388	102248	59.9	-13.8
	HON	8	1131.7	170636	894	106389	64247	37.7	8.5
	SRI	8	1131.7	170636	861	98734	71902	42.1	4.0
LG656	ASU	1	967.5	124717	342	15614	109102	87.5	-11.0
	ASU	8	967.5	124717	506	34064	90652	72.7	3.8
	HON	1	967.5	124719	362	17420	107300	86.0	-9.6
	HON	8	967.5	124719	566	42610	82109	65.8	10.6
	SRI	8	967.5	124719	537	38433	86286	69.2	7.3
LG657	ASU	1	830.0	91786	446	26558	65228	71.1	28.9
	ASU	8	830.0	91786	495	32628	59158	64.5	35.5
	SRI	8	830.0	91786	508	34373	57413	62.6	37.4
LG688	ASU	1	870.8	101040	601	48098	52942	52.4	7.8
	ASU	2	870.8	101040	598	47650	53390	52.8	7.4
	SRI	2	870.8	101040	590	46314	54725	54.2	6.1
LG692	ASU	1	885.0	104356	719	68805	35551	34.1	19.6
	ASU	2	885.0	104356	701	65500	38857	37.2	16.4
	SRI	2	885.0	104356	700	65365	38991	37.4	16.3
LG594	ASU	1	844.2	89885	583	42936	46949	52.2	14.8
	ASU	2	844.2	89885	582	42678	47207	52.5	14.5
	SRI	2	843.9	89810	584	42941	46868	52.2	14.8
LG689	ASU	1	896.7	106847	681	61623	45223	42.3	4.3
	ASU	2	896.7	106847	657	57328	49519	46.3	0.2
	SRI	2	896.3	106751	665	58755	47996	45.0	1.6
LG620	ASU	1	894.2	103948	367	17483	86465	83.2	-25.4
	ASU	2	894.2	103948	515	34503	69445	66.8	-9.0
	SRI	2	893.8	103861	578	43356	60505	58.3	-0.5

To further ascertain the capability of material model version 3.1 and to quantify improvements, Honeywell decided a more detailed comparison with simulation results using material version 2.1 was necessary. The complete comparison included the following additional steps:

1. For test cases in Phase I, results from simulations using Honeywell single FE shell layer models and Kevlar material model versions 2.1 and 3.1 were added.
2. For test cases in Phase II, a Honeywell model was available for case LG655 only, and was added for simulations with both material models.
3. For all test cases where SRI's multiple FE shell layer modeling approach (one FE shell layer simulating four fabric wraps) was possible, simulations using two approaches were performed. The first approach, used by Honeywell throughout all phases of the program, involved a shell-element layer thickness equal to the analytical fabric shell thickness. (The analytical fabric shell thickness is half of the physical fabric shell thickness, as explained in reference 1). This approach was named "tight" due to the small distance between the FE shell layers of the models. The second approach, introduced by SRI and used in the SRI-developed models, involved a shell-element layer thickness equal to the physical fabric shell thickness and was named "loose," as the distance between the FE shell layers is greater.

For material version 2.1, no friction was considered, as this was not studied during the material model definition process. For material model version 3.1, friction was introduced for all simulations in Phase II using the LS-DYNA parameter FS=FD=0.2.

The results (table 5) show the absorbed kinetic energy for the latest comparison between the two material models performed by Honeywell. The comparison of results was more meaningful when a qualitative visual assessment of the damaged fabric was performed. For example, figure 5 shows the deformed and damaged fabric that was used in simulations for case LG572.

The absorbed kinetic energy and visual comparison of fabric deformation were not the only methods used when assessing a simulation's success. Numerical stability was also required. Detailed plots of all energies calculated during the LS-DYNA simulations were examined for this purpose. Plots (for example, figure 6) using the glstat LS-DYNA output files, were used to examine the energy balance during a simulation. The first general rule is that the ratio between the total energy and the kinetic or internal energy should be less than unity. Thus, plots where either the kinetic energy or the internal energy was greater than the total energy indicated numerical errors in the simulation. The second general rule is that values higher than 10 percent of the total energy for any energy component other than kinetic, or internal, energy indicates numerical deficiencies with the simulation. The plots using the matsum LS-DYNA output files were used to examine the energy balance for individual parts of interest, in this case the fabric layers. Figure 7 shows such a plot for case LG572.

Table 5. The ASU, Honeywell, and SRI Simulation Results for Kevlar Material Model Versions 2.1 and 3.1 Using Both SRI and Honeywell Models

NASA-GRC Test No.	Run By	Material Version/ FE Shells No./ Model Type	Before Impact		After Impact		Absorbed Energy		Difference vs Test (%)
			Velocity (ft/sec)	Energy (ft*lb)	Velocity (ft/sec)	Energy (ft*lb)	(ft*lb)	(%)	
LG403	ASU	v.3.1_1s	900.0	106032	855.5	95806	10226	9.6%	1.7
	HON	v.3.1_1s	900.0	106032	852.6	95162	10870	10.3%	1.1
	SRI	v.3.1_1s	900.0	106032	855.1	95712	10320	9.7%	1.6
	HON	v.2.1_1h	904.1	107007	846.1	93714	13293	12.4%	-1.1
	HON	v.3.1_1h	904.1	107007	855.4	95788	11219	10.5%	0.9
LG404	ASU	v.3.1_1s	896.7	105048	808.7	85447	19601	18.7%	-2.5
	ASU	v.3.1_2sl	896.7	105048	803.4	84339	20709	19.7%	-3.6
	HON	v.3.1_1s	896.7	105048	808.9	85496	19553	18.6%	-2.5
	HON	v.3.1_2sl	896.7	105048	811.2	85968	19080	18.2%	-2.0
	SRI	v.3.1_2sl	896.7	105048	808.9	85496	19553	18.6%	-2.5
	HON	v.2.1_1h	875.0	100034	765.0	76464	23571	23.6%	-7.4
	HON	v.3.1_1h	875.0	100034	777.0	78881	21153	21.1%	-5.0
LG411	ASU	v.3.1_1s	885.8	101558	539.8	37718	63840	62.9%	15.4
	ASU	v.3.1_6sl	885.8	101558	535.9	37175	64383	63.4%	14.8
	HON	v.3.1_1s	885.8	101558	539.2	37625	63932	63.0%	15.3
	HON	v.3.1_6sl	885.8	101558	557.0	40148	61410	60.5%	17.8
	SRI	v.3.1_6sl	885.8	101558	508.2	33422	68136	67.1%	11.1
	HON	v.2.1_1h	886.0	101597	497.0	31969	69628	68.5%	9.7
	HON	v.3.1_1h	886.0	101597	454.6	26743	74854	73.7%	4.5
LG432	ASU	v.3.1_1s	895.8	105578	679.9	60816	44763	42.4%	5.0
	ASU	v.3.1_4sl	895.8	105578	671.0	59227	46352	43.9%	3.5
	HON	v.3.1_1s	895.8	105578	694.5	63449	42129	39.9%	7.5
	HON	v.3.1_4sl	895.8	105578	677.1	60309	45269	42.9%	4.5
	SRI	v.3.1_4sl	895.8	105578	675.5	60032	45547	43.1%	4.3
	HON	v.2.1_1h	913.7	109824	673.6	59696	50128	45.6%	1.8
	HON	v.3.1_1h	913.7	109824	628.4	51957	57867	52.7%	-5.3
LG449	HON	v.2.1_1h	345.0	16882	262.9	9803	7079	41.9%	-7.4
	HON	v.3.1_1h	345.0	16882	216.5	6648	10234	60.6%	-26.1

Table 5. The ASU, Honeywell, and SRI Simulation Results for Kevlar Material Model Versions 2.1 and 3.1 Using Both SRI and Honeywell Models (Continued)

NASA-GRC Test No.	Run By	Material Version/ FE Shells No./ Model Type	Before Impact		After Impact		Absorbed Energy		Difference vs Test (%)
			Velocity (ft/sec)	Energy (ft*lb)	Velocity (ft/sec)	Energy (ft*lb)	(ft*lb)	(%)	
LG655	ASU	v.3.1_1s	1131.7	170632	718.7	68818	101814	59.7%	-13.5
	ASU	v.3.1_8sl	1131.7	170632	894.0	106496	64136	37.6%	8.5
	HON	v.3.1_1s	1131.7	170636	716.4	68388	102248	59.9%	-13.8
	HON	v.3.1_8sl	1131.7	170636	893.6	106389	64247	37.7%	8.5
	HON	v.3.1_8sl	1131.7	170636	860.8	98734	71902	42.1%	4.0
	HON	v.2.1_1h	1131.7	170636	820.0	89592	81044	47.5%	-1.4
LG657	HON	v.3.1_1h	1131.7	170636	601.6	48227	122409	71.7%	-25.6
	ASU	v.3.1_1s	830.0	91786	446.5	26558	65228	71.1%	28.9
	ASU	v.3.1_8sl	830.0	91786	494.9	32628	59158	64.5%	35.5
	SRI	v.3.1_8sl	830.0	91786	507.9	34373	57413	62.6%	37.4
	HON	v.2.1_1s	830.0	91786	95.2	1207	90580	98.7%	1.3
	HON	v.3.1_1s	830.0	91786	413.9	22826	68961	75.1%	24.9

Note for column 3:

v.3.1 or 2.1—material model version

1, 2, 4, 6, and 8 are the number of FE shell layers simulating the total number of fabric layers

h = Honeywell model

s = SRI model

For the SRI model, 1 = loose fabric layers

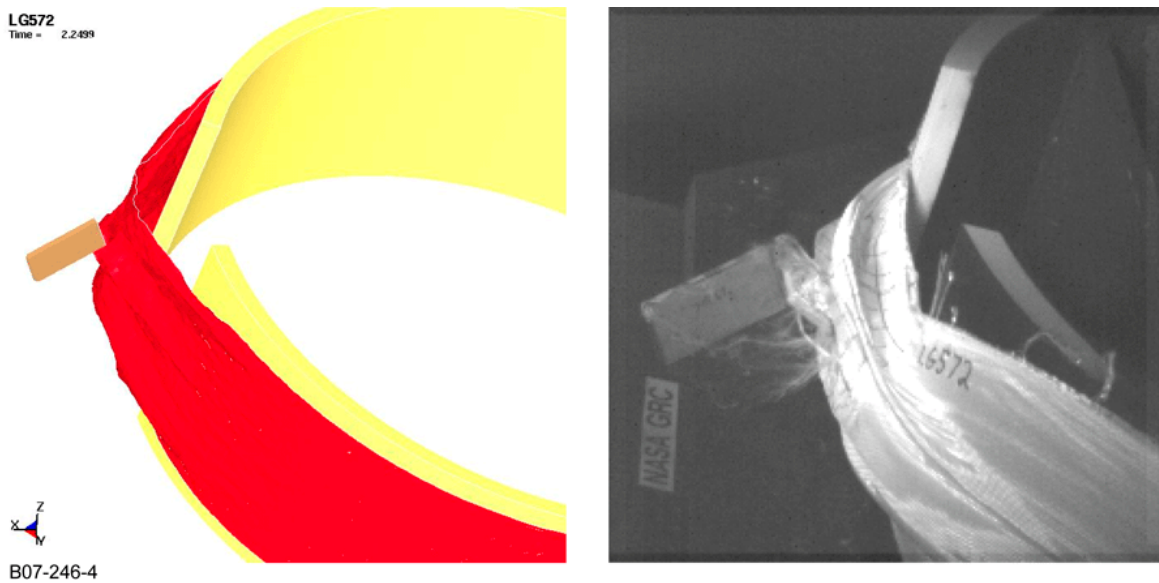


Figure 5. The NASA-GRC Test LG572 Versus Analysis for One FE Shell Layer Simulation, SRI Model, Material Version 3.1

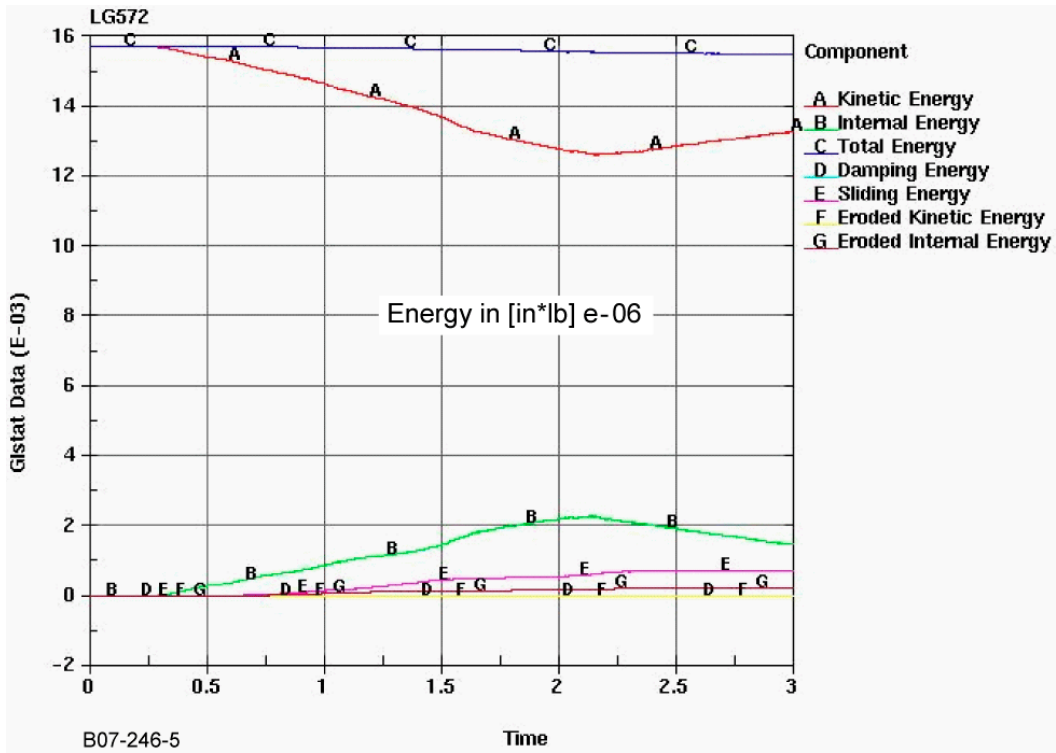


Figure 6. The NASA-GRC LG572-Glstat Data for One FE Shell Layer Simulation, SRI Model, Material Version 3.1

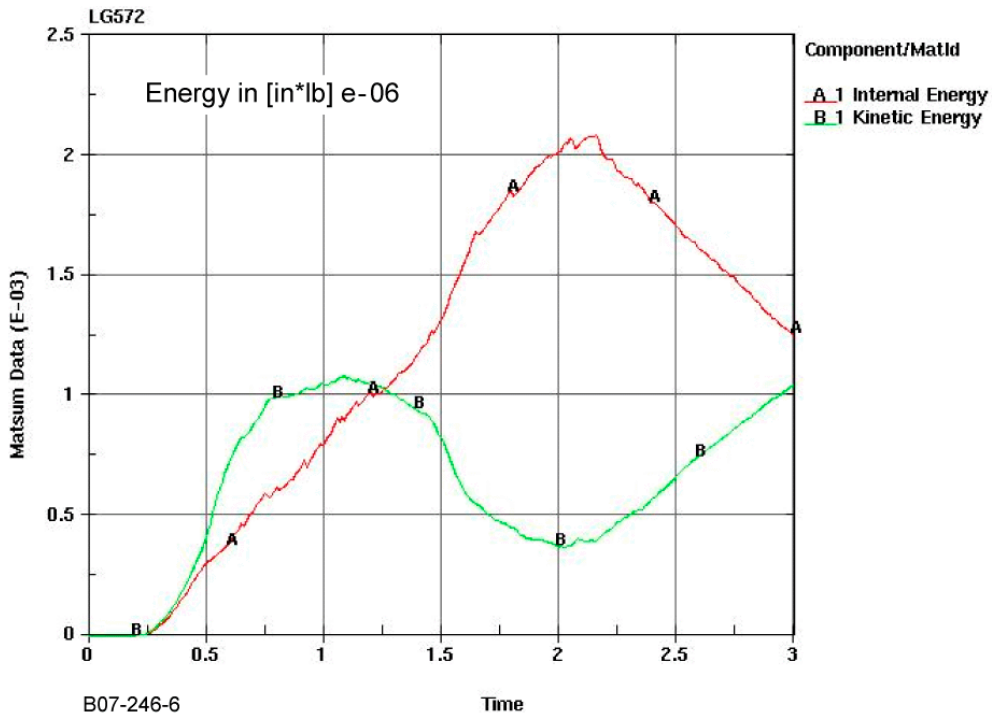


Figure 7. The NASA-GRC LG572-Fabric Matsum Data for One FE Shell Layer Simulation, SRI Model, Material Version 3.1

The plot of the projectile velocity is also very important in analyzing a simulation. Plots of projectile velocity versus time for the tests used for material model version comparison are in figures 8 through 13. A point showing the final test projectile velocity is also introduced in these plots for reference. The naming convention used for figures 8 through 13 is the same as the one used for table 5.

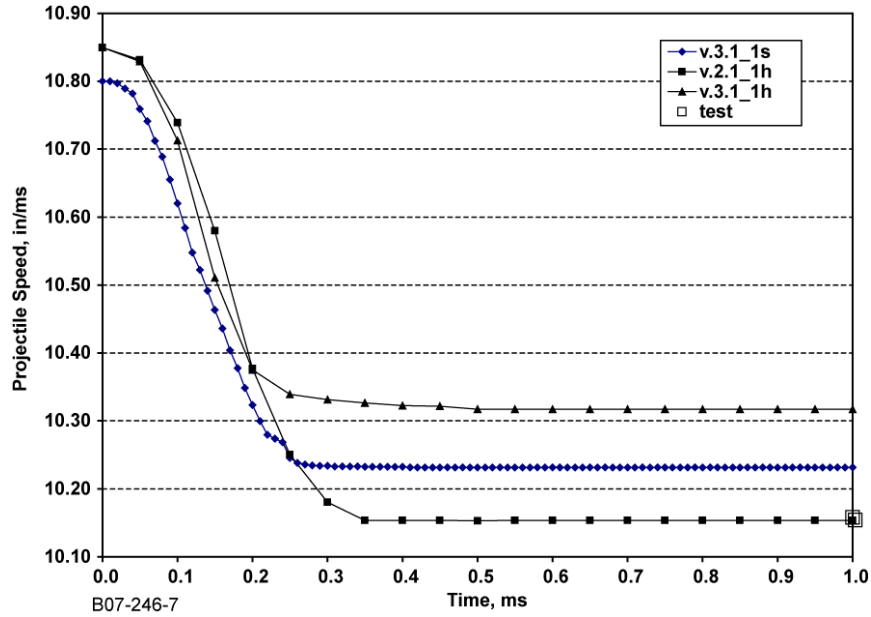


Figure 8. Simulation Results Showing Velocity Versus Time Compared to Test Final Projectile Velocity for NASA-GRC Test LG403

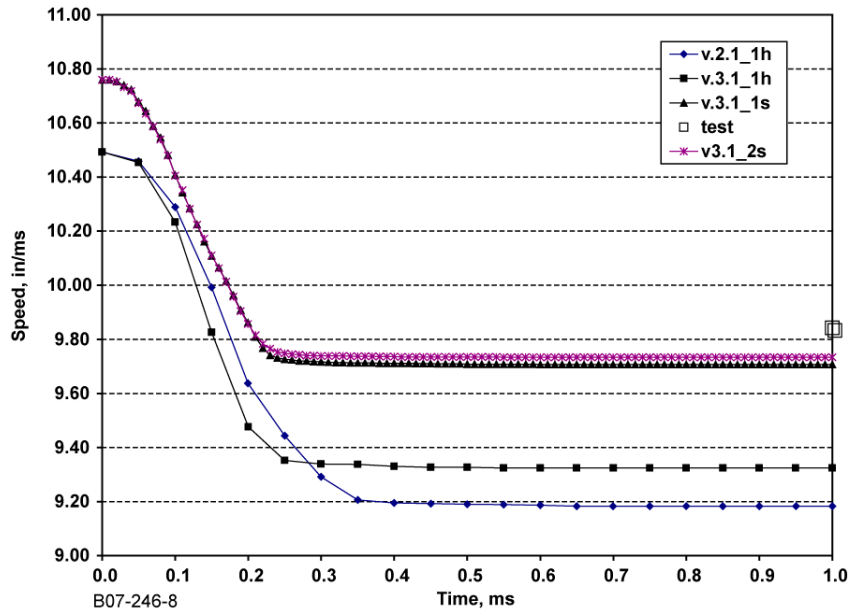


Figure 9. Simulation Results Showing Velocity Versus Time Compared to Test Final Projectile Velocity for NASA-GRC Test LG404

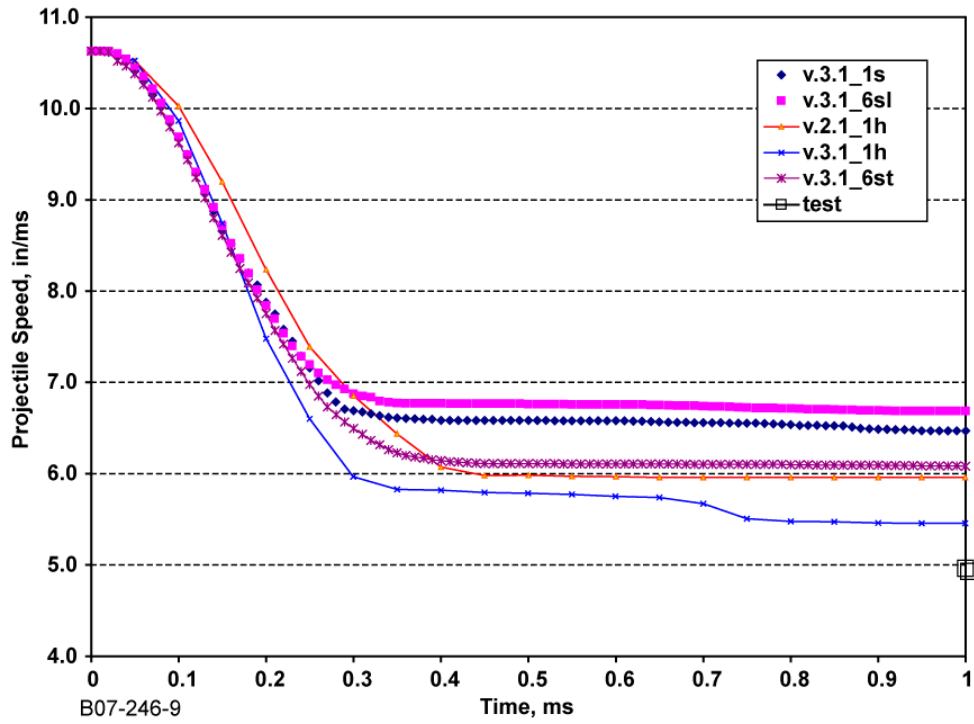


Figure 10. Simulation Results Showing Velocity Versus Time Compared to Test Final Projectile Velocity for NASA-GRC Test LG411

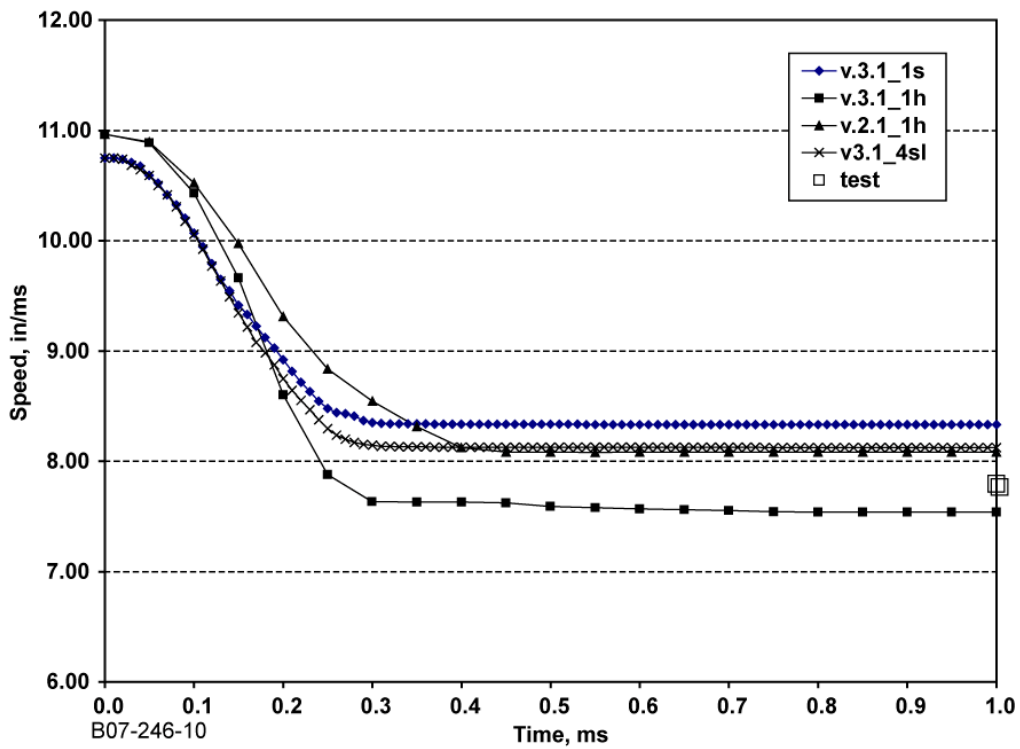


Figure 11. Simulation Results Showing Velocity Versus Time Compared to Test Final Projectile Velocity for NASA-GRC Test LG432

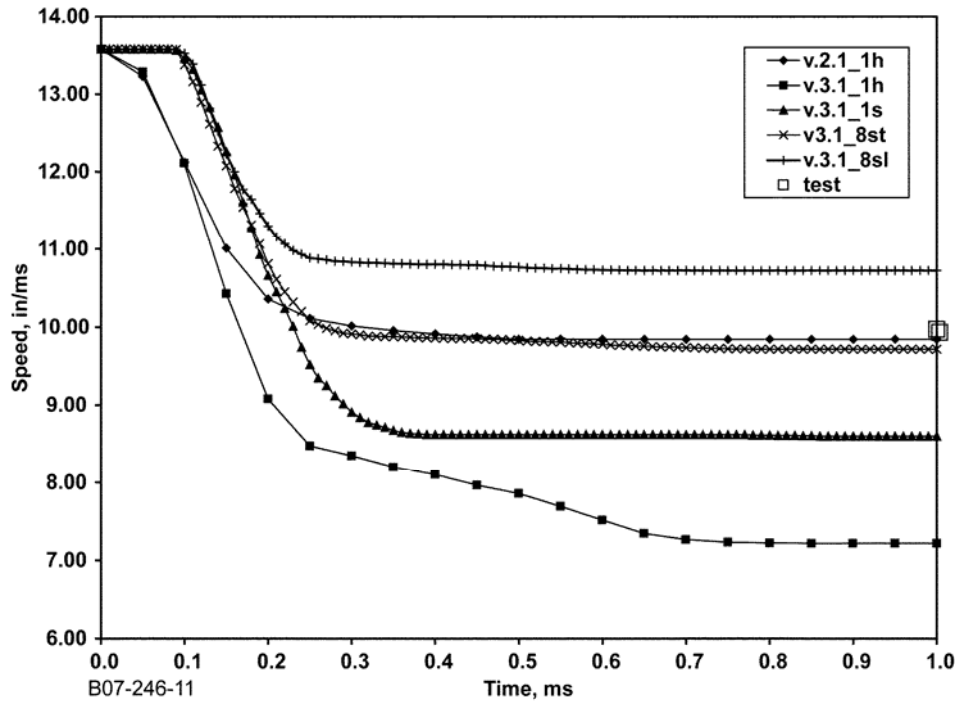


Figure 12. Simulation Results Showing Velocity Versus Time Compared to Test Final Projectile Velocity for NASA-GRC Test LG655

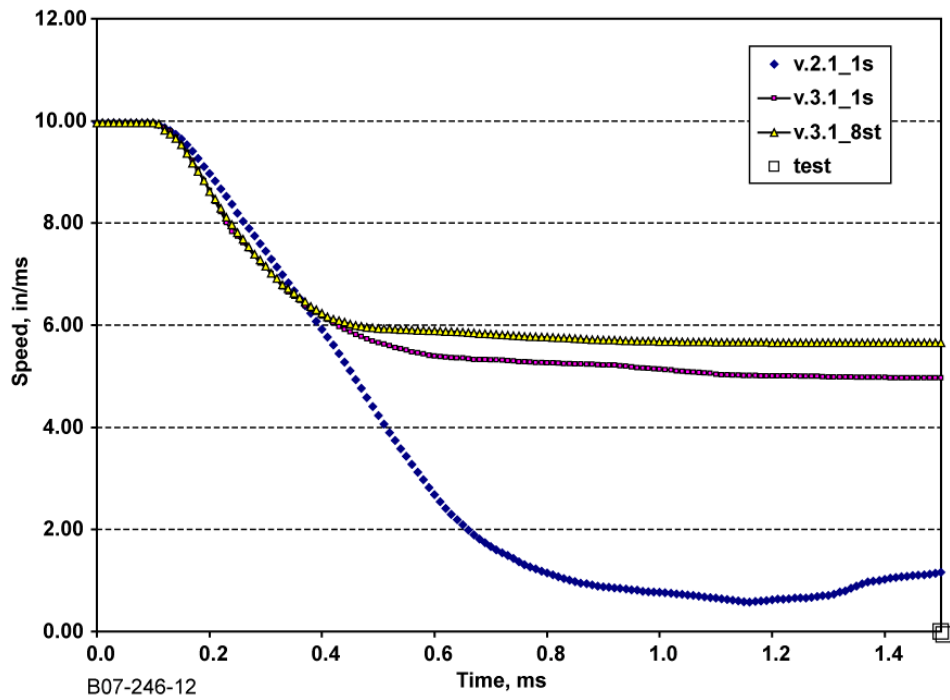


Figure 13. Simulation Results Showing Velocity Versus Time Compared to Test Final Projectile Velocity for NASA-GRC Test LG657

2.6 CONCLUSIONS FOR TASK 1.

Examination of all results using the methods described in section 2 resulted in the following conclusions for Task 1:

1. Material version 3.1 is better than 2.1 for simulations of ballistic tests using rotated projectiles with models involving a single FE layer, based on examination of projectile velocity and absorbed kinetic energy. Energy plots using glstat/matsum confirm this conclusion.
2. Visual examination of fabric damage or displacement does not always show a consistent match with the tests for both versions, which means that the physics of the fabric failures is not adequately captured yet. Although difficult, a comparison of the magnitude of the fabric displacement during test and simulation could shed more light on this issue.
3. SRI's approach with loose fabric for multiple shell layer models introduced more numerical error, and the absorbed energy difference was opposite in sign to the single-layer model results (i.e., loose underpredicts and single layer overpredicts). If the tight Phase I approach is used, the simulation is slightly better and the difference in absorbed energy is similar to the single-layer simulation results.
4. The previous conclusions are confirmed by examination of the energy plots from LS-DYNA. One run can show excellent visual agreement with the test and no difference between tight or loose fabric modeling in energy absorbed, but the energy plots show errors, such as kinetic energy higher than total energy.
5. The stiffness-based hourglass control (parameter IHQ = 4 in the *CONTROL_HOURGLASS card) is recommended for material version 3.1.
6. For material version 3.1 simulations, the magnitude of the projectile velocity for single and multiple shell layer models is very close.
7. Material version 2.1 is very sensitive to the hourglass control type (parameter IHQ). Using IHQ = 4 produced failed simulations. It is possible that IHQ = 3 could produce better results.
8. Using individual contact cards for each contact in the simulation produces better results than using a single global contact card.
9. Further work is needed for multiple-layer simulations to understand: (1) the best material model, 2.1 or 3.1, and (2) the optimum number of fabric wraps to be simulated by one FE shell layer.

3. MULTIPLE SHELL-ELEMENT LAYER MODELING (TASK 2).

3.1 BACKGROUND AND OBJECTIVE.

In Phase I, most of the LS-DYNA models used a single element through the thickness to model the fabric, which ranged from 1 to 24 layers. Although this technique is simple, it does not provide the predictive capability of computing the number of fabric layers that will be penetrated during an actual containment event. Therefore, the containment margin in terms of the number of unpenetrated layers versus total number of layers cannot be calculated. In Phase I, modeling the fabric layers using multiple layers of shell elements exhibited two problems. First, for the ballistic tests, the calculated energy absorbed was not constant for different model configurations, e.g., modeling 16 layers of fabric using 16 layers of shell elements absorbed significantly less energy than a single (thicker) layer of shell elements. Also, there appeared to be significant instability in the numerical algorithm for the contact. Second, for simulations of the engine blade containment, the analysts were unable to use multiple element layers without the simulation failing prematurely.

The objective of Phase II, Task 2 was to improve the modeling capability for multiple layers of fabric using multiple layers of shell elements. The following steps were performed to achieve this goal.

3.2 PERFORM SYSTEMATIC STUDY—BOUND THE PROBLEM (TASK 2.1.2).

The objective of this task was to perform simulations over a typical range of parameter choices to establish the boundaries for the problem identified in section 3.1. The focus was to create simple, projectile ballistic impact or engine containment simulations with multiple fabric layers in which the multilayer shell modeling was not successful with previously used techniques.

A Honeywell generic engine model was built based on the HTF7000 (previously called AS907) engine model used in Phase I. Two FE models, (figure 14) were derived: one model used one shell FE layer simulating all fabric wraps, and one model used three shell FE layers simulating all fabric wraps. The following parameters were varied:

1. Model complexity, where three models were used:
 - a. basic (blade and fabric only)
 - b. intermediate (blade, fabric, and the containment housing only)
 - c. complex (blade, fabric, containment housing, and all containment layers, including abrasion coating, graphite-epoxy shell, and honeycomb)
2. Blade mesh type: shell or solid elements
3. Fabric mesh refinement through element size: coarse (0.25 inch), locally refined (0.15 inch at the blade contact area), or refined (0.15 inch)
4. Element formulation type: 16 (used in Phase I) and 2

5. Hourglass control type in LS-DYNA contact cards: stiffness-based (IHQ = 4) or viscous-based (IHQ = 3) formulations
6. SFS (penalty stiffness scale factor) and TSSFAC (time-step scale factor) in conjunction with IHQ

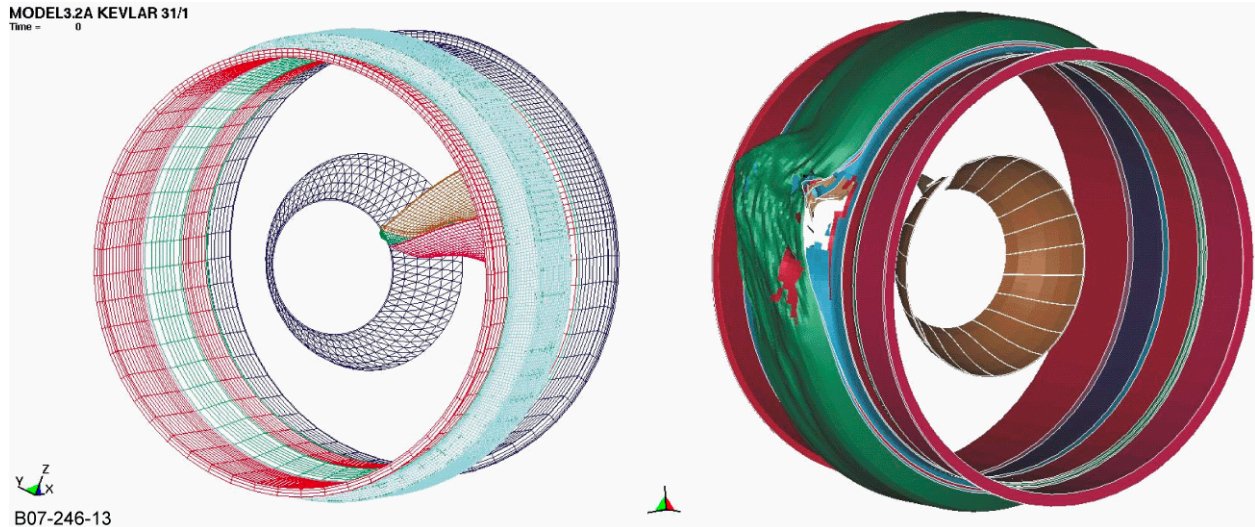


Figure 14. Honeywell Generic Engine Model Versions

It should be noted that material model version 1.0 was initially used for simulations in this task.

At the end of the process, all analyses were running, exhibiting different levels of stability. The following conclusions were formulated at the end of all simulations.

- A mesh of solid elements works best for the blade.
- A uniform, refined mesh with no local changes in mesh density works best. An element size of 0.25 inch provides sufficient refinement.
- Increased model size deteriorates the analysis stability.
- Element formulation 16, recommended by Livermore Software Technology Corporation (LSTC), does not improve stability.
- Material model version 1.0 does not seem to work well for multiple layers and is suspected to yield inconsistent results.

The resulting recommendations from Task 2 are that the material model and element formulation influence are the factors targeted for change and improvement.

3.3 PROBLEM REVIEW WITH LIVERMORE SOFTWARE TECHNOLOGY CORPORATION (TASK 2.2).

Honeywell worked closely with the LS-DYNA vendor, LSTC, to determine whether the problems could be solved for issues experienced with multiple shell-element layer analysis. LSTC was consulted to learn whether different choices of existing controls, parameters, and algorithms should be used, or whether code development would be needed. The first review of results with LSTC occurred in November 2004. The following conclusions were formulated.

- An improvement to the material model algorithm is needed.
- SFS is a major contributor to instability.
- TSSFAC is a major contributor to instability.
- Viscous hourglass formulation (IHQ = 2 or 3) is recommended.
- Projectile sharp corners are contributors to instability.
- Change to element formulation 2 is recommended for improving stability.

The second review of results with LSTC occurred in January 2005. The following conclusions were formulated.

1. Regarding the use of element formulation 2:
 - High sliding energy was noticed.
 - High total energy and initial energy ratio was noticed.
 - High hourglass and internal energy were noticed.
2. Element formulation 16 should be abandoned due to the incompatibility between the LS-DYNA code and SRI's material model regarding failure definition. LSTC may examine the problem if resources are available.

Thus, most of the issues experienced with multiple shell-element layer analysis are due to the LS-DYNA code and material model interactions and type of hourglass control (viscous- or stiffness-based). The following changes to the LS-DYNA input deck were recommended to improve the Honeywell generic engine fan blade-out model simulation:

- Increase speed for penetration in the basic model
- Use *DAMPING_PART_STIFFNESS (0.02 damping coefficient)
- Use one single *CONTACT_ERODING_SINGLE_SURFACE sliding interface (with several transducers on the parts of interest) (SFS = 1 and SFM = 1)
- Use *CONTROL_SHELL with parameters BWC = 1, PROJ = 1
- Use *CONTROL_ACCURACY (INN = 2)
- Use *CONTROL_TIMESTEP with TSSFAC = 0.7

- Use *CONTROL_ENERGY (HGEN = 2)
- Increase the d3plot output
- Use double precision executable
- Use LS-DYNA 970 release 5434a
- Use material model version 2.1

Several analyses were performed using the Honeywell generic fan blade containment models with the changes agreed upon with LSTC and material model version 2.1 for Kevlar. The stability of the analyses improved substantially when the hourglass control was changed to the viscous formulation (IHQ = 3). In addition, the difference in absorbed energy between the single and multiple shell-element layer models was very small. An example of an analysis performed using the latest recommendations and Kevlar material version 2.1 is in figure 15, where fabric deformation is shown. The verification process went further than in Phase I involving assessment of the energies during the simulations, as described in section 2 and exemplified in figure 16 for the model in figure 15. The models developed in this task were used to create the generic fan blade containment model described in section 4.

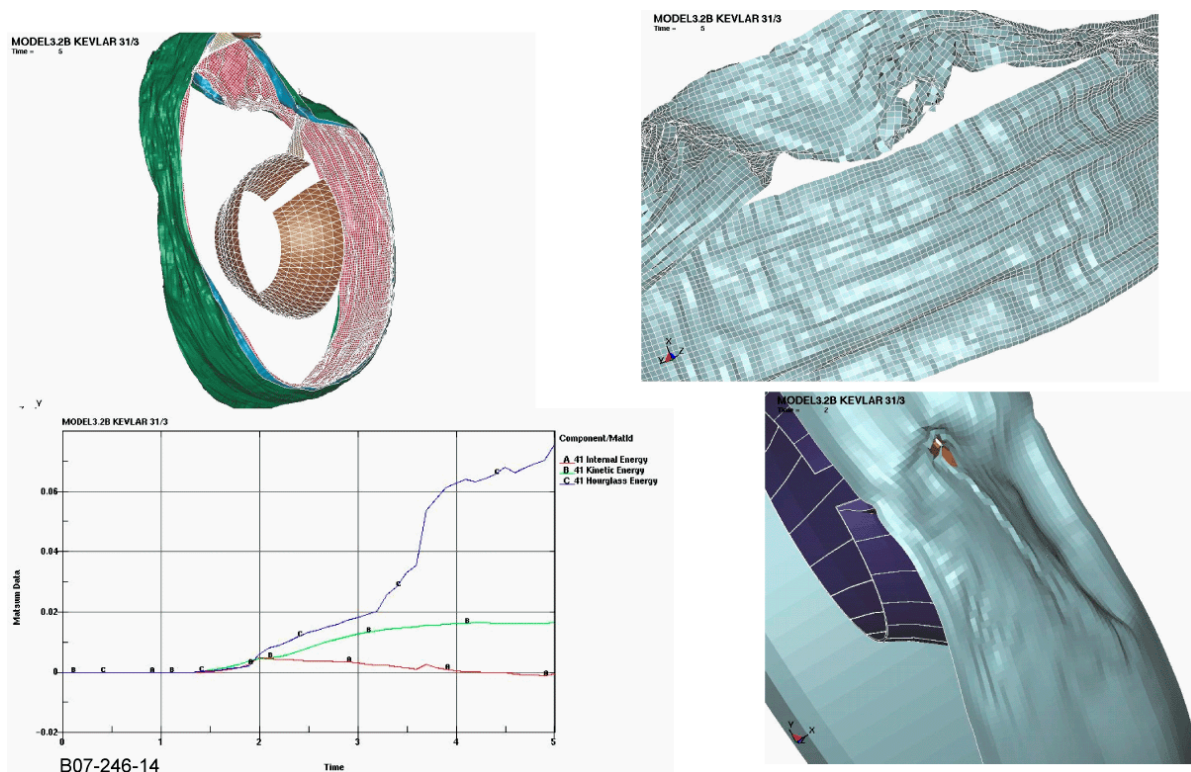


Figure 15. Results for Basic Honeywell Generic Engine Model, Three Layers, IHQ = 3, Material Model Version 2.1

time.....	4.99811E+00
time step.....	2.42813E-05
kinetic energy.....	5.79501E-01
internal energy.....	6.61538E-02
spring and damper energy.....	1.00000E-20
hourglass energy	1.59908E-01
system damping energy.....	0.00000E+00
sliding interface energy.....	-2.74015E-01
external work.....	0.00000E+00
eroded kinetic energy.....	1.68840E-01
eroded internal energy.....	5.66197E-02
total energy.....	5.31548E-01
total energy / initial energy..	1.10131E+00
energy ratio w/o eroded energy.	6.34182E-01
global x velocity.....	-5.98124E-04
global y velocity.....	2.08517E-02
global z velocity.....	2.41114E-02

B07-246-15

Figure 16. Energy Balance From the Gostat File for Figure 14

3.4 DEMONSTRATE RESULTS (TASK 2.3).

During this stage, it was concluded that simulations using the multiple shell-element layer approach were feasible, and a streamlined process for validation of a material model was needed. Also, both single and multiple shell-element layer simulations needed to be validated for the same material model. Moreover, to quantify achieved progress compared to previous models developed in this program, both material versions 2.1 and 3.1 needed to be assessed for their capability of simulating ballistic impact tests when multiple shell-element layer models are used.

The comparison between material model versions 2.1 and 3.1, when the single FE shell layer modeling approach was used, was described in section 2.5. Both straight and rotated projectile ballistic impact test cases were simulated. Section 2.5 also contains the results for test case simulations involving rotated projectiles and multiple shell-element layer models using the SRI-developed approach with loose layers and one shell-element layer simulating four fabric wraps.

The following three steps needed to be performed for a complete picture of the material model validation process.

1. The question of how many shell-element layers to use to simulate all fabric wraps needed to be answered, or equivalently, how many fabric wraps should be represented by a shell-element layer? For one test case, LG411 (a straight-projectile case with 24 Kevlar wraps, shown in figure 17), Honeywell built a set of several multiple FE shell layer models, using 2, 4, 8, 12, and 24 shell layers, respectively, and the analytical fabric shell thickness. Simulations were run using Honeywell's approach of individual contact between each part, stiffness hourglass formulation (IHQ = 4), and material versions 2.1 and 3.1. The simulation results for these models, using material version 3.1, are shown in figures 17 through 26. No results were reported for the multiple-layer simulations using

Kevlar material model version 2.1, as all failed when the methodology defined during Task 1 (section 2.5) was used.

2. A final comparison of the two approaches for fabric thickness definition was needed. For two test cases with 32 fabric layers, LG655 and LG657, where SRI's multiple FE shell layer modeling approach (one FE shell layer simulating four fabric wraps) was possible, simulations using the two fabric thickness definition approaches described in section 2.5 were used: the tight fabric approach, used by Honeywell, and the loose fabric approach, introduced by SRI. Test cases LG655 and LG657 are important because the fabric thickness is similar to the one used in an actual engine case. Also, the projectile was not contained for test case LG655, but was contained for test case LG657. Simulation for these models using material versions 2.1 and 3.1 were performed. For these cases, simulations using Kevlar material model version 2.1 failed when the methodology defined during Task 1 (section 2.5) was used.
3. The conclusions for the methodology developed for ballistic test simulations were applied to the generic engine model described in section 3.3. The final Honeywell generic fan blade containment model (figure 27), consisted of a fan containment housing, a fan blade, and three FE shell layers simulating several Kevlar wraps. The model was used to perform several simulations with the Honeywell individual contact approach and SRI's single contact approach using material versions 2.1 and 3.1 and viscous hourglass control (IHQ = 3).



Figure 17. Simulation of NASA-GRC Test LG411—Two FE Shell Layers, Honeywell Model, Material Version 3.1

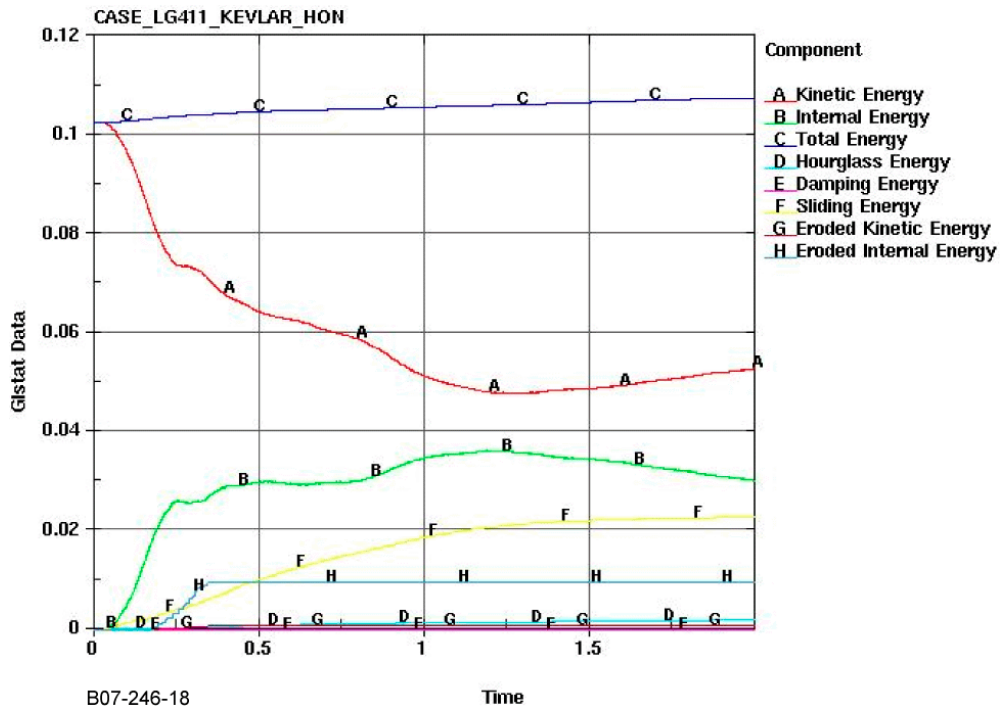


Figure 18. The NASA-GRC Test LG411—Gistat Data for the Two FE Shell Layer Simulations, Honeywell Model, Material Version 3.1

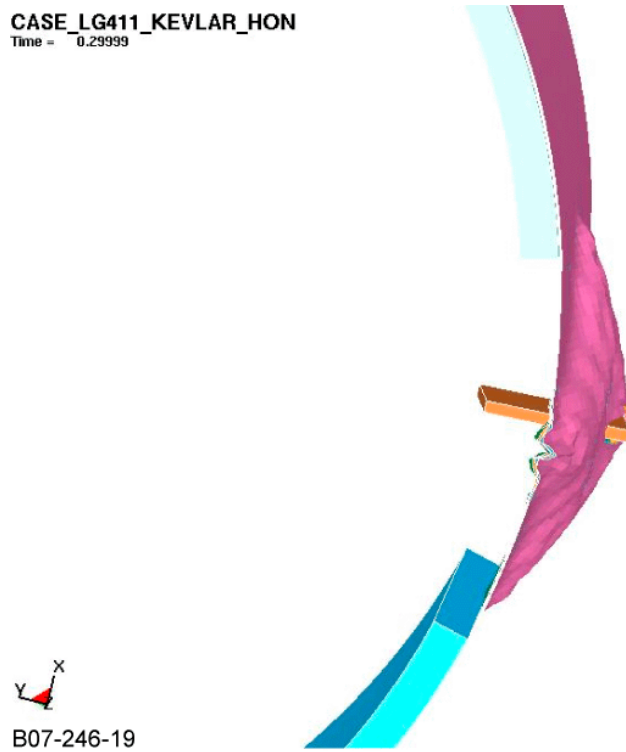


Figure 19. Simulation of NASA-GRC Test LG411—Four FE Shell Layers, Honeywell Model, Material Version 3.1

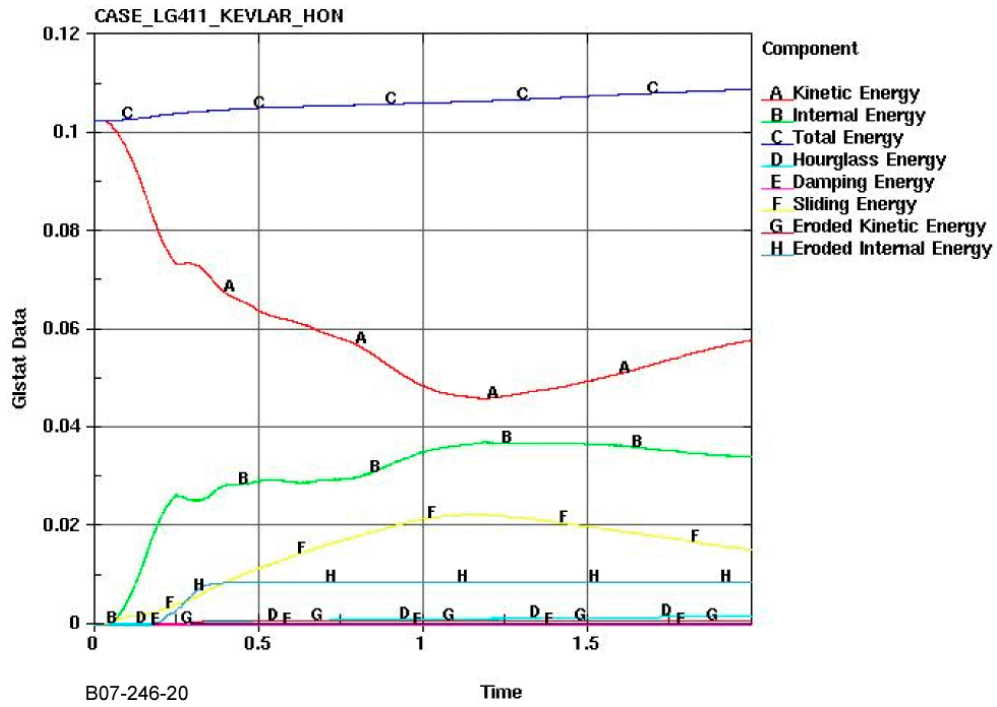


Figure 20. The NASA-GRC Test LG411—Gistat Data for the Four FE Shell Layer Simulations, Honeywell Model, Material Version 3.1

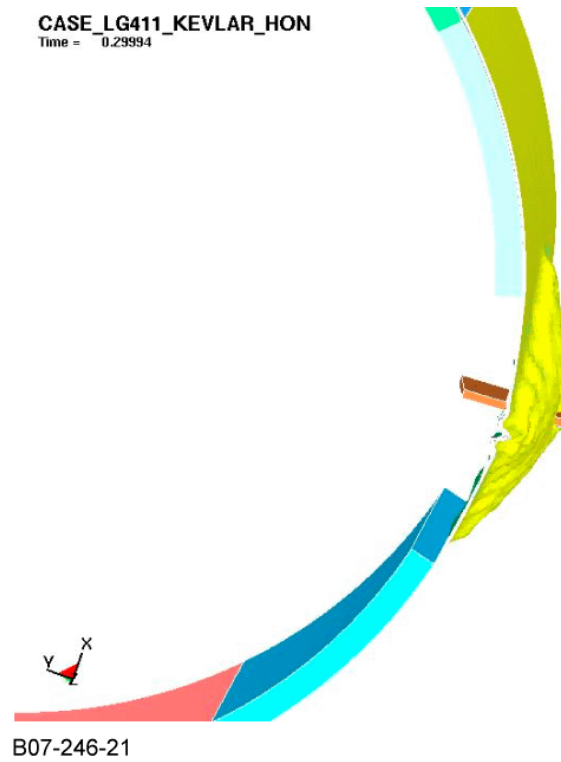


Figure 21. Simulation of NASA-GRC Test LG411—Eight FE Shell Layers, Honeywell Model, Material Version 3.1

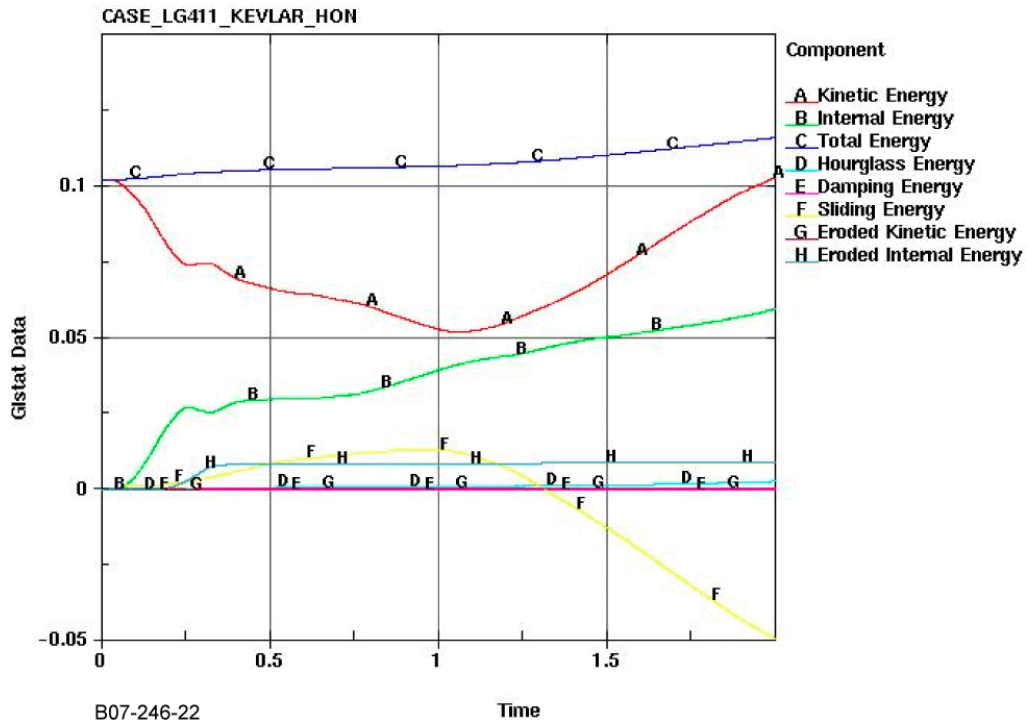


Figure 22. The NASA-GRC Test LG411—Gistat Data for the Eight FE Shell Layer Simulations, Honeywell Model, Material Version 3.1



Figure 23. Simulation of NASA-GRC Test LG411—12 FE Shell Layers, Honeywell Model, Material Version 3.1

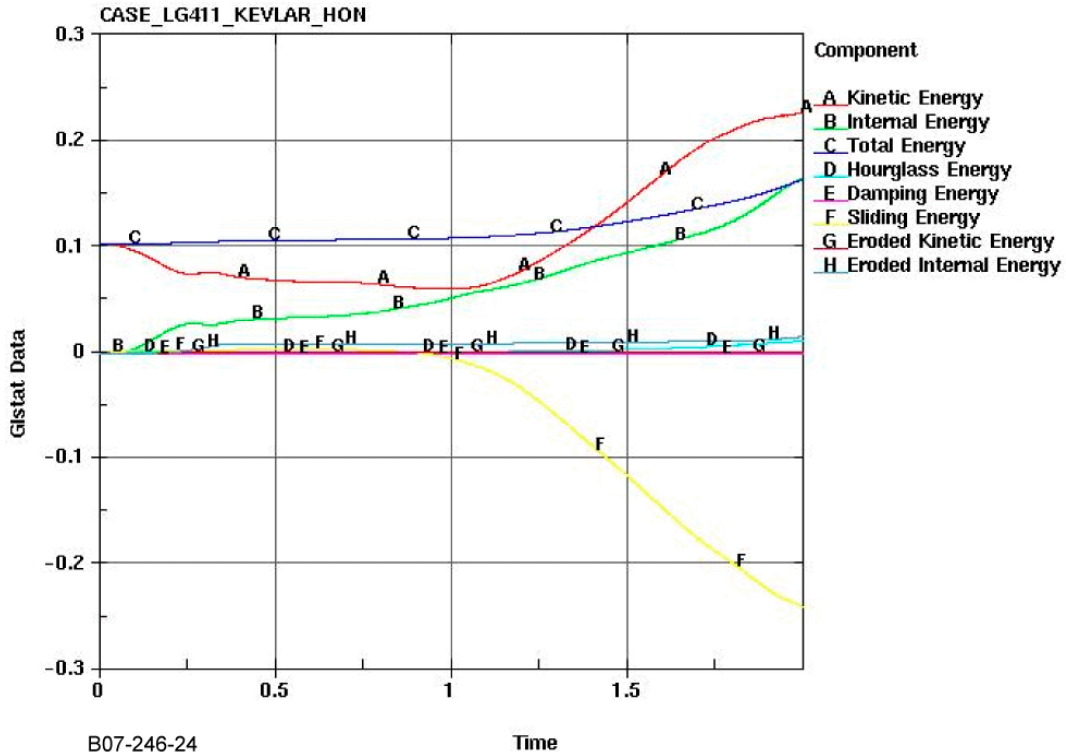


Figure 24. The NASA-GRC Test LG411—Gistat Data for the 12 FE Shell Layer Simulations, Honeywell Model, Material Version 3.1

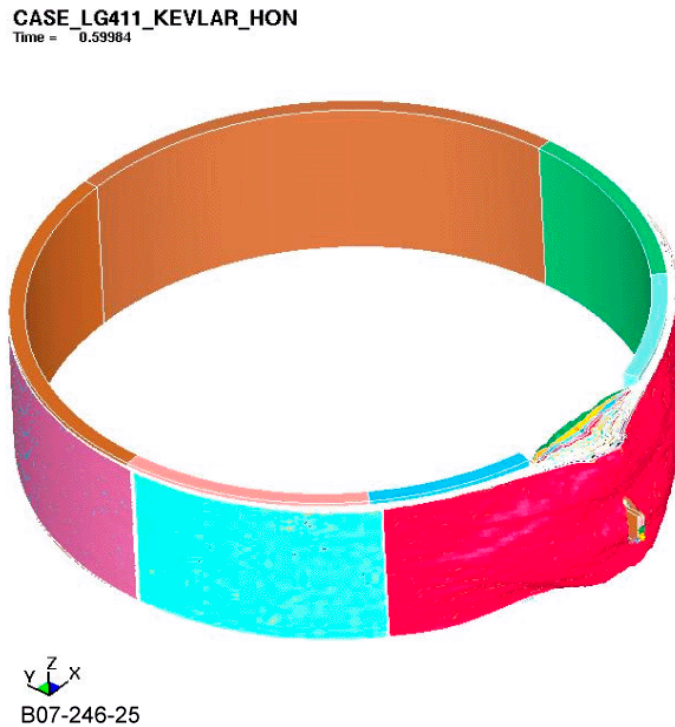


Figure 25. Simulation of NASA-GRC Test LG411—24 Shell Layers, Honeywell Model, Material Version 3.1

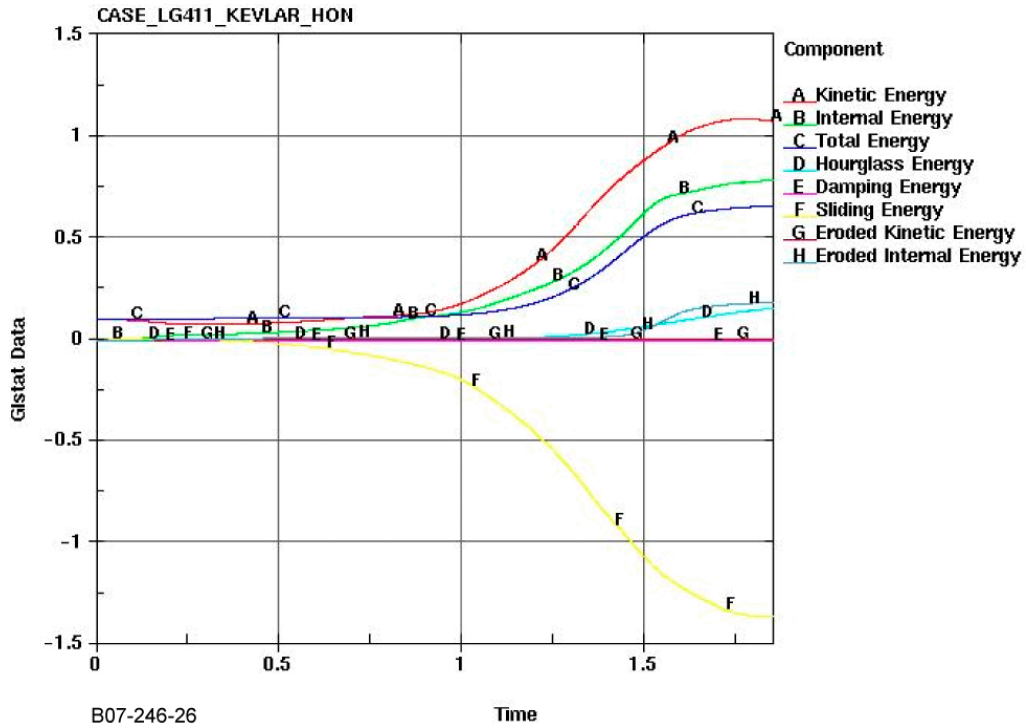


Figure 26. The NASA-GRC Test LG411—Glistat Data for the 24 FE Shell Layer Simulations, Honeywell Model, Material Version 3.1

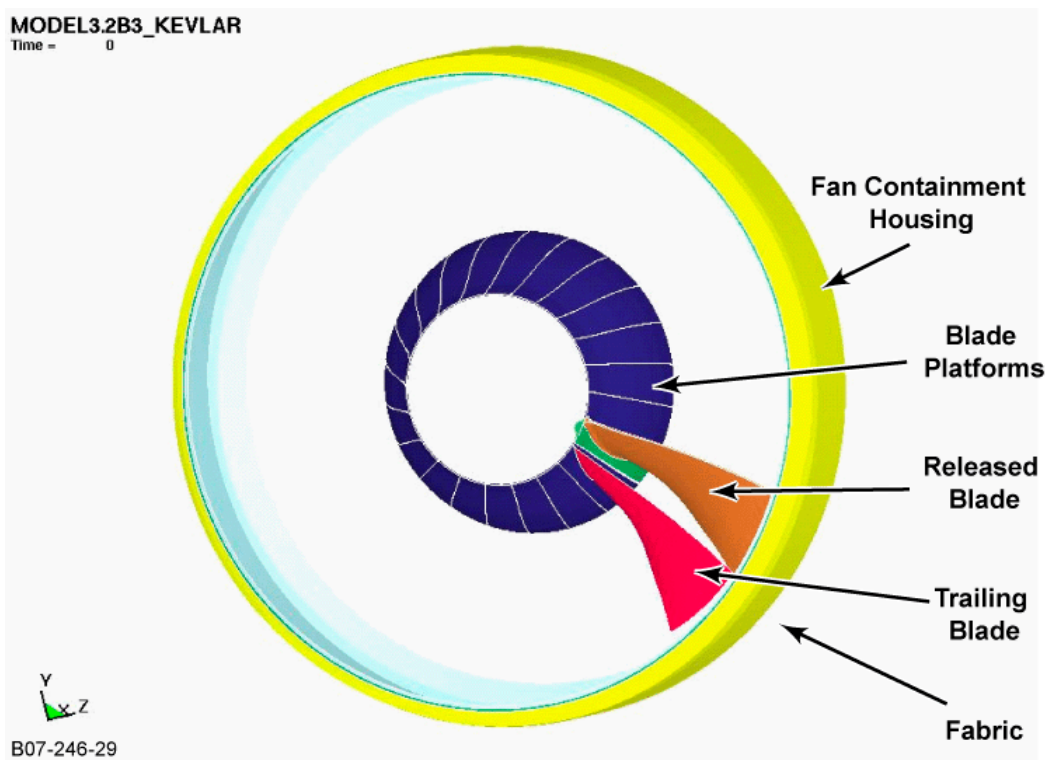


Figure 27. The FE Model of the Honeywell Basic Generic Blade Containment Model

The straight projectile ballistic test simulation results showing the absorbed kinetic energy for the latest comparison between the two material models are shown in table 6. For completeness, results from all simulations of straight projectiles tests using Kevlar material model versions 2.1 and 3.1 are included from section 2.5.

Table 6. The ASU, Honeywell, and SRI Simulation Results, Kevlar Material Model Versions 3.1 and 2.1, Both SRI and Honeywell Ballistic Models

NASA-GRC Test No.	Run By	Material Version/ FE Shells No./ Model Type	Before Impact		After Impact		Absorbed Energy		Difference vs Test (%)
			Velocity (ft/sec)	Energy (ft*lb)	Velocity (ft/sec)	Energy (ft*lb)	(ft*lb)	(%)	
LG404	ASU	v.3.1_1s	896.7	105048	808.7	85447	19601	18.7%	-2.5
	ASU	v.3.1_2sl	896.7	105048	803.4	84339	20709	19.7%	-3.6
	HON	v.3.1_1s	896.7	105048	808.9	85496	19553	18.6%	-2.5
	HON	v.3.1_2sl	896.7	105048	811.2	85968	19080	18.2%	-2.0
	SRI	v.3.1_2sl	896.7	105048	808.9	85496	19553	18.6%	-2.5
	HON	v.2.1_1h	875.0	100034	765.0	76464	23571	23.6%	-7.4
	HON	v.3.1_1h	875.0	100034	777.0	78881	21153	21.1%	-5.0
LG411	ASU	v.3.1_1s	885.8	101558	539.8	37718	63840	62.9%	15.4
	ASU	v.3.1_6sl	885.8	101558	535.9	37175	64383	63.4%	14.8
	HON	v.3.1_1s	885.8	101558	539.2	37625	63932	63.0%	15.3
	HON	v.3.1_6sl	885.8	101558	557.0	40148	61410	60.5%	17.8
	SRI	v.3.1_6sl	885.8	101558	508.2	33422	68136	67.1%	11.1
	HON	v.2.1_1h	886.0	101597	497.0	31969	69628	68.5%	9.7
	HON	v.3.1_1h	886.0	101597	454.6	26743	74854	73.7%	4.5
	HON	v.3.1_2h	886.0	101597	466.8	28201	73397	72.2%	6.0
	HON	v.3.1_4h	886.0	101597	443.2	25420	76177	75.0%	3.2
	HON	v.3.1_8h	886.0	101597	452.7	26524	75073	73.9%	4.3
	HON	v.3.1_12h	886.0	101597	417.0	22503	79094	77.9%	0.4
	HON	v.3.1_24h	886.0	101597	416.9	22496	79101	77.9%	0.4
	HON	v.3.1_6st	885.8	101558	507.2	33288	68270	67.2%	11.0
LG432	ASU	v.3.1_1s	895.8	105578	679.9	60816	44763	42.4%	5.0
	ASU	v.3.1_4sl	895.8	105578	671.0	59227	46352	43.9%	3.5
	HON	v.3.1_1s	895.8	105578	694.5	63449	42129	39.9%	7.5
	HON	v.3.1_4sl	895.8	105578	677.1	60309	45269	42.9%	4.5
	SRI	v.3.1_4sl	895.8	105578	675.5	60032	45547	43.1%	4.3
	HON	v.2.1_1h	913.7	109824	673.6	59696	50128	45.6%	1.8
	HON	v.3.1_1h	913.7	109824	628.4	51957	57867	52.7%	-5.3

Table 6. The ASU, Honeywell, and SRI Simulation Results, Kevlar Material Model Versions 3.1 and 2.1, Both SRI and Honeywell Ballistic Models (Continued)

NASA-GRC Test No.	Run By	Material Version/ FE Shells No./ Model Type	Before Impact		After Impact		Absorbed Energy		Difference vs Test (%)
			Velocity (ft/sec)	Energy (ft*lb)	Velocity (ft/sec)	Energy (ft*lb)	(ft*lb)	(%)	
LG655	ASU	v.3.1_1s	1131.7	170632	718.7	68818	101814	59.7%	-13.5
	ASU	v.3.1_8sl	1131.7	170632	894.0	106496	64136	37.6%	8.5
	HON	v.3.1_1s	1131.7	170636	716.4	68388	102248	59.9%	-13.8
	HON	v.3.1_8sl	1131.7	170636	893.6	106389	64247	37.7%	8.5
	HON	v.3.1_8sl	1131.7	170636	860.8	98734	71902	42.1%	4.0
	HON	v.2.1_1h	1131.7	170636	820.0	89592	81044	47.5%	-1.4
	HON	v.3.1_1h	1131.7	170636	601.6	48227	122409	71.7%	-25.6
	HON	v.3.1_8st	1131.7	170636	809.4	87284	83352	48.8%	-2.7
LG657	ASU	v.3.1_1s	830.0	91786	446.5	26558	65228	71.1%	28.9
	ASU	v.3.1_8sl	830.0	91786	494.9	32628	59158	64.5%	35.5
	SRI	v.3.1_8sl	830.0	91786	507.9	34373	57413	62.6%	37.4
	HON	v.2.1_1s	830.0	91786	95.2	1207	90580	98.7%	1.3
	HON	v.3.1_1s	830.0	91786	413.9	22826	68961	75.1%	24.9
	HON	v.3.1_8st	830.0	91786	471.5	29614	62172	67.7%	32.3

Note for column 3:

v.3.1 or 2.1—material model version

1, 2, 4, 6, 8, 12, and 24 are the number of FE shell layers simulating the total number of fabric layers

h = Honeywell model

s = SRI model

For SRI model, l = loose fabric layers, t = tight fabric layers

The absorbed kinetic energy is not the only factor used to compare test results to simulation results. The plot of the projectile velocity is also very important in analyzing a simulation. Plots of projectile velocity versus time for cases LG411, LG655, and LG657 used for material model version comparison are in figures 28 through 30. A point showing the final test projectile velocity is also introduced in these plots for reference. Plots of projectile velocity versus time for the simulations using the generic blade containment model are shown in figure 31. Note in figures 28 through 31, the legend notation is defined as v.3.1 or 2.1—material model version; h = Honeywell model; s = SRI model (for this model, l = loose fabric layers, t = tight fabric layers); 1, 2, 4, 6, 8, 12, and 24 are the number of FE shell layers simulating the actual number of fabric layers.

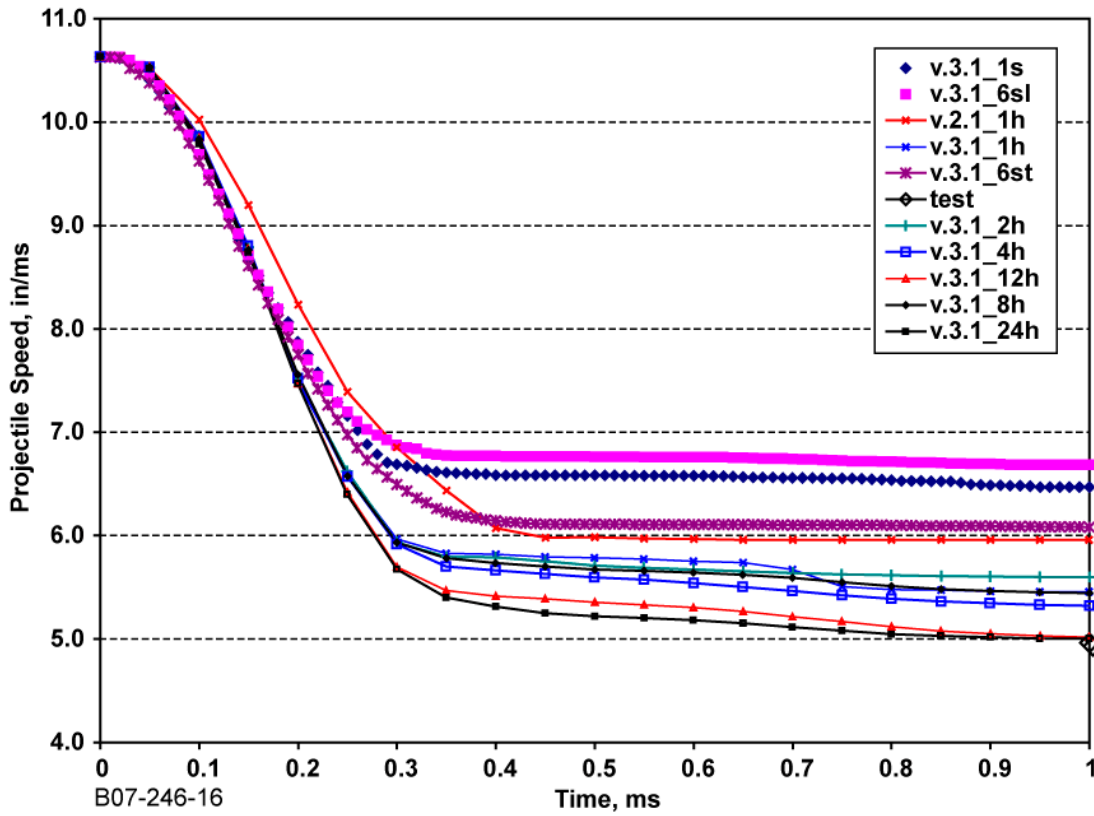


Figure 28. Ballistic Test Case Simulations Results Showing Velocity Versus Time Compared to Test Final Projectile Velocity for NASA-GRC Test LG411

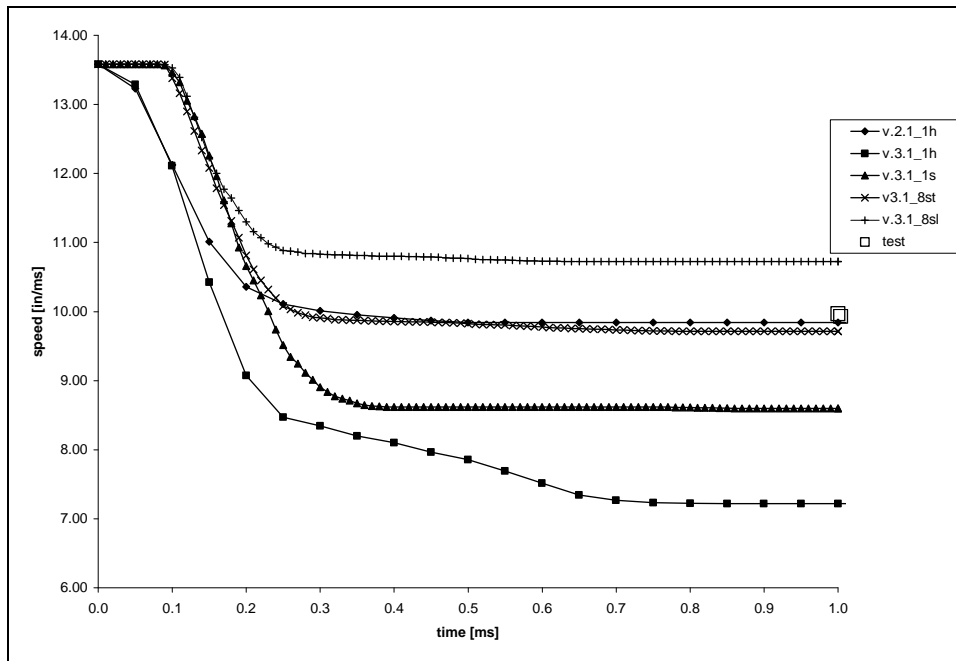


Figure 29. Ballistic Test Case Simulations Results Showing Velocity Versus Time Compared to Test Final Projectile Velocity for NASA-GRC Test LG655

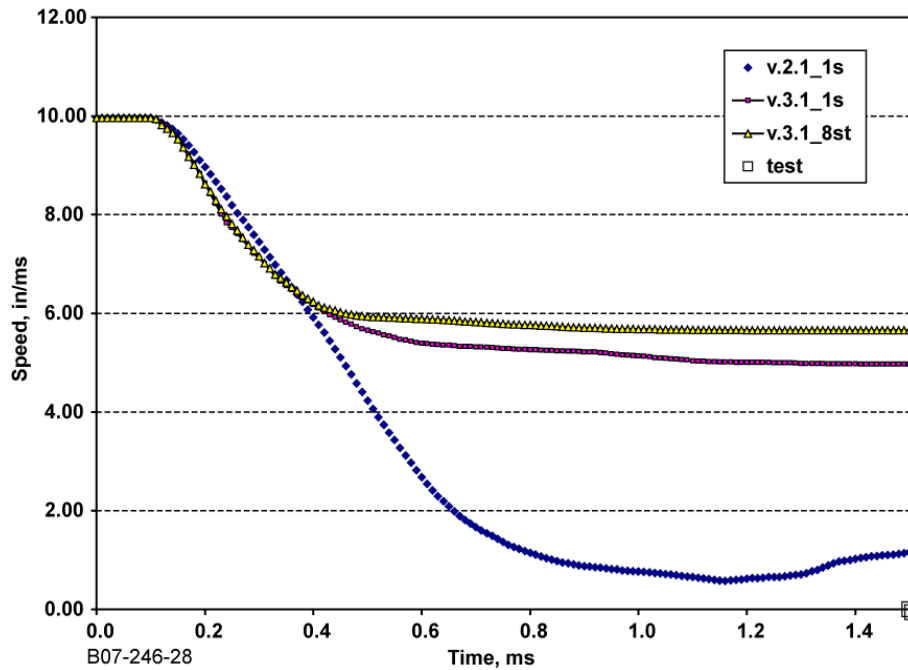
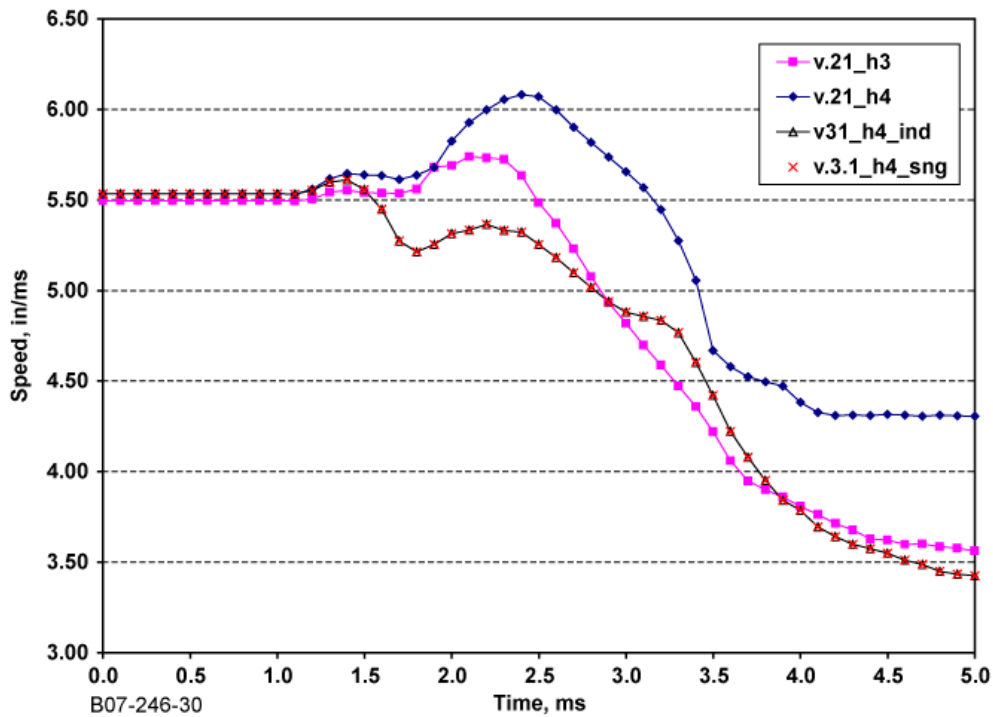


Figure 30. Ballistic Test Case Simulations Results Showing Velocity Versus Time Compared to Test Final Projectile Velocity for NASA-GRC Test LG657



Notes: h3 or h4 = hourglass formulation
ind = individual part contact
sng = single contact

Figure 31. Velocity Plots for Simulations Using the Basic Generic Blade Containment Model

The comparison of results is also meaningful when detailed plots of all energies calculated during the LS-DYNA simulations are examined. Plots using the glstat LS-DYNA output files were used to examine the energy balance during a simulation. These plots are shown for cases LG411 in figures 18, 20, 22, 24, and 26. Section 2.5 provides guidelines on plot interpretation.

3.5 CONCLUSIONS FOR TASK 2.

Examination of all results using the methods described in section 3 produced the following conclusions.

- Material model version 3.1 works well for multiple FE shell layer models based on examination of absorbed kinetic energy and projectile velocity. Energy plots using glstat confirm the conclusion. Material model version 2.1 simulations failed when IHQ = 4 was used for multiple-layer simulations.
- A comparison of absorbed energies shows that multiple-layer simulation produced similar results with single-layer simulations when material model version 3.1 and up to eight shell-element layers were used.
- Examination of energy plots revealed that simulations involving more than four FE shell layers in the model produce erroneous results, even though the absorbed kinetic energy was close to the energy absorbed during the actual test. This is considered to be the result of LS-DYNA error accumulation and confirms the conclusions of the work done in Phase I. However, the absorbed energy comparison results are very good, meaning that a multiple-layer modeling approach may be very successful once software and material model issues are optimized.
- The multiple-layer modeling validity conclusion is also supported by the simulation projectile velocity being closest to the test velocity when the number of FE shell-element layers is increased.
- SRI's approach with loose fabric introduces more numerical errors, and the absorbed energy difference is opposite of the tight model results (i.e., tight underpredicts and loose overpredicts). If the tight Phase I approach is used, the simulation is slightly better and the difference in absorbed energy is similar to the single-layer simulation results. This conclusion is confirmed by examination of the energy plots from LS-DYNA. One run shows excellent visual agreement with the test and no difference between tight or loose fabric modeling in the energy absorbed, but the energy plots show errors, such as kinetic energy higher than total energy.
- Ballistic impact test simulations using material model version 2.1 and multiple shell-element layers failed when IHQ = 4 was used, but generic engine fan blade-out simulations using the same material model version converged when IHQ = 3 was used. This indicates that the material model version is very sensitive to the hourglass control parameter.

- The stiffness-based hourglass control (IHQ = 4) is recommended for material model version 3.1.
- Results for models with 32 fabric layers do not match the test when the projectile is contained (the projectile is not contained for all simulations, regardless of material model or number of FE shell layers), and seem to contradict the trends for all other tests. Because this conclusion is based on single test case, further work is needed to understand this issue.
- With regard to the methodology, simulations performed using Honeywell's approach, which has several contact cards for the parts in the model, produced results closer to the ballistic tests than the results using SRI's single contact card approach.
- Each computer platform yielded slightly different results for the same models. The double-precision UNIX runs were the most accurate.
- Different LS-DYNA parameters (SFS and TSSFAC in conjunction with IHQ) need to be used when simulating a ballistic impact test or an engine fan blade-out test. The main explanation for this phenomenon in these cases is the shape of the projectile and the difference in the impact and fabric damage mechanism.

After finalizing this task, the process needed to validate a material model was clearly understood. The following steps are recommended for a sound material model validation process: (Figure 32 shows a flow chart of this process.)

1. Establish a matrix of variation for the most critical LS-DYNA parameters. Among them, IHQ in conjunction with TSSFAC and SFS are the most important. The matrix will be used for all simulations to determine the best combination.
2. Run simulations for one single shell-element layer model and one multiple shell-element layer model for two ballistic impact test cases: one where the projectile was contained and one where the projectile was not contained. Use three shell layers initially on the available models. Using the matrix of step 1, decide on the best LS-DYNA parameters to use for single and multiple shell-element layer simulations, respectively.
3. Simulate a straight projectile ballistic impact test for 1 through 24 shell-element layers (for example, case LG411) using the multiple shell-element layer modeling approach. Determine the number of shell-element layers for which the simulation is error-free and, hence, the number of shell-element layers that makes sense to use in the following simulations.
4. Simulate straight projectile ballistic impact tests (cases LG403, LG404, LG411, LG432, and LG572) using the single shell-element layer modeling approach.
5. Simulate rotated projectile ballistic impact tests (cases LG594, LG609, LG610, LG611, LG612, LG618, LG620, LG655, LG657, LG688, LG689, LG692, and LG694) using the single shell-element layer modeling approach.

6. Simulate straight projectile ballistic impact tests of Step 3 using the multiple shell-element layers modeling approach for the methodology obtained in Step 3.
7. Simulate rotated projectile ballistic impact tests of Step 4 using the multiple shell-element layers modeling approach for the methodology obtained in Step 3.
8. Use an engine fan blade-out, generic, reduced-size model to verify and optimize simulation parameters for the single shell-element layer modeling approach, if available; this would be derived from the generic engine fan blade-out model. Verify that the simulations for blade, case, and fabric damage match with actual test results. A matrix for variation of LS-DYNA parameters, like the one of Step 1, may be necessary.
9. Based on results from Step 3, use the generic engine fan blade-out model for the number of shell-element layers that makes sense. Establish the number of multiple shell-element layers that best matches the fabric damage for the actual tests.

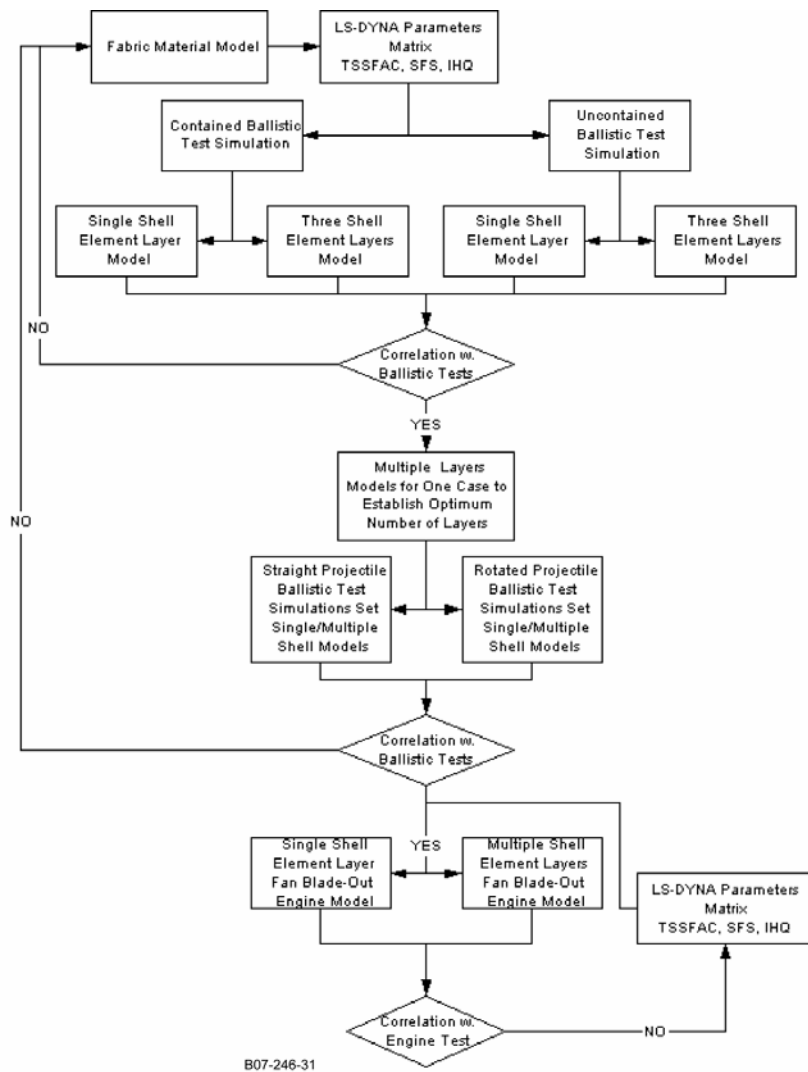


Figure 32. Material Model Calibration Thought Process Map

3.6 PHASE II MODEL IMPROVEMENTS.

The following improvements were made compared to Phase I.

- The assessment of the simulations was improved by introducing the examination of the energies from the glstat and matsum files. In the past, the simulation was assessed mostly visually. With the current methodology, simulations with numerical errors can be discarded.
- A process for material model validation was developed.
- Simulations using multiple shell-elements layers greatly improved with the latest material model version 3.1 and LS-DYNA technology. The energy absorbed during simulations was very close to the energy absorbed during test using the single shell-element layer approach.
- A process for continuously collaborating and benchmarking with LSTC was developed. LSTC is now fully involved in developing and validating new material models and methodologies.

3.7 RECOMMENDATIONS FOR TASKS 1 AND 2.

Based on conclusions drawn from work on Tasks 1 and 2, Honeywell recommended the following:

1. Further material model improvement and work should be performed with LSTC to understand the optimum number of fabric wraps to be simulated by one FE shell layer.
2. More ballistic impact tests are needed for cases when the projectiles are contained. Until now, the majority of the tests focused on cases with projectile penetration. A material model must be able to correctly simulate both contained and uncontained projectile cases.
3. A methodology to measure fabric displacement during the tests is desirable. Currently, fabric deformation is mostly visually compared.
4. The physics of a ballistic impact test is different than that of a fan blade-out test; this becomes more evident through the fact that different LS-DYNA parameters are needed for generic fan blade-out model simulations. Spin pin tests are recommended if a material model that accurately captures the physics of the blade-fabric interaction is desired.

4. NUMERICAL SIMULATION OF ENGINE FAN BLADE-OUT TESTS (TASK 4).

4.1 BACKGROUND AND OBJECTIVE.

In Phase I, the HTF7000 engine fan blade-out event was successfully simulated using the fabric material models and analytical methodologies were developed. Acceptable correlation was

obtained between the simulation results and the engine fan blade containment test results, using the Kevlar material model version 1.0 and the single shell layer modeling technique. Prediction capability significantly improved with the new material model and the associated modeling techniques, with respect to previously used methodologies [1]. However, despite successful results during the ballistic impact test simulations, further analytical enhancement with multilayer modeling was not possible due to extensive element distortion and numerical instabilities.

As in Phase I, the objective of Task 4 was to validate improvements to the material models and FE methods developed under Phase II as they relate to propulsion engine fan blade containment. The primary objective of Task 4 was to validate the Kevlar material models developed for use in LS-DYNA fan containment analyses; the Zylon material model development was eliminated from this study due to environmental-deterioration issues of the fabric. Both the single and multiple shell-element layer methodologies developed in Tasks 1 and 2 were planned to be validated.

4.2 ANALYTICAL PROCEDURE.

To achieve the objectives of Task 4, Honeywell simulated two actual engine fan blade-out tests using the material model and the analysis techniques developed during Tasks 1 and 2. The detailed steps for the analytical effort were:

1. Two Honeywell turbofan engine models were chosen to validate the techniques developed in Tasks 1 and 2. The first engine model was of the HTF7000 fan blade-out development test used in Phase I. The second was a model developed to simulate the CFE738 engine Federal Aviation Administration (FAA) certification fan blade-out test performed in March 1993.
2. The fabric material model codes (developed in previous tasks) were used in the Task 4 analyses to simulate the engine fan blade containment. The typical LS-DYNA input deck included the model file (FE nodes and elements), the user-controlled material input parameters, the contact file defining the contact types to be used, and LS-DYNA control parameters from Tasks 1 and 2.
3. The analytical predictions were compared to the two engine fan blade-out tests results, in the form of engine hardware pre- and posttest pictures, which allowed qualitative comparison of the ability of LS-DYNA to predict various failure modes against actual engine test results.
4. The qualitative comparison was complemented with the examination of the LS-DYNA results from the glstat and matsum files for all simulations to determine the correctness of the numerical simulation.
5. Plots of the blade kinetic energy versus time were also examined to comparatively assess all results.

4.2.1 Engine Fan Blade-Out Test Results.

In 1999, during development of the new Honeywell HTF7000 turbofan engine, a containment test was conducted on a full-scale engine, to verify the fan blade-out containment and related design features, prior to the official certification test required by the FAA. An overall view of this engine is shown in figure 33. The HTF7000 fan containment design incorporates composite fabric wraps with material properties equivalent to Kevlar. The number of layers required to adequately contain a possible fan blade separation was calculated using empirical Kevlar penetration design curves, based on Honeywell experience with similar designs. The diameter of the HTF7000 containment system was comparable to the diameter of the ballistic impact test target ring in this project.



B07-246-32
Figure 33. The HTF7000 Honeywell Turbofan Engine Overall View

During the engine fan blade-out containment test, a fan blade was intentionally released (by artificial means) while the engine continued to operate for 15 seconds; then, the engine was shut down by the operator. Fan blade-out containment was achieved. The released blade penetrated the containment system, but stopped between the fan housing and the fabric wraps. Figure 34 shows the disassembled fan housing (immediately after the test) with the intentionally released blade at its resting position. The airfoil penetrated the containment system up to approximately mid span, but the heavier root section, including the platform and the shank, was contained within the fabric wraps. The blade tip was damaged and bent due to the resulting impact. More details and photographs of post-blade-out test HTF7000 engine hardware are shown in reference 1. Although this containment test was successful, the design was modified for certification tests by increasing the number of layers by approximately 15 percent to achieve an additional safety

margin. As a result, during the official HTF7000 certification test, the intentionally separated fan blade was entirely contained within the fabric containment system.

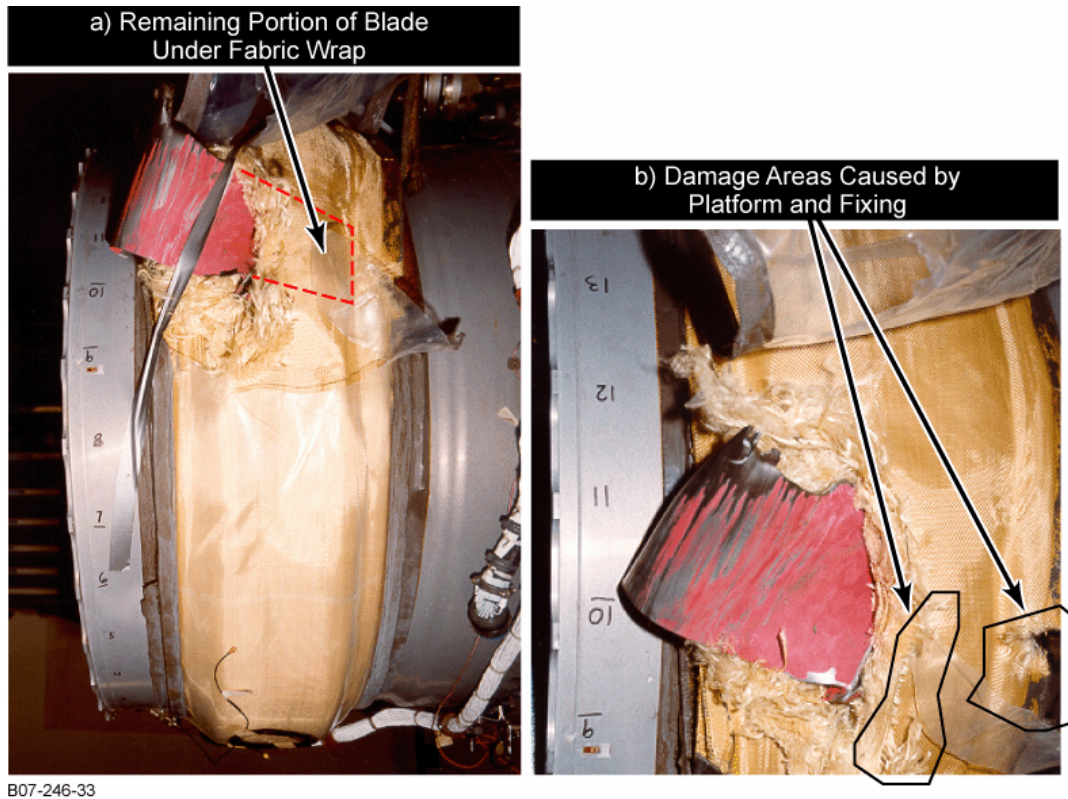


Figure 34. The HTF7000 Fan Containment Housing Following Blade-Out Test (Fabric and blade damage areas are shown.)

The same design philosophy was used for the CFE738 engine (figure 35) fan blade containment case, incorporating composite fabric wraps with material properties equivalent to Kevlar. An FAA certification test was performed in 1993. The number of layers required to contain a separated fan blade was calculated using empirical Kevlar penetration design curves. The fan blade-out test was performed in a similar manner to the test described above for the HTF7000 engine. Complete fan blade-out containment was achieved and the released blade penetrated the containment system, but stopped between the fan housing and the fabric wraps (figures 36 and 37). The airfoil penetrated the containment system, up to approximately the mid-span dampers level, but the heavier root section, including the platform and the shank, was properly contained within the fabric wraps. The blade tip was fractured above the damper (figure 36). Figure 38 shows the damage sustained by the trailing blade.



B07-246-34

Figure 35. The CFE738 Turbofan Engine Overall View



B07-246-67

Figure 36. The CFE738 Fan Containment Housing Following Blade-Out Test, Internal View (Housing and blade damage areas of are shown.)

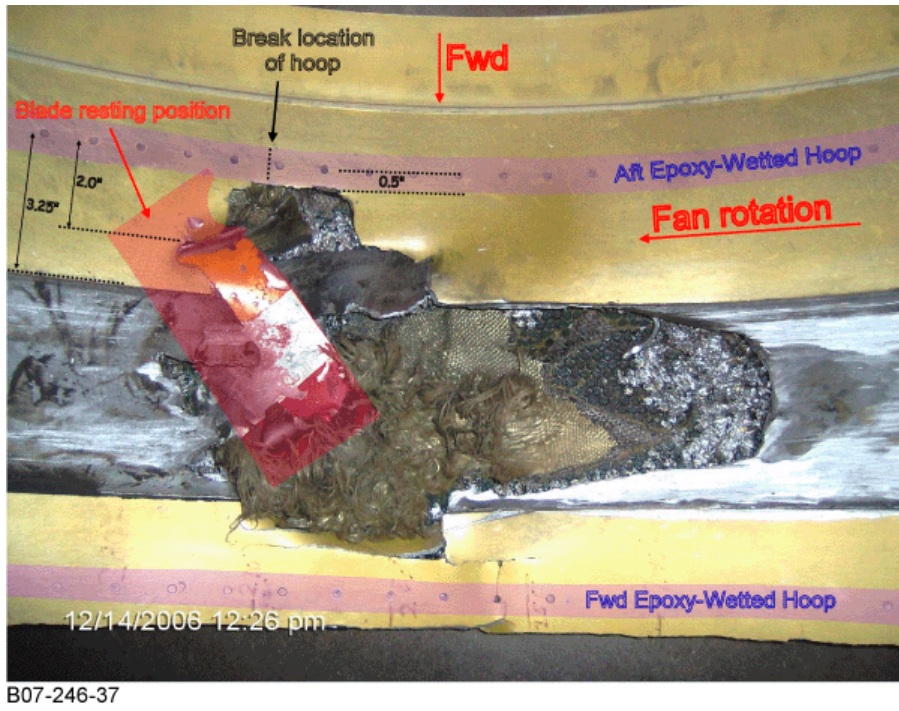


Figure 37. The CFE738 Trailing Fan Blade Damage After the Fan Blade-Out Test

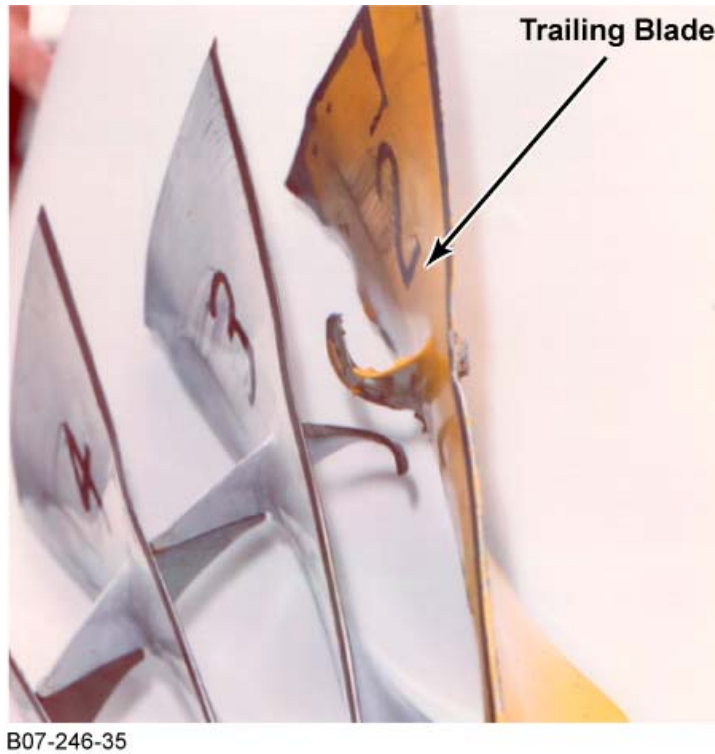


Figure 38. The CFE738 Fan Containment Housing Following Blade-Out Test, External View (Fabric and blade damage areas are shown.)

4.2.2 The FE Engine Fan Blade-Out Models.

The same FE model of Phase I was used for simulating the HTF7000 engine fan blade-out. This reduced model includes two blades (one released and one trailing) and the fan containment hardware, with one shell-element layer representing all fabric layers and the other layers including the metallic housing, abrasion coating, honeycomb, and graphite epoxy shell (figure 39). The conclusions from Tasks 1 and 2 were applied to guide the multiple shell-element layers modeling approach. Two additional versions of the model were built: a second version with three shell-element layers, representing all fabric wraps, and a third version with four shell-element layers, representing all fabric wraps.

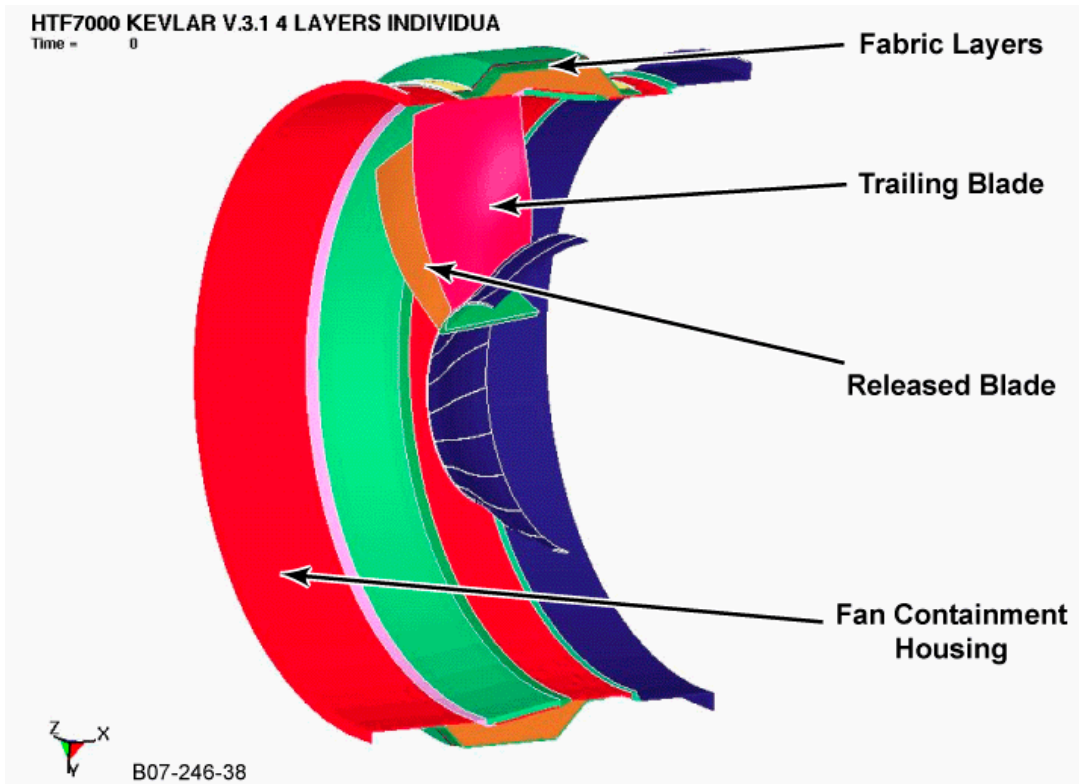


Figure 39. The HTF7000 LS-DYNA Model for Fan Blade-Out Containment Analysis

The FE model for simulating the CFE738 engine fan blade-out had more inherent complexity. Based on results of Phase I, all fan blades were modeled in this phase, as they hit the released blade and have an influence on its final position. A fan inlet housing and a front frame were also modeled (figure 40). Similar to the HTF7000 model, one, three, and four shell-element layers were used to represent all fabric layers. Solid hexahedron and shell elements were used to represent the metallic housing, abrasion coating, honeycomb, and the graphite epoxy shell.

Both FE engine models incorporated technology developed in Phase I and Phase II. The blades were modeled with solid hexahedron elements and the size of the Kevlar shell elements was maintained at 0.25 inch.

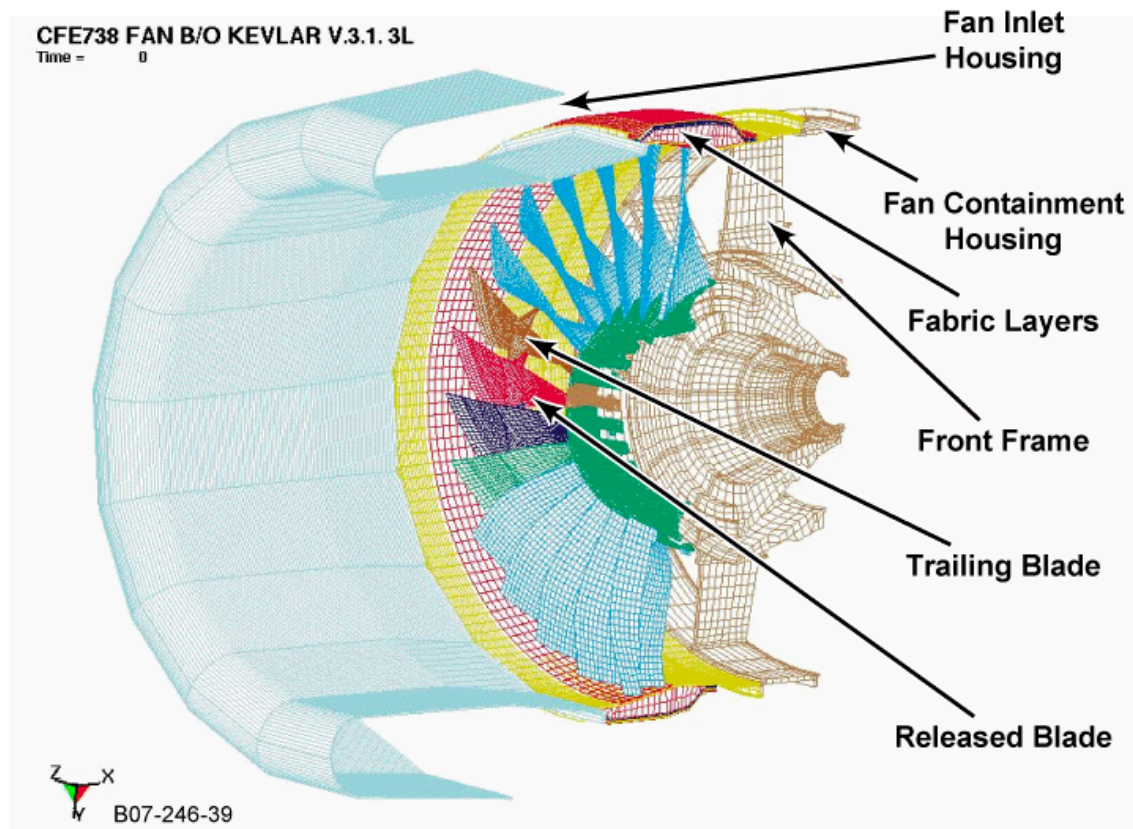


Figure 40. The CFE738 LS-DYNA Model for Fan Blade-Out Containment Analysis

4.2.3 Qualitative Comparisons Between the Simulations and Tests.

The focus of the predictions was to match the overall behavior in both engine tests. Predictions obtained with the simulation technology of the Phase I for the HTF7000 engine are shown in figure 41. Predicted damage to the internal (non-fabric) components of the containment system is shown. The extent of damage made by the blade, the size of the opening before reaching the fabric layers, and the location of the impact of the heavy blade shank with the housing wall were captured realistically. Similarly, the deformed posttest shape of the blade was successfully predicted; for example, the tip section curved opposite to the direction of rotation, the tip leading edge and the shank trailing edge were severely damaged, and the platform was severed by the impact of the trailing blade. This type of detailed information permits the containment designer to consider other aspects of the fan containment problem, such as support structure integrity, blade design, etc. Using the latest technology, the same level of fidelity of prediction was expected during Phase II for both engine models. Moreover, a successful simulation would predict that the fabric layers would be punctured by the blade tip at the front portion of the containment system, and that the blade tip would be exposed in both engine tests (figure 34 for the HTF7000 engine and figure 36 for the CFE738 engine, respectively). The damage caused by the heavy root portion of the blade at the aft section of the fabric system would also be realistically captured. The puncture of the fabric layers by the blade tip was only partially predicted in Phase I. There, the simulations exhibited high deformation of the fabric, but the penetration was not complete.

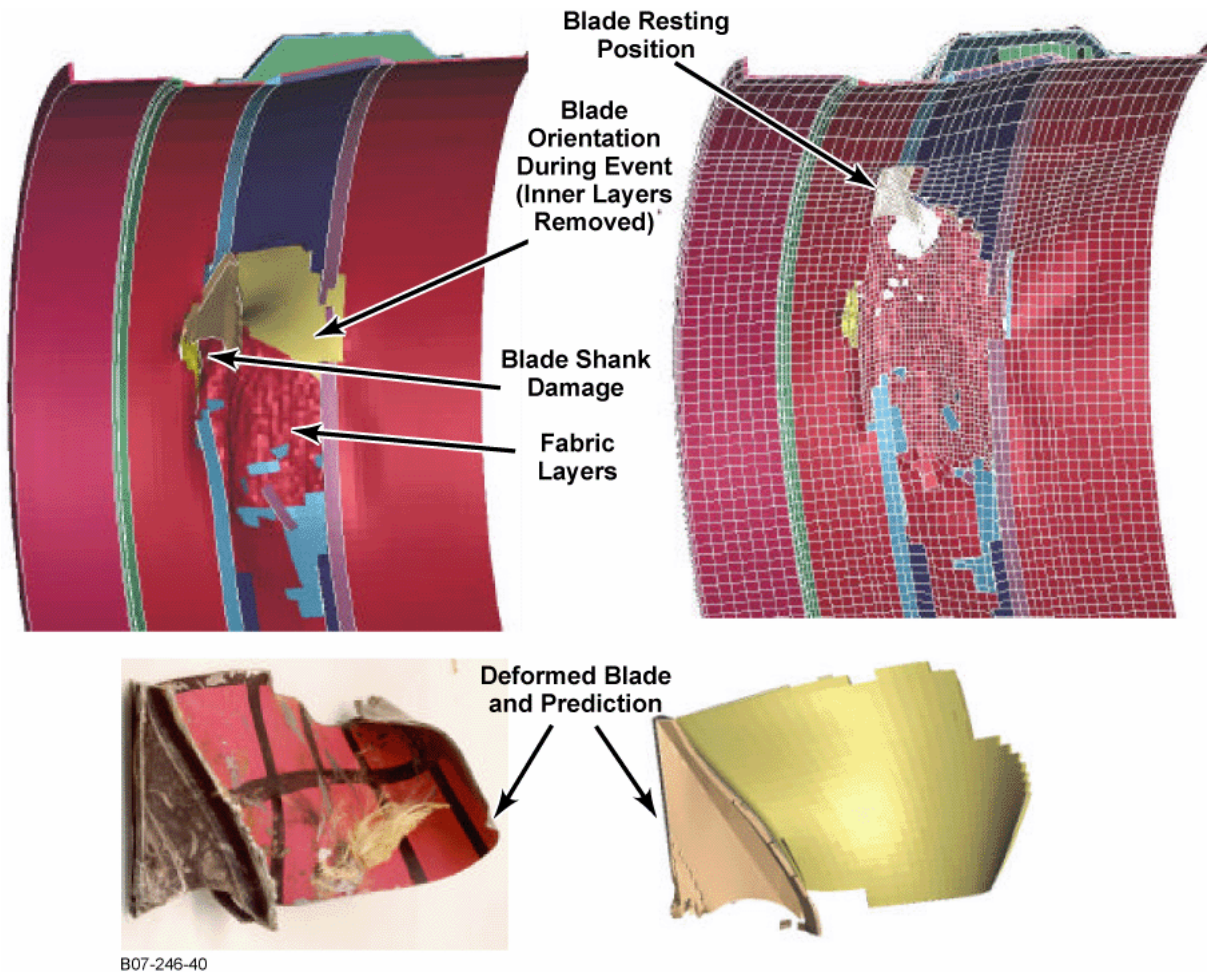


Figure 41. The HTF7000 Fan Blade-Out Simulation Results of Phase I [4]

4.2.4 The LS-DYNA Simulation Procedure.

The same combination of LS-DYNA parameters (SFS and TSSFAC in conjunction with IHQ), as in the ballistic test simulations, were used initially. After poor results, the combinations used in the generic fan blade-out engine model simulations were exercised. Viscous (IHQ = 3) hourglass control was used for material model version 2.1 simulations based on the conclusions from Tasks 1 and 2 (sections 2 and 3). Both stiffness (IHQ = 4) and viscous (IHQ = 3) hourglass control parameters were used for material model version 3.1 simulations, based on SRI's conclusions that there is no major difference between them (see Phase II, Part 3).

Friction was not considered for material model version 2.1 simulations, as it was not studied during the material model definition process. For material model version 3.1, friction was introduced using the LS-DYNA contact parameter $FS=FD=0.2$, based on SRI's recommendation and the tests performed by ASU. The effect of using DAMPING_PART_STIFFNESS was not studied, but should be studied in the material model validation process.

The following parameters were varied in the analyses.

1. For the HTF7000 engine fan blade-out model simulations:
 - (a) Material model version 2.1, fabric simulated by a single shell-element layer:
 - Global, single contact card, no friction, IHQ = 3
 - Individual contact cards, no friction, IHQ = 3
 - Five percent increase in blade release speed, no friction, IHQ = 3
 - Epoxy-wetted ends of fabric layers was simulated by fixing the ends of the single shell-element layer, no friction, IHQ = 3
 - (b) Material model version 3.1, fabric simulated by a single shell-element layer:
 - Individual contact cards, no friction
 - Global, single contact card with friction
 - Individual contact cards with friction and IHQ = 4
 - Individual contact cards with friction and IHQ = 3
 - (c) Material model version 2.1, fabric simulated by three shell-element layers:
 - Global, single contact card, no friction, IHQ = 4
 - Individual contact cards, no friction, IHQ = 3
 - (d) Material model version 3.1, fabric simulated by three shell-element layers:
 - Individual contact cards with friction and IHQ = 4
 - Individual contact cards with friction and IHQ = 3
 - (e) Material model version 3.1, fabric simulated by four shell-element layers:
 - Individual contact cards with friction and IHQ = 4
 - Individual contact cards with friction and IHQ = 3
2. For the CFE738 engine fan blade-out model simulations:
 - (a) Material model version 2.1, fabric simulated by a single shell layer:
 - Global, single contact card, no friction, IHQ = 3
 - Individual contact cards, no friction, IHQ = 3
 - Individual contact cards, no friction, IHQ = 4

- (b) Material model version 3.1, fabric simulated by a single shell layer:
 - Individual contact cards with friction and IHQ = 4
 - Individual contact cards with friction and IHQ = 3
- (c) Material model version 3.1, fabric simulated by three shell-element layers:
 - Individual contact cards with friction and IHQ = 3
 - Individual contact cards with friction and IHQ = 4
- (d) Material model version 3.1, fabric simulated by four shell-element layers:
 - Individual contact cards with friction and IHQ = 3
 - Individual contact cards with friction and IHQ = 4

4.3 ANALYSIS RESULTS.

The assessment of the simulation results involved the following three methods: a qualitative comparison of the ability of LS-DYNA to predict various failure modes against actual engine test results, the examination of the LS-DYNA results from the glstat and matsum files, and a comparison of the plots of the blade kinetic energy versus time. Only results of the most successful predictions are presented.

4.3.1 Results for the HTF7000 Engine Simulations.

- Simulations using the single shell-element layer technology with material model version 2.1 were generally similar to simulations of Phase I, as the modifications to the Kevlar material model were minor. For blade orientation, deformed blade shape and damage, and containment housing damage, the majority of the simulations predictions were close to the test. Figure 42 shows an example of the predictions. Fabric damage was relatively underpredicted when no change was made to the model used in Phase I; considerable fabric deformation was present, but no blade penetration or fabric failure occurred. The best case was when the epoxy-wetted ends of the fabric were simulated. Fabric damage at both ends was properly predicted (figure 43). Another simulation with a 5% increase in blade release speed produced similarly improved results. Thus, fabric penetration was not accurately predicted in the Phase I due to two factors: (1) the lack of simulation of the epoxy-wetted ends of the fabric and (2) the lack of presence of all blades, which pushed the released blade further inside the containment area.

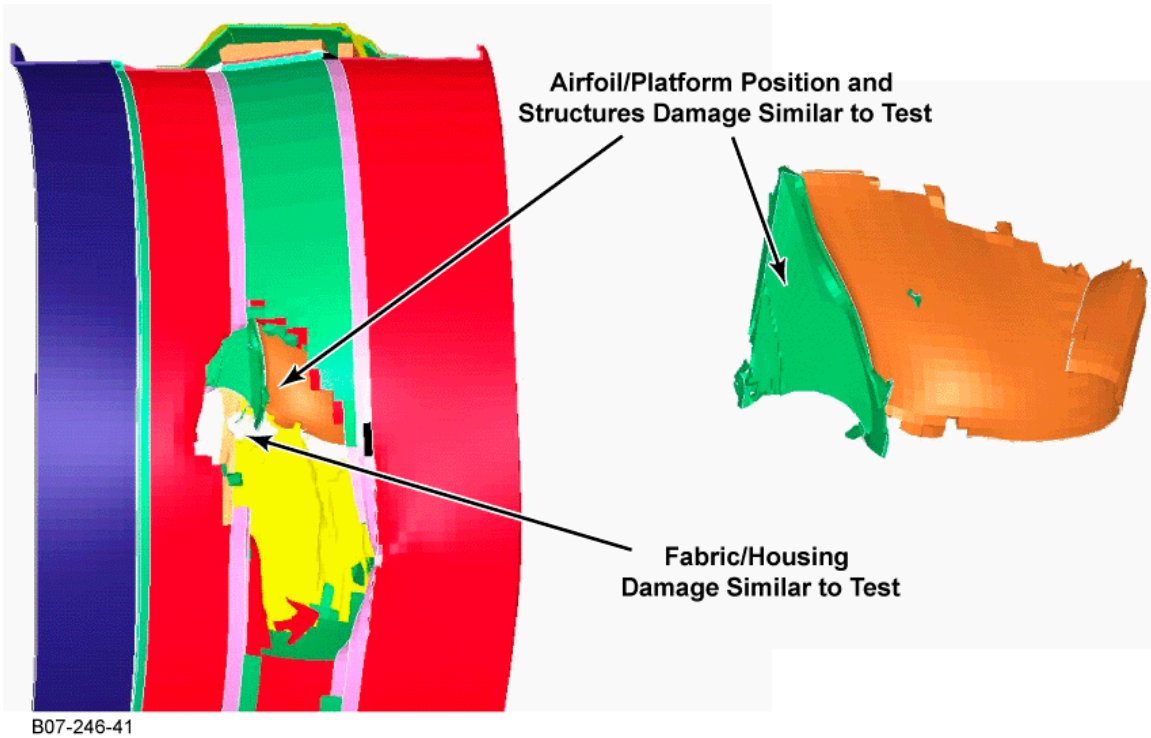


Figure 42. The HTF7000 Engine Blade Orientation and Deformed Blade Prediction for Simulation Using One Kevlar Shell Layer With Wetted Ends, Material Model Version 2.1, and Individual Contact Cards

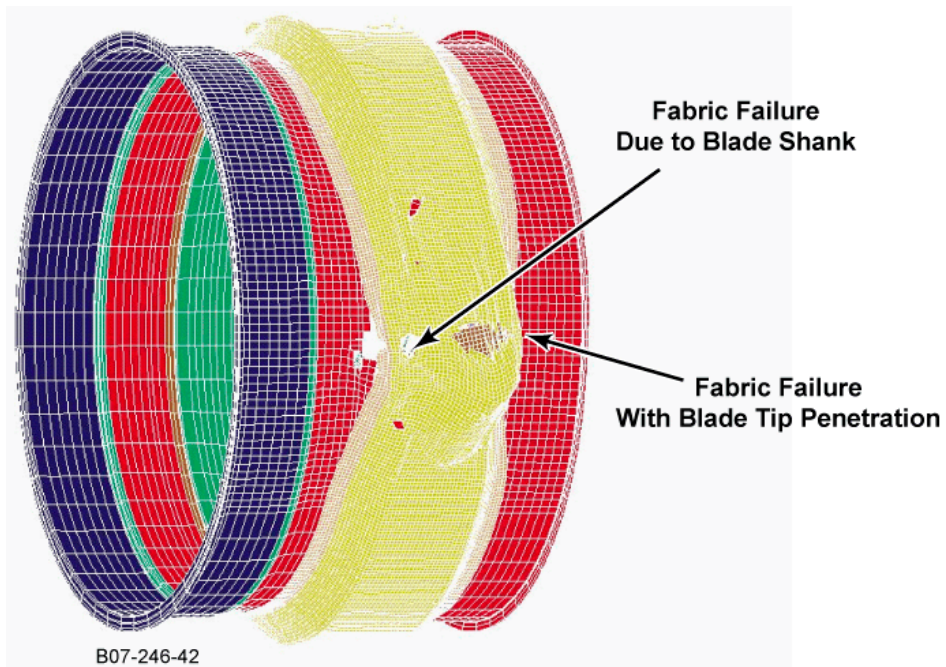


Figure 43. The HTF7000 Engine Fabric Aspect Showing Penetration for Simulation Using One Kevlar Shell Layer With Wetted Ends, Material Model Version 2.1, and Individual Contact Cards

- Examination of the glstat and matsum plots for single shell-element layer simulations revealed that for material model version 2.1 simulations using IHQ = 3, the results were normal, but the hourglass energy for the fabric was high (figures 44 and 45).
- For material model version 2.1 single shell-element layer simulations, plots of the blade kinetic energy versus time revealed that all simulations using individual contact cards for each contact between parts produced very close results. Simulations using a single global contact card, while faster, resulted in some difference in blade kinetic energy (figure 46). In addition, the analysis exhibited numerical instability.
- Simulations using multiple shell-element layer technology with material model version 2.1 converged, but the results were not correct, showing complete erosion of too many aluminum housing elements. Comparison with successful simulations using Honeywell's generic engine fan blade-out model led to the conclusion that the instability and excessive element distortion were probably due to the presence of thick shell elements in the HTF7000 model. Thus, thick shell elements were not included in the CFE738 model. Another reason may be that the use of IHQ = 4 as simulations using IHQ = 3 exhibited less element erosion and less hourglass effect.
- Simulations using the single shell-element layer technology with material model version 3.1 were also successful when predictions compared the blade orientation, deformed blade shape and damage, and containment housing damage, to the test results. Fabric damage prediction was slightly better. Damage was noticed at the wetted hoop, which was produced by the released blade shank, as observed in the test (figure 47).
- Examination of the glstat and matsum plots (figures 48 and 49) showed that for single shell-element layer simulations using material model version 3.1 and IHQ = 4, the simulation was error-free, but the hourglass energy for the fabric was high (figure 49).
- Simulations using multiple shell-element layer technology with material model version 3.1 converged successfully and predicted the housing and blade deformation and damage very well. When IHQ = 4 was used, the fabric damage was slightly underpredicted; high deformation was noticed, but no failure of the last shell-element layer occurred. However, when IHQ = 3 was used, for the simulations using a total of three shell-element layers for all fabric wraps (figure 50), damage for the third (last) layer was similar to the test, with failures due to both the blade shank and the blade tip. The blade tip did not completely penetrate the shell layer. Simulations using a total of four shell-element layers for all fabric wraps did not exhibit failure of the last shell-element layer, thus underpredicting the fabric damage.
- Examination of the glstat and matsum plots (figures 51 and 52) showed that for three shell-element layer simulations using material model version 3.1 and IHQ = 3, the simulation was error-free, but the hourglass energy for the fabric was high.

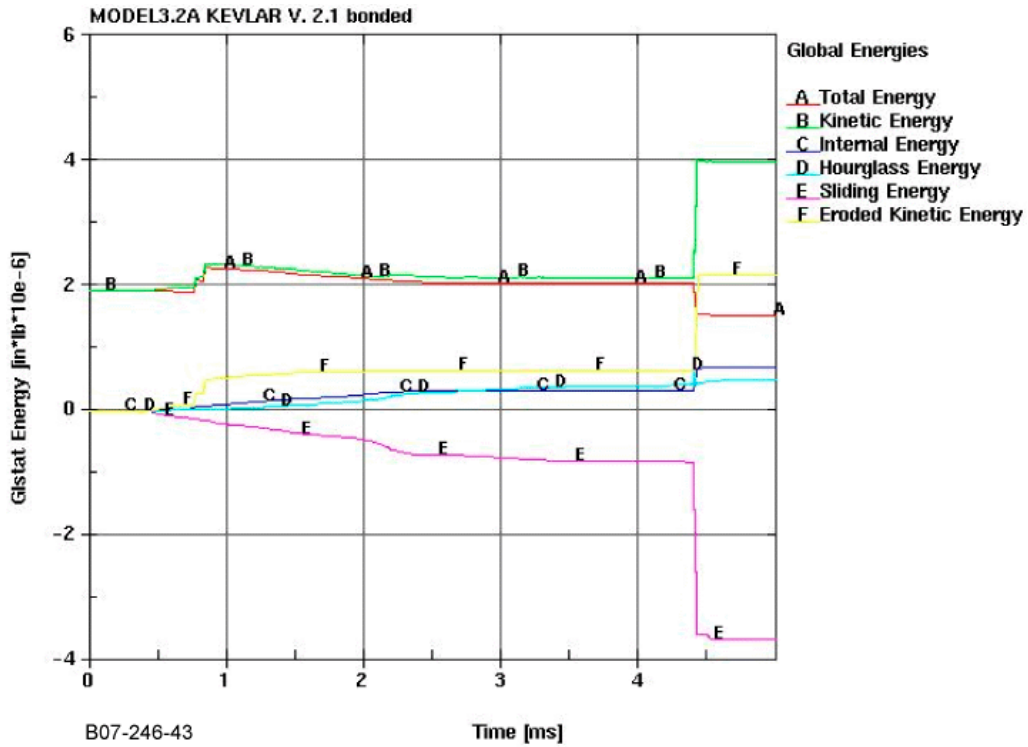


Figure 44. The HTF7000 Engine Global Gstat Data for Simulation Using One Kevlar Shell Layer With Wetted Ends, Material Model Version 2.1, and Individual Contact Cards

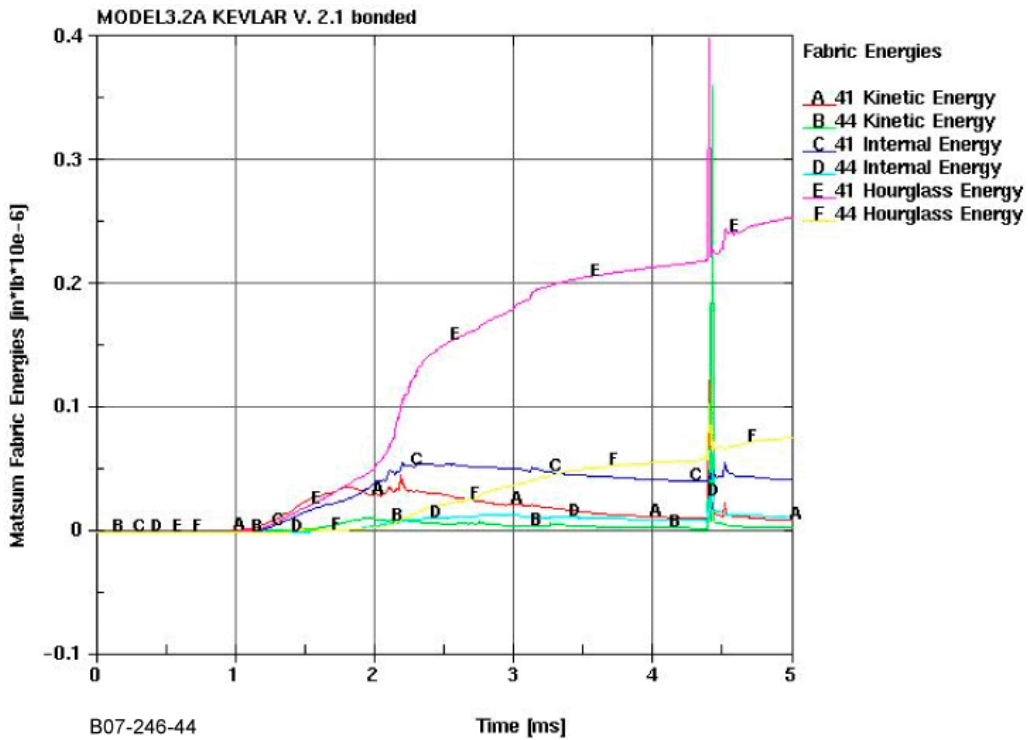


Figure 45. The HTF7000 Engine Fabric Matsum Data for Simulation Using One Kevlar Shell Layer With Wetted Ends, Material Model Version 2.1, and Individual Contact Cards

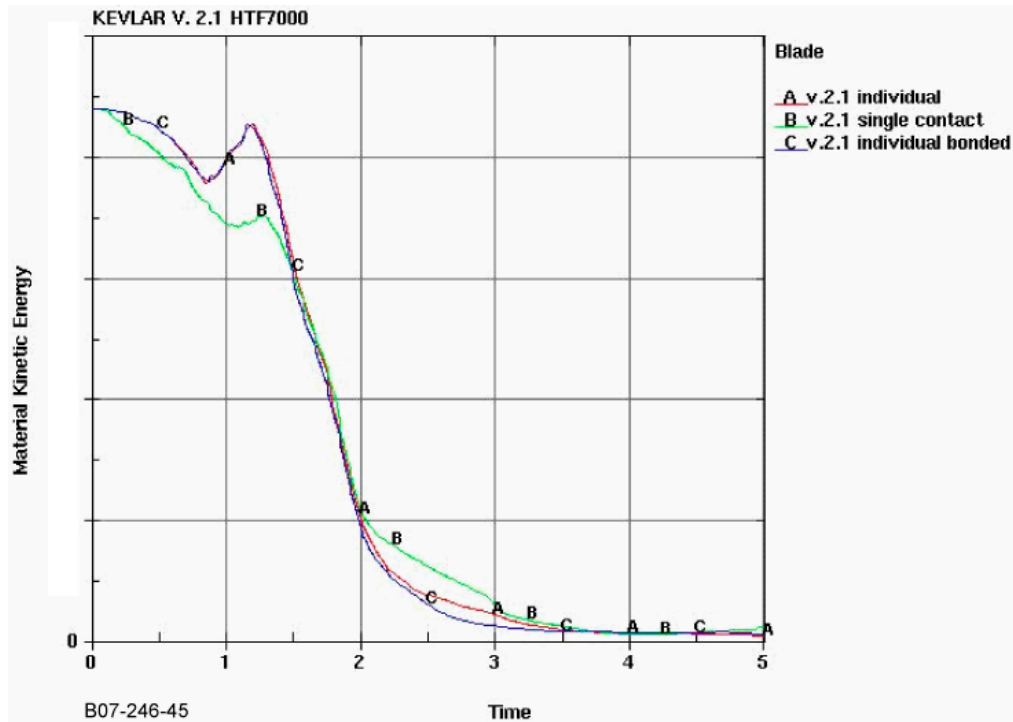


Figure 46. The HTF7000 Engine Blade Kinetic Energy Data for Simulations Using One Kevlar Shell Layer and Material Model Version 2.1



Figure 47. The HTF7000 Engine Fabric Aspect for Simulation Using One Kevlar Shell Layer, Material Model Version 3.1, Individual Contact Cards With Friction, and IHQ = 4

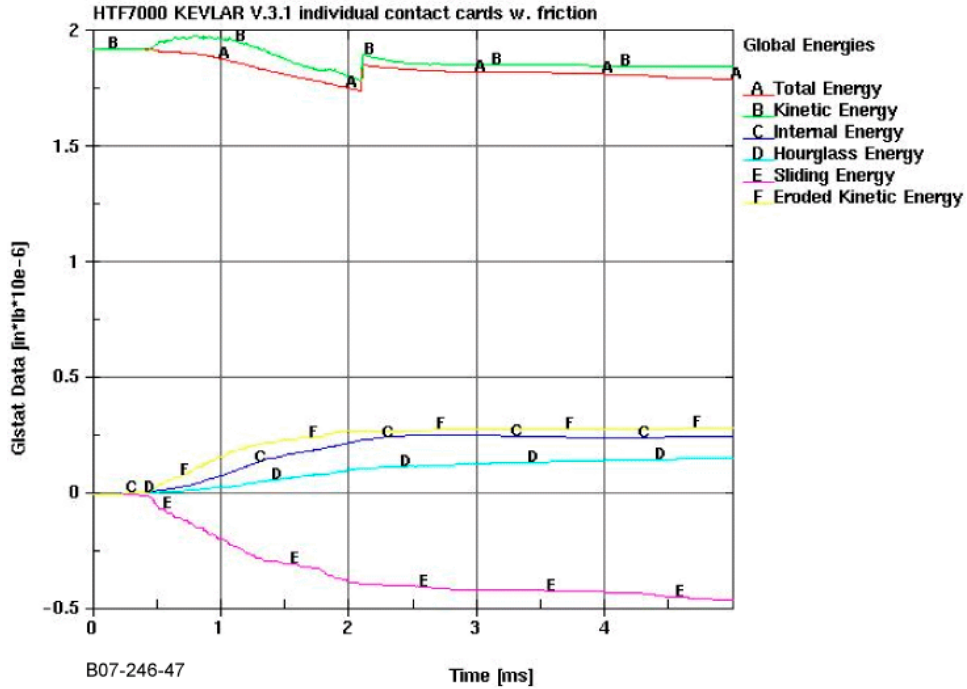


Figure 48. The HTF7000 Engine Global Gstat Data for Simulation Using One Kevlar Shell Layer, Material Model Version 3.1, Individual Contact Cards With Friction, and IHQ = 4

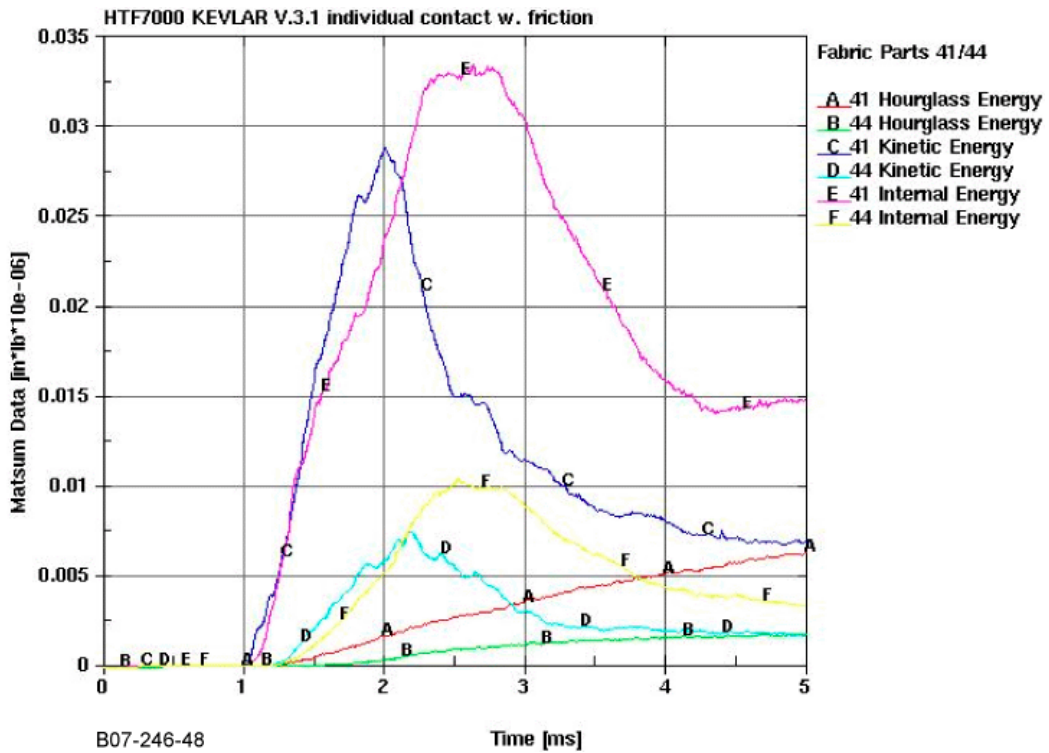


Figure 49. The HTF7000 Engine Fabric Matsum Data for Simulation Using One Kevlar Shell Layer, Material Model Version 3.1, Individual Contact Cards With Friction, and IHQ = 4

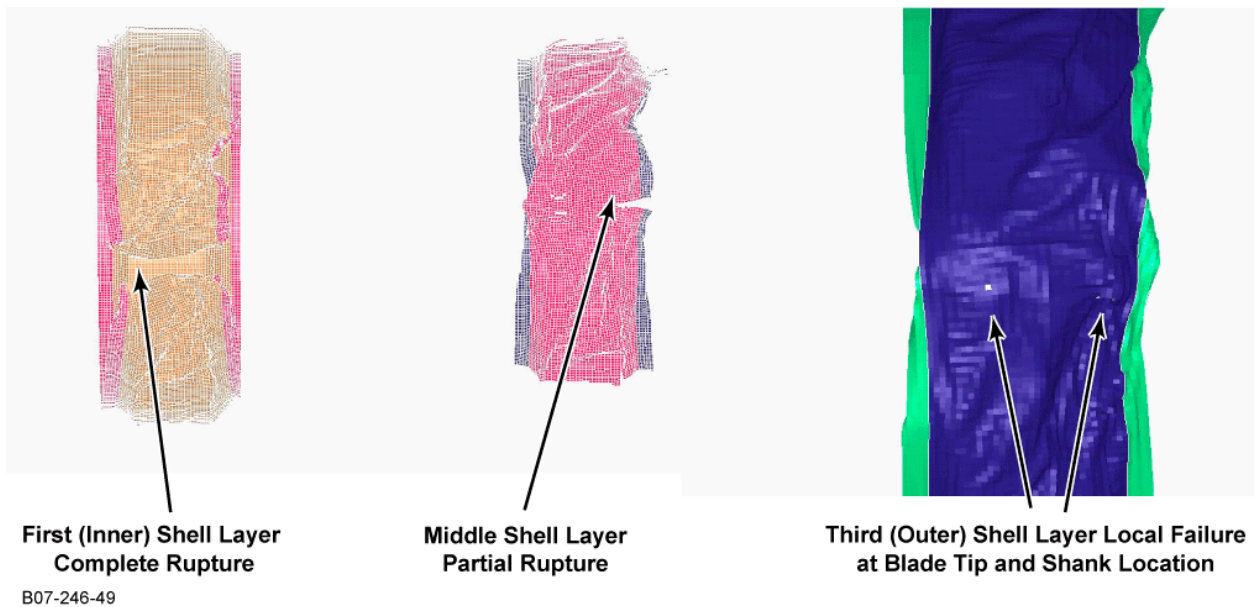


Figure 50. The HTF7000 Engine Fabric Aspect for Simulation Using Three Kevlar Shell Layers, Material Model Version 3.1, Individual Contact Cards With Friction, and IHQ = 3

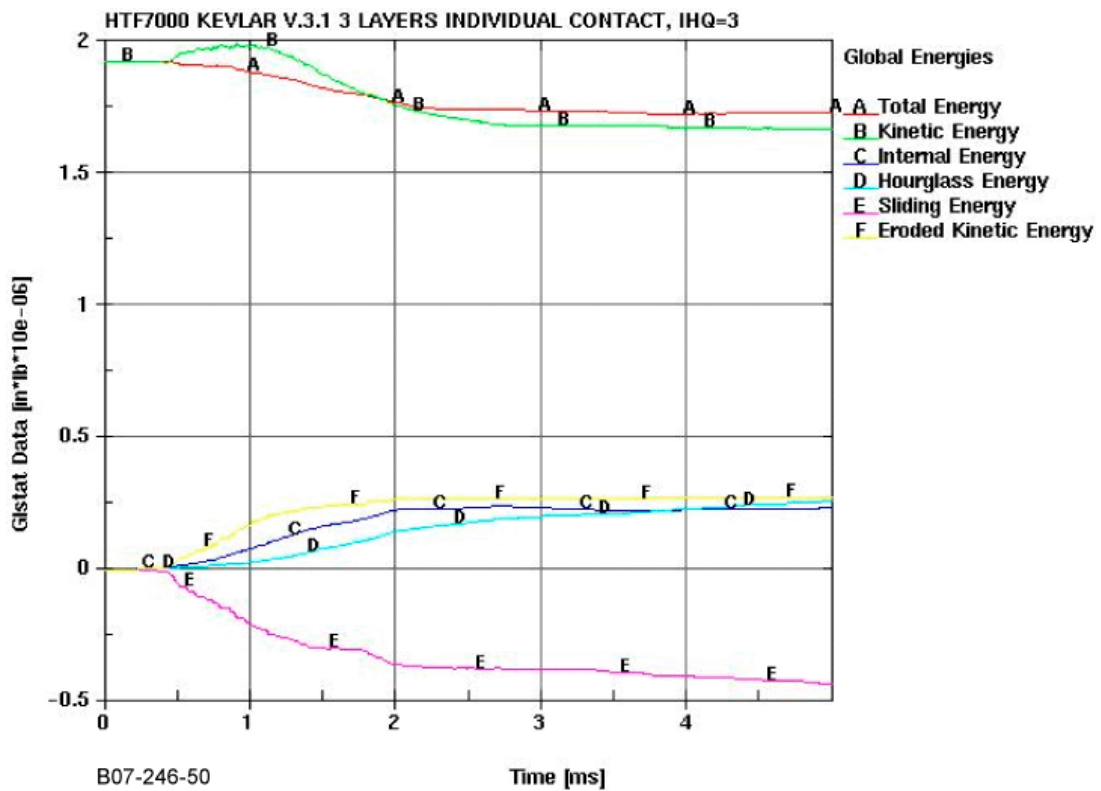


Figure 51. The HTF7000 Engine Global Glistat Data for Simulation Using Three Kevlar Shell Layers, Material Model Version 3.1, Individual Contact Cards With Friction, and IHQ = 3

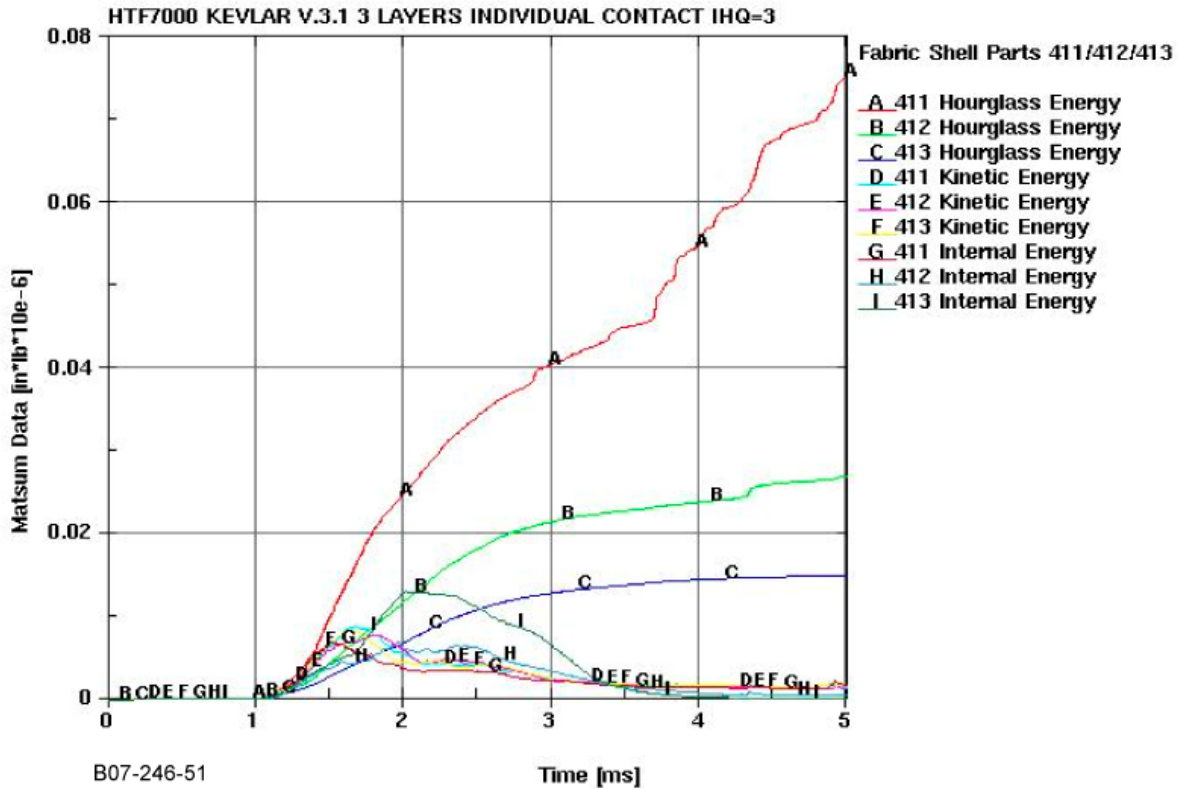


Figure 52. The HTF7000 Engine Fabric Matsum Data for Simulation Using Three Kevlar Shell Layers, Material Model Version 3.1, Individual Contact Cards With Friction, and IHQ = 3

- Plots of the blade kinetic energy versus time revealed that all simulations using material model version 3.1 and individual contact cards for each contact between parts produced very close results (figure 53). Simulations using a single global contact card, while faster, resulted in some difference in blade kinetic energy. The analysis using version 3.1 did not exhibit instability like the analysis using material version 2.1.
- For all analyses using material version 3.1, the effect of simulating the epoxy-wetted ends of the fabric was not studied.

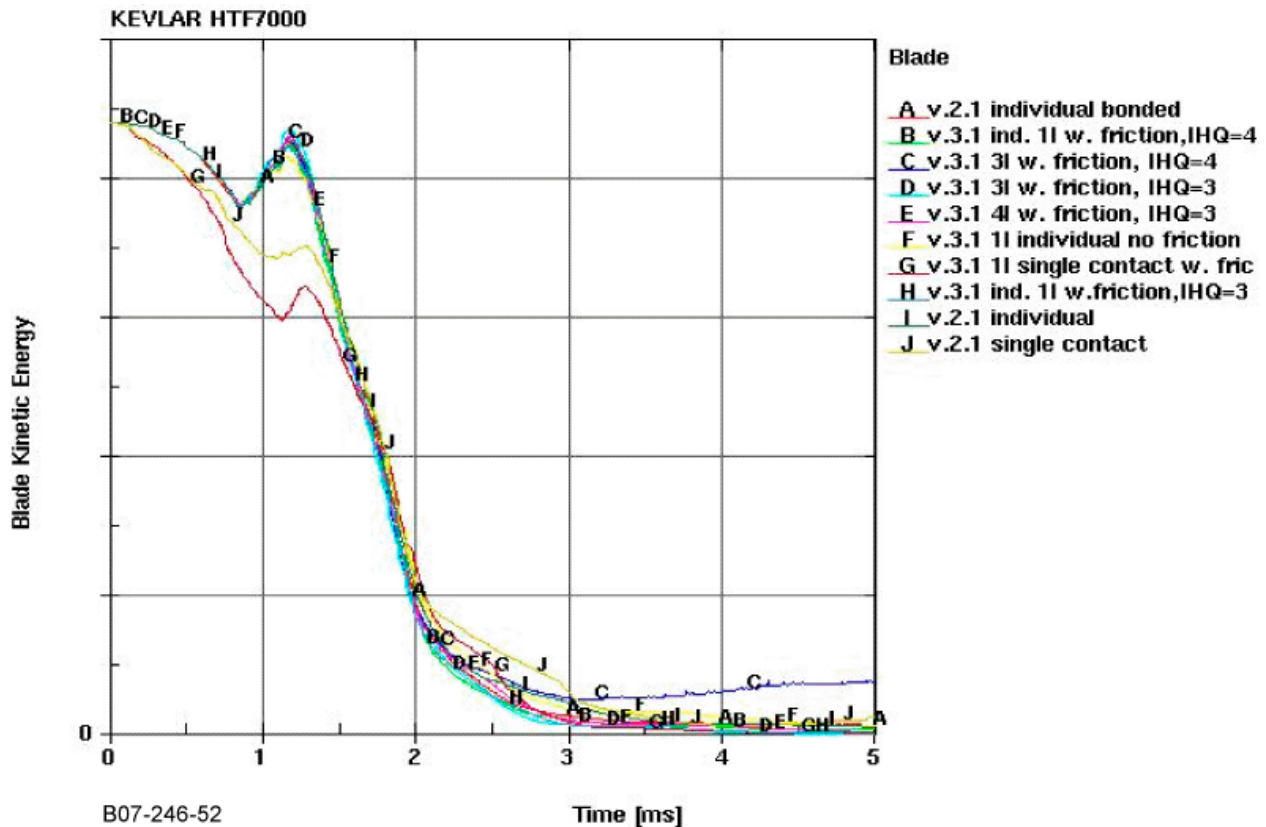
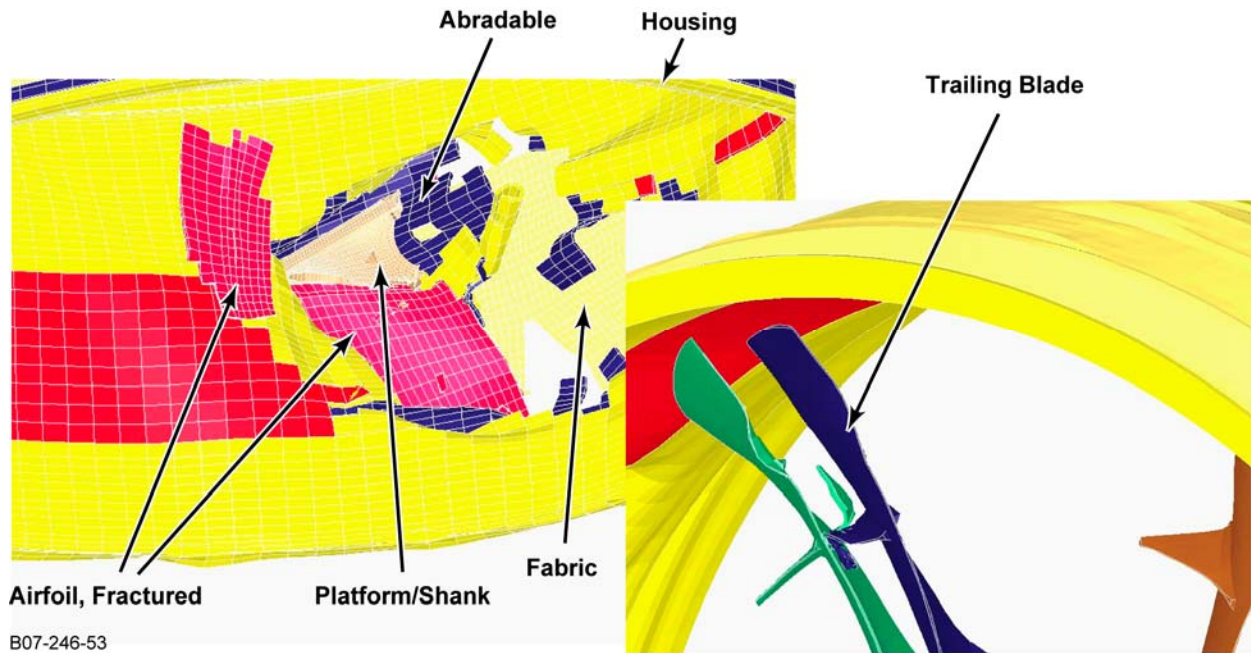


Figure 53. The HTF7000 Engine Blade Kinetic Energy Data for Simulations Using Kevlar Material Model Versions 2.1 and 3.1, and Single and Multiple Shell Layers

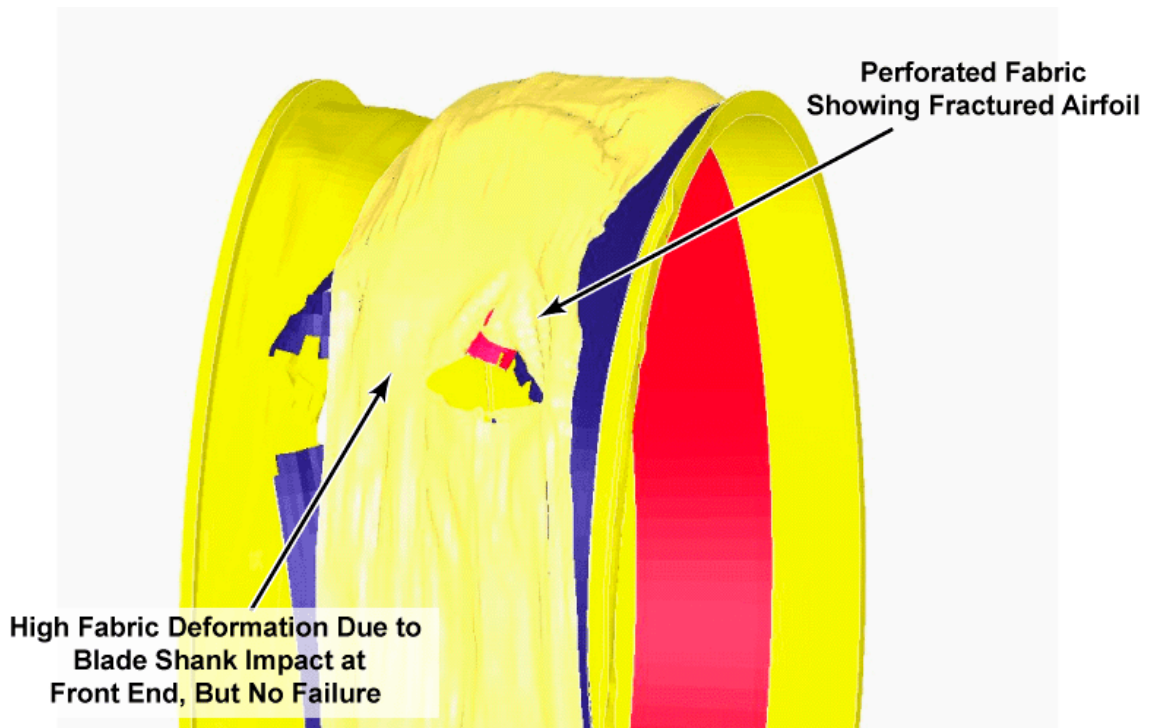
4.3.2 Results for the CFE738 Engine Simulations.

- The majority of predictions for simulations using the single shell-element layer technology with material model version 2.1 were reasonably close to the test. A typical example of a simulation result is shown in figure 54. The released blade orientation, deformed blade shape and damage, and containment housing damage were similar to the orientation and damage noticed in the actual test (figure 37). Damage to the trailing blades (figure 54) was also similar to the damage during the test (figure 38). Fabric damage was predicted better than that for the HTF7000 simulations (figure 55). In the model, the damage made by the blade tip, as well as the rupture of the blade above the dampers, matched the test damage (figure 36). The fabric was also heavily deformed at the front portion, but did not fail. The best case occurred when individual contact cards and IHQ = 3 were used. It was clear that the presence of all blades in the model, which pushed the released blade further inside the containment area, made the simulation results closer to the test results. Cases with fixed fabric ends were not simulated.
- Examination of the glstat and matsum plots for single shell-element layer simulations using material model version 2.1 showed that, if IHQ = 3 was used, the simulation did not present any anomalies from the energy balance point of view (figure 56), but the fabric hourglass energy was high (figure 57).



B07-246-53

Figure 54. The CFE738 Engine Blade Orientation and Deformed Trailing Blade for Simulation Using One Kevlar Shell Layer, Material Model Version 2.1, Individual Contact Cards, No Friction, and IHQ = 3



B07-246-54

Figure 55. The CFE738 Engine Fabric Aspect for Simulation Using One Kevlar Shell Layer, Material Model Version 2.1, Individual Contact Cards, No Friction, and IHQ = 3

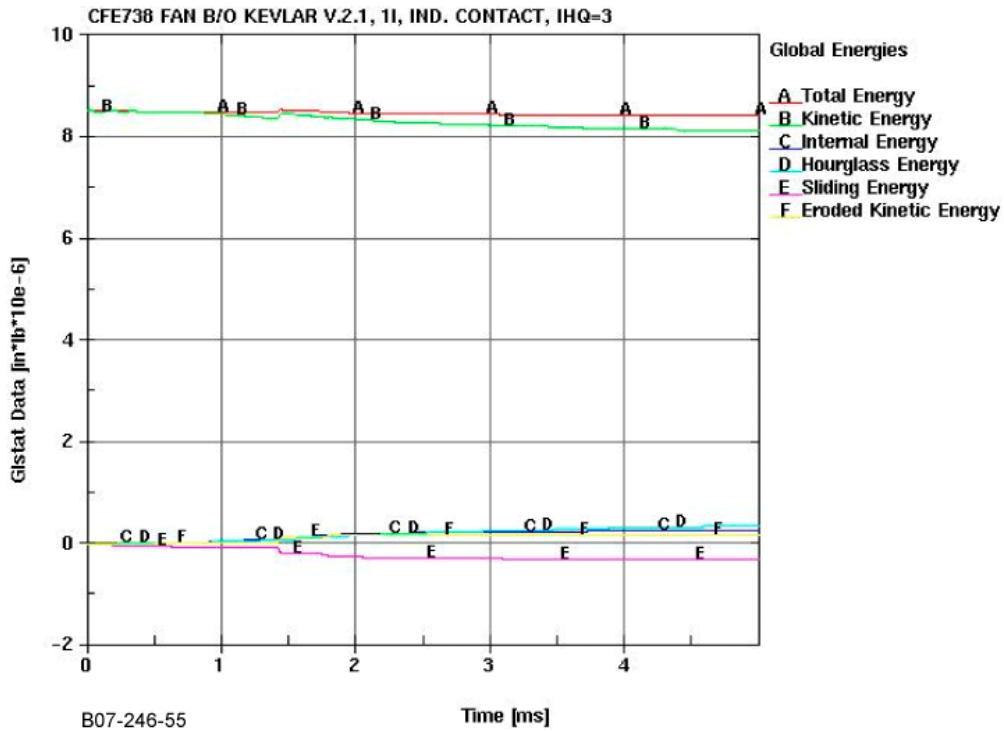


Figure 56. The CFE738 Engine Global Gistat Data for Simulation Using One Kevlar Shell Layer, Material Model Version 2.1, Individual Contact Cards, No Friction, and IHQ = 3

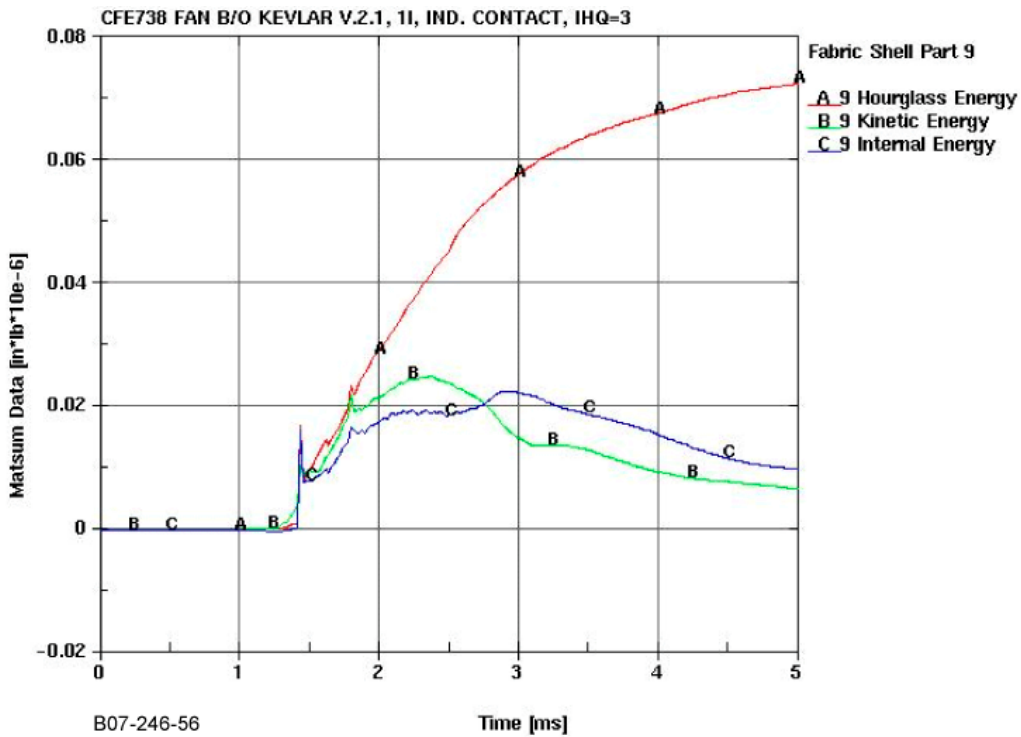


Figure 57. The CFE738 Engine Fabric Matsum Data for Simulation Using One Kevlar Shell Layer, Material Model Version 2.1, Individual Contact Cards, No Friction, and IHQ = 3

- Simulations using multiple shell-element layer technology with material model version 2.1 and IHQ = 3 converged, but the analysis exhibited some instability. Visual matching versus test results was acceptable.
- Simulations using the single shell-element layer technology and material model version 3.1 with IHQ = 4 (figure 58) were successful when predictions compared the blade orientation, the deformed blade shape and damage, and the containment housing damage to the test results. Fabric damage prediction was similar to that for material model version 2.1: damage caused by the blade tip matched, but damage at the aft end (produced by the released blade shank) was underpredicted. The failure of the blade tip above the dampers was also predicted correctly (figure 58).
- Examination of the glstat and matsum plots (figures 59 and 60) showed that for single shell-element layer simulations using IHQ = 4, the simulation was error-free and the hourglass energy for the fabric was lower.
- Simulations using multiple shell-element layer technology with material model version 3.1 successfully converged, and all adequately predicted the housing and blade deformation and damage. When IHQ = 3 was used, the fabric damage was slightly underpredicted; high deformation was noticed, but no fabric failure of the last shell-element layer was present (therefore, blade penetration would occur). However, when IHQ = 4 was used for the simulation modeling, a total of four shell-element layers for all fabric wraps (figure 61). Damage for the fourth (last) layer was similar to the test with failure at both aft end (due to the blade shank) and front end (due to the blade tip). The blade tip completely penetrated the shell layer. An examination of actual fabric damage after the test (figure 62) revealed the presence of four areas of successive failure, decreasing in size. Even though the simulations did not perfectly match the size and the mechanism of the fabric failure, the results were very close and showed that multiple shell-element layer simulations work. Simulations using a total of three shell-element layers for all fabric wraps did not exhibit failure of the last shell layer, thus underpredicting the test.
- Examination of the glstat and matsum plots showed that for multiple shell-element layer simulations using IHQ = 4, the simulation is error-free and the hourglass energy for the fabric is lower (figures 63 and 64).
- Plots of the blade kinetic energy versus time revealed that all simulations using individual contact cards for each contact between parts produced very close results (figure 65), regardless of whether material model version 2.1 or 3.1 was used. Simulation using a single global contact card, while faster, was abandoned due to the instability of the analysis.
- For all analyses using material model version 3.1, the effect of simulating the epoxy-wetted ends of the fabric was not studied due to their very small area compared to the area of the HTF7000 application.

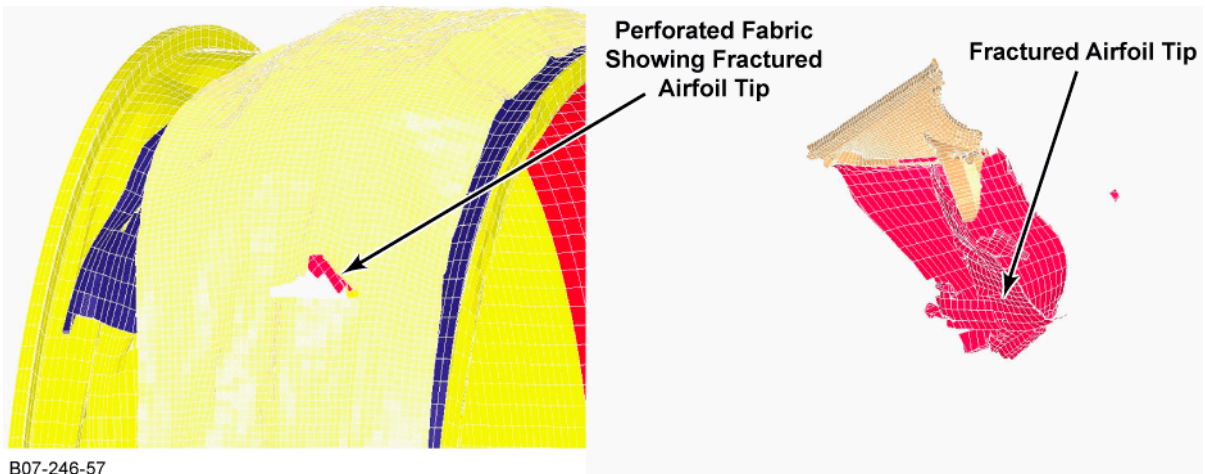


Figure 58. The CFE738 Engine Fabric and Blade Aspect for Simulation Using One Kevlar Shell Layer, Material Model Version 3.1, Individual Contact Cards With Friction, and IHQ = 4

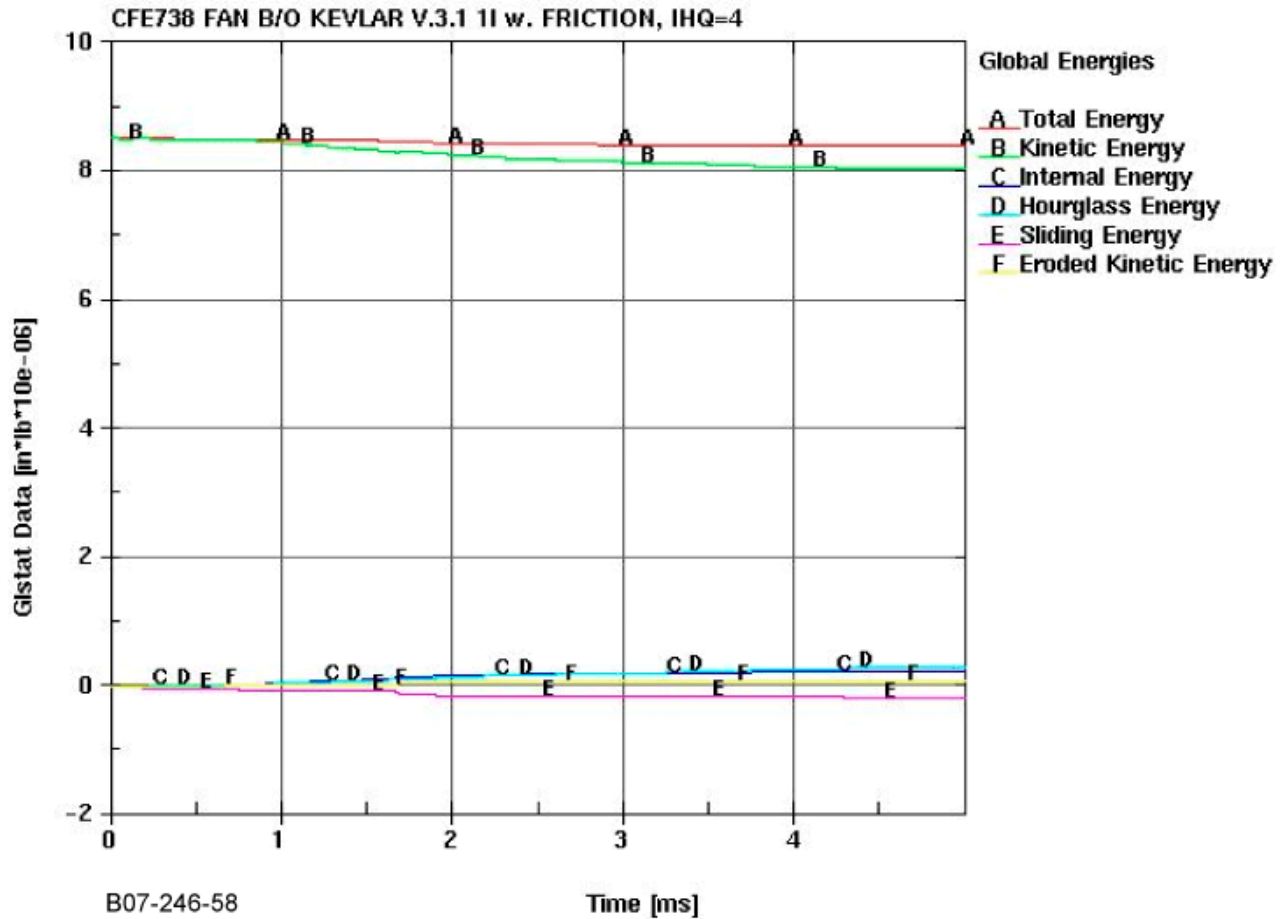


Figure 59. The CFE738 Engine Global Gistat Data for Simulation Using One Kevlar Shell Layer, Material Model Version 3.1, Individual Contact Cards With Friction, and IHQ = 4

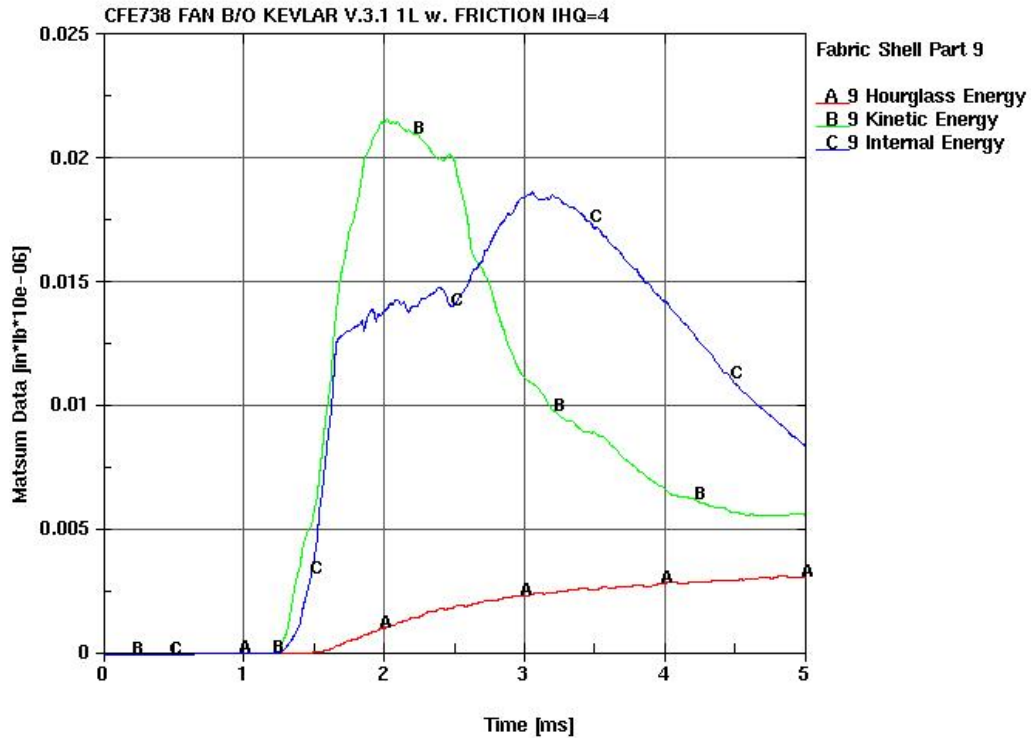


Figure 60. The CFE738 Engine Fabric Matsum Data for Simulation Using One Kevlar Shell Layer, Material Model Version 3.1, Individual Contact Cards With Friction, and IHQ = 4

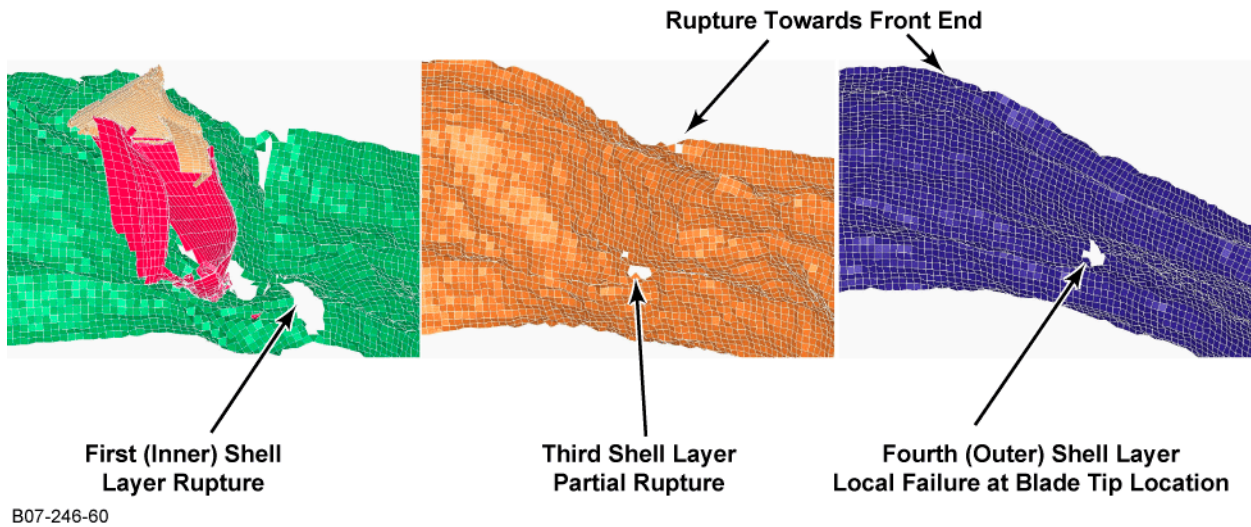
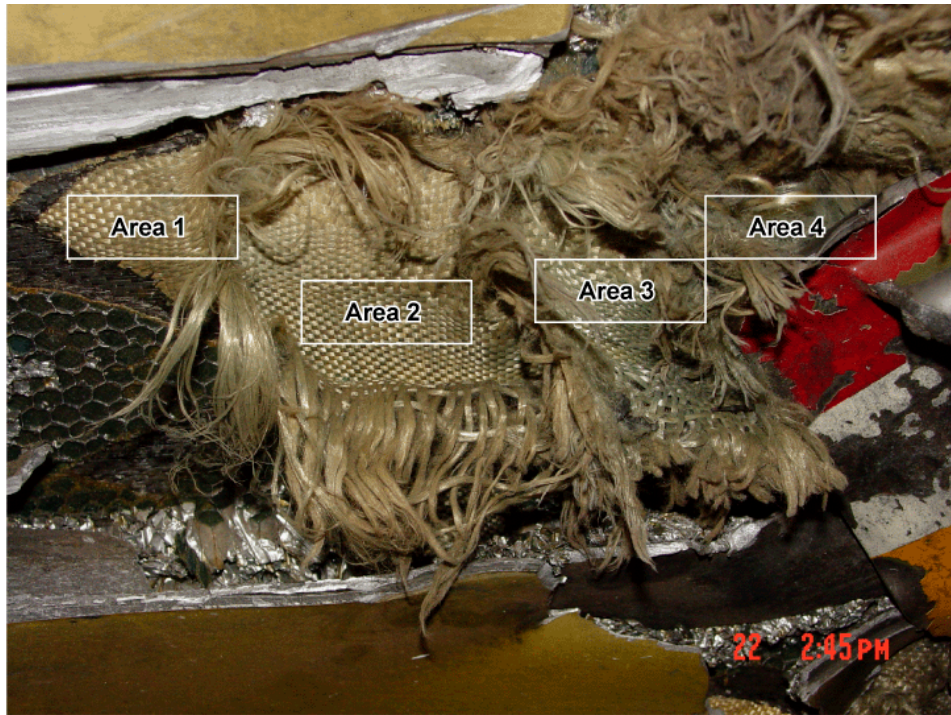
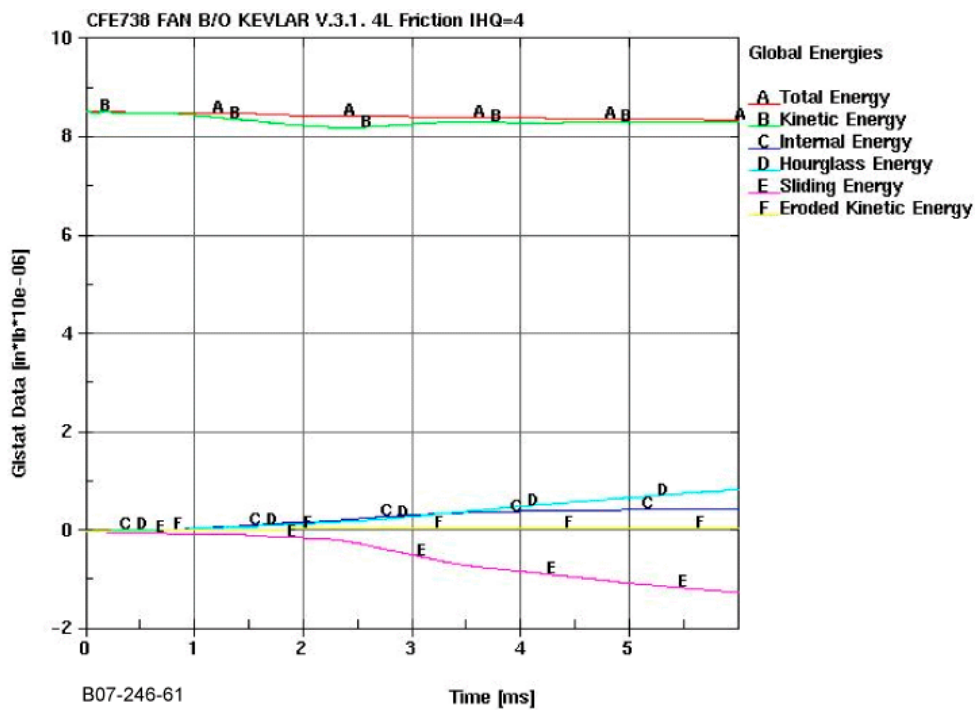


Figure 61. The CFE738 Engine Fabric and Blade Aspect for Simulation Using Four Kevlar Shell Layers, Material Model Version 3.1, Individual Contact Cards With Friction, and IHQ = 4



B07-246-66

Figure 62. The CFE738 Engine Close-Up of the Damaged Fabric in the Blade-Out Test Containment Housing



B07-246-61

Figure 63. The CFE738 Engine Global Gistat Data for Simulation Using Four Kevlar Shell Layers, Material Model Version 3.1, Individual Contact Cards With Friction, and IHQ = 4

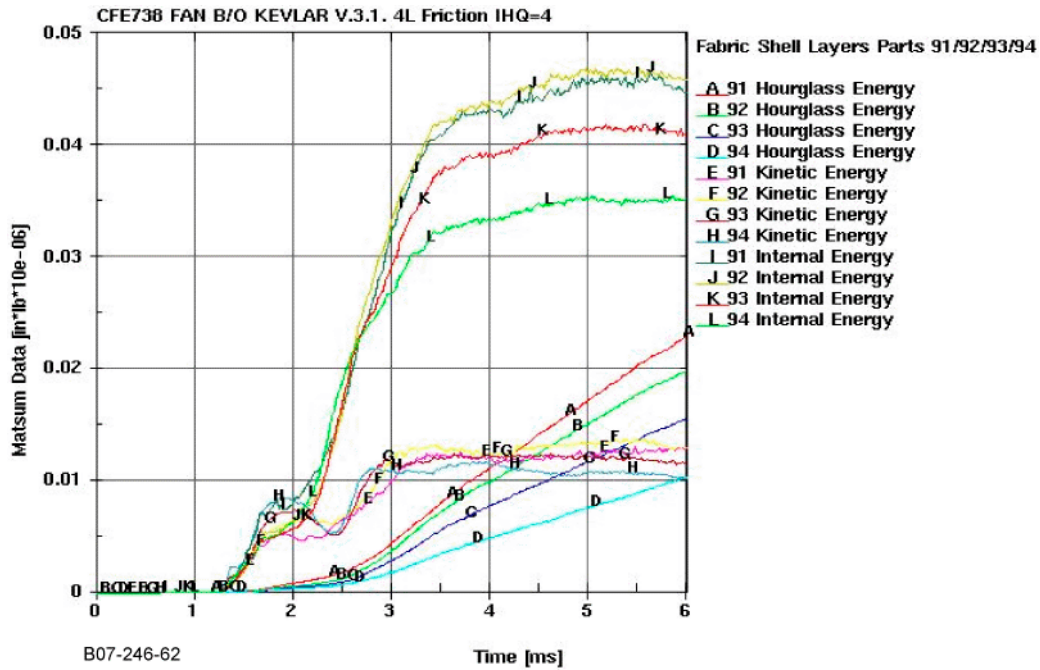


Figure 64. The CFE738 Engine Fabric Matsum Data for Simulation Using Four Kevlar Shell Layers, Material Model Version 3.1, Individual Contact Cards With Friction, and IHQ = 4

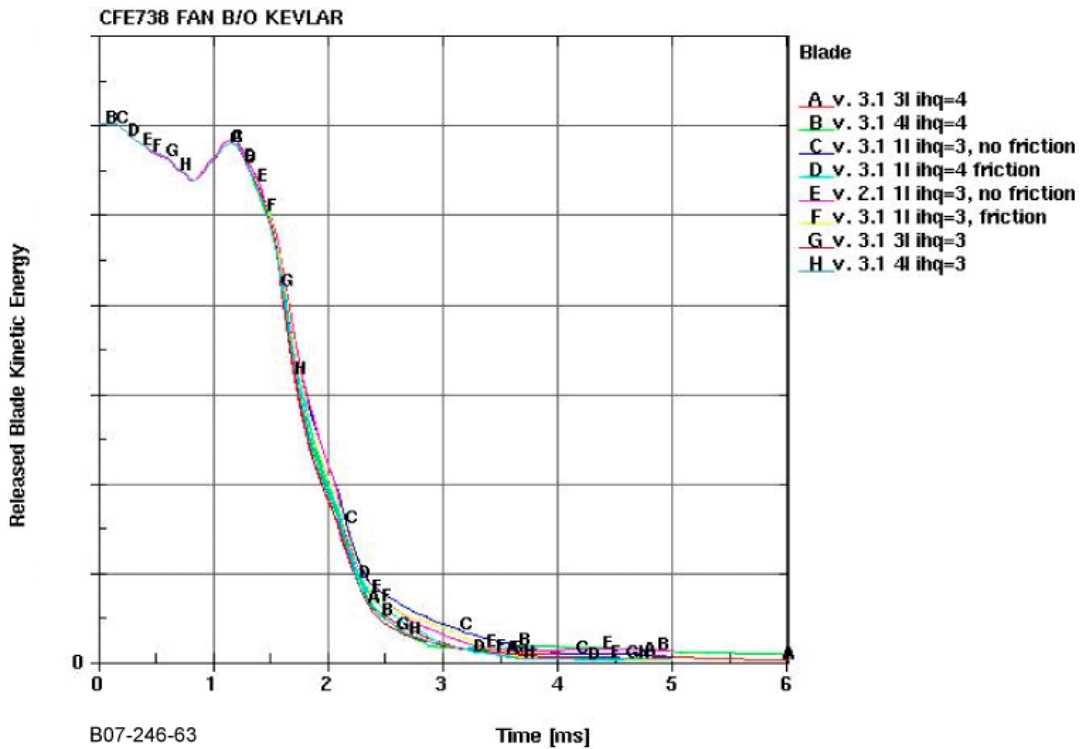


Figure 65. The CFE738 Engine Blade Kinetic Energy Data for Simulations Using Kevlar Material Model Versions 2.1 and 3.1, and Single and Multiple Shell Layers

4.4 CONCLUSIONS FOR TASK 4.

The conclusions drawn from the Task 4 results are summarized as follows:

1. Two engine fan blade-out events were successfully simulated using the latest fabric material models and analytical methodologies.
2. Acceptable correlation was obtained between the simulation results and the engine fan blade containment test results, using the new Kevlar material models 2.1 and 3.1, and both single and multiple shell-element layers modeling techniques.
3. Prediction capability significantly improved with the new material models and the associated modeling techniques with respect to the methodology used in Phase I.
4. Material model version 2.1 was reliable for single shell-element layer simulations when $IHQ = 3$ was used. The fact that simulations with multiple shell-element layer models failed frequently makes it unsuitable for this purpose.
5. Material model version 3.1 is reliable for both single and multiple shell-element layer modeling approaches. $IHQ = 4$ seems the best option for this material model. Further work is needed to assess the most accurate value for the coefficient of friction.
6. For both material models and single shell-element layer simulations, the fabric failure simulation was considerably better, but needs improvement in matching fabric deformation and failure mechanism of the tests.
7. The most significant material model improvement is in the successful use of multiple shell-element layer modeling techniques, with three and four shell-element layers simulating all fabric wraps. The fabric failure simulation was considerably better, but needs improvement in matching fabric deformation and failure mechanism of the tests. Further work with more than four shell-element layers is required, as ballistic tests simulations in Task 2 showed improved prediction of final projectile speed with increasing number of shell-element layers.
8. The mesh density was kept constant during Phases I and II. Based on results obtained in Task 2, only one model had three shell-element layers. Further investigation of the effects of mesh sensitivity, contact parameters, and multilayer numerical instabilities are recommended.
9. During the Phase II study, the best engine fan blade-out simulations were obtained with different LS-DYNA contact parameters than those used for ballistic impact test simulations. This fact points, again, to the conclusion that the fabric failure mechanism is different between the two containment events. This is obvious when considering the difference in motion and impact directions: the ballistic test projectile has an axial impact motion versus a fan blade moving in a radial and circumferential impact direction. The differences in motion and impact directions are also reasons why ballistic impact test simulations with multiple shell-element layers were successful during Phase I, but engine

fan blade-out test simulations with multiple shell-element layers failed when the same LSDYNA contact parameters were used. Thus, simulations of more complex spin pit tests are recommended as the best way to validate a fabric material model for engine fan containment simulations.

4.5 GENERIC ENGINE FAN BLADE-OUT CONTAINMENT MODEL.

4.5.1 Objective.

An objective of this research project was to build and provide a generic fan blade containment FE model for Kevlar or Zylon wrap materials. The purpose of the model is to provide LS-DYNA users with generic guidelines for modeling composite fabric wraps in impact- and containment-related applications.

4.5.2 Background.

During the planning stage of this project, the specifics of the generic model were undefined and left to the project participants and were dependent upon the outcome of the previous tasks. Two possible considerations were studied. One was to consider improving the generic model from Phase I, which was a simulation of a ballistic impact test and could be verified with experimental data. The second consideration for the generic model was to build a model of a simplified engine containment system including fabric layers, a metallic support housing, and a generic blade as the projectile. During completion of Task 4, it was concluded that the latter objective was the best way to develop an industry standard that would best serve the community of aircraft engine manufacturers. Even though the downfall of a fictitious engine containment model was the proprietary nature of experimental test data needed to verify the accuracy of predictions, the model would be a useful starting point for collaborative development. This model could then be improved with input from the aerospace industry users' community and eventually could become the industry guideline standard, for such a simulation, for design and certification by analysis.

It was therefore decided, in principle, to provide a tool that included only the numerical model, the actual fabric LS-DYNA material model, and fictitious material models for the rest of the parts. This gave users the possibility to study and calibrate their own analytical systems, using material properties specific to their applications. The electronic version of the LS-DYNA FE model used (figure 66) was provided to the FAA to satisfy the requirements of the generic containment model. This model will be made available to the Aerospace Users Group being supported by LSTC. Potential users will be able to run this model, already set up with the appropriate contact algorithms, boundary conditions, etc., with their respective software versions, operating systems, and computer platforms. The only modification will be to insert their specific material properties for the application considered. A brief discussion of the model file is given below. This discussion, together with the ballistic test generic model delivered in Phase I, will guide the users to experiment with the simulations, with corresponding experimental results as the goal.

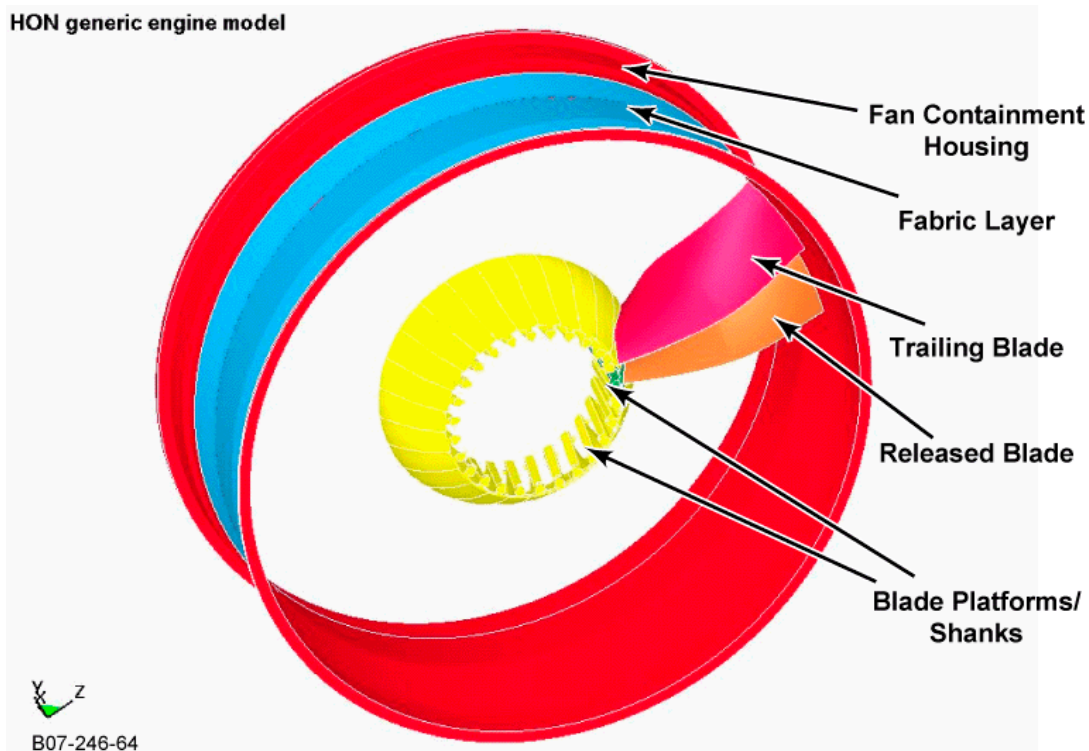


Figure 66. Generic Engine Fan Blade Containment Model

4.5.3 Generic Engine Model File Description.

The computer file consisting of the generic engine fan blade containment model contains the following:

1. FE model: The LS-DYNA input deck includes the nodes and elements of the following parts:
 - Part 1, Fan housing. Built with solid hexahedron elements, the *MAT_PIECEWISE_LINEAR_PLASTICITY card was used for the corresponding material with ID = 2, with fictitious entries. Usually an engine fan containment housing is made of aluminum or titanium. The user can input actual material properties as appropriate.
 - Part 2, Containment fabric layer. Built with shell elements, the *MAT_USER_DEFINED_MATERIAL_MODELS card was used for the corresponding material with ID = 292. This card is the actual card for material properties of Kevlar version 3.1 developed in Phase II. No change is needed, unless a different fabric material model is desired.

- Part 3, Platform_1, the platform of the blade to be released. Built with solid hexahedron elements, the *MAT_PIECEWISE_LINEAR_PLASTICITY card was used for the corresponding material with ID = 10, with fictitious entries. Usually an engine fan blade is made of titanium. The user can input actual material properties as appropriate.
 - Part 4, Platforms_4, the platforms of the rest of the blades. Built with solid hexahedron elements, the *MAT_RIGID card was used for the corresponding material with ID = 142, with fictitious entries. Usually an engine fan blade is made of titanium. The user can input actual material properties as appropriate.
 - Part 5, Blade_0, the airfoil of the blade to be released. Built with solid hexahedron elements, the *MAT_PIECEWISE_LINEAR_PLASTICITY card was used for the corresponding material with ID = 10, with fictitious entries. Usually an engine fan blade is made of titanium. The user can input actual material properties as appropriate.
 - Part 6, Blade_1, the airfoil of trailing blade. Built with solid hexahedron elements, the *MAT_PIECEWISE_LINEAR_PLASTICITY card was used for the corresponding material with ID = 10, with fictitious entries. Usually an engine fan blade is made of titanium. The user can input actual material properties as appropriate.
 - Shell thickness definition for Kevlar, card *SECTION_SHELL, fictitious. For Kevlar analyses, change the thickness to appropriate thickness of all Kevlar wraps.
2. *CONTROL cards. Same controls as in the ballistic test simulations were used. The user would optimize these for a particular simulation.
 3. *CONTACT cards. The global, single contact card approach was used to simulate the contact between the released blade and the other structures with the same parameters as in the ballistic test simulations. The user would optimize these for a particular simulation. Tied contact was used to connect the blade airfoils with their platforms.
 4. *INITIAL_VELOCITY_GENERATION cards. These cards are used to specify the rotating speed of the blades. One option, to simulate the release of a blade, is using this card for all blades and use *PART_INERTIA for the platforms of all blades, except the released blade. This is not the only method to simulate a blade release; the user should involve the best-suited method.

4.5.4 General Model Recommendations.

The following recommendations provide potential users of the generic engine fan blade containment model with important tips on capability and limitations.

1. The user should choose the appropriate version of LS-DYNA to compile the user-defined material model. The binary models can be downloaded from a special file transfer protocol website maintained by the LSTC. Not all LS-DYNA versions and revisions for different operating systems and platforms have a user-defined material capability. Note that example problems and results were obtained with a specific computer setup, as noted in sections 2 and 3.
2. The user should establish a baseline capability of the LS-DYNA version on the available computer hardware. If more than one computer platform is available to the user, it is strongly recommended to compare the results of ballistic test simulations to results of ballistic tests (see Tasks 1 and 2, sections 2 and 3 of this document) using each of the platforms. The results might be different, especially if the same problem is analyzed using single processing or parallel processing.
3. For a given computer platform, the largest source of variation in the results is due to the various contact algorithms available in LS-DYNA. The user should read the methodologies discussed in sections 2 through 4 to learn more about the effects of the contact parameters.
4. The same contact type and parameters were consistent throughout the simulation analyses reported in previous sections. Particularly in the fabric containment problem where a stiff projectile hits a low-stiffness fabric, the successful contact parameters are difficult to pick. Throughout the analyses of the current research, segment-based SOFT = 2 automatic surface-to-surface contact type was consistently used and is recommended. The SOFT = 2 option causes the contact stiffness to be determined, based on stability considerations, taking into account the time step and nodal masses. This approach is generally more effective for contact between materials of dissimilar stiffness or dissimilar mesh densities. The influence of slave and master contact penalty factor (SFS and SFM) is very important.
5. Another parameter closely related to the successful contact modeling is the time step. The TSSFAC in the *CONTROL_TIMESTEP control card is very important.
6. It is recommended that individual contact cards be used for each contact between parts. The global, single contact card option does not produce reliable results, especially when big-engine models are involved.

5. REFERENCES.

1. Rajan, S.D., Mobasher, B., Sharda, J., Yanna, V., Deenadayla, C., Lau, D., and Dhah, D., “Explicit Finite Element Modeling of Multilayer Composite Fabric for Gas Turbine Engines Containment System, Part 1: Static Tests and Modeling,” FAA report DOT/FAA/AR-04/40,P1, November 2004.
2. Periera, M. and Revlock, D., “Explicit Finite Element Modeling of Multilayer Composite Fabric for Gas Turbine Engines Containment System, Part 2: Ballistic Impact Testing,” FAA report DOT/FAA/AR-04/40,P2, November 2004.
3. Simons, J., Erlich, D., and Shockey, D., “Explicit Finite Element Modeling of Multilayer Composite Fabric for Gas Turbine Engines Containment System, Part 3: Model Development and Simulation of Experiments,” FAA report DOT/FAA/AR-04/40,P3, November 2004.
4. Gomuc, R., “Explicit Finite Element Modeling of Multilayer Composite Fabric for Gas Turbine Engines Containment System, Part 4: Model Simulations for Ballistic Tests, Engine Fan-Out, and Generic Engine,” FAA report DOT/FAA/AR-04/40,P4, November 2004.